WCIO 2012

14 – 17 June 2012
Sheraton Chicago Hotel and Towers
Chicago, Illinois, USA

Contents

Message from the Chairs

Dear Colleagues:

We are pleased to welcome you to the World Conference on Interventional Oncology (WCIO), 14-17 June 2012 at the Sheraton Chicago Hotel and Towers in Chicago, Illinois, USA. WCIO 2012 is a scientific forum designed to establish, nurture, and support Interventional Oncology (IO) therapies that use imaging technology to diagnose and treat localized cancers in ways that are precisely targeted and minimally or non-invasive.

Over the course of the next four days, we will gather to promote meaningful dialogue on available and emerging therapies in Radiology, Medical Oncology, Surgical Oncology, Interventional Oncology, Hepatology, and Radiation Oncology. In keeping with the innovative nature of Interventional Oncology, WCIO 2012 is pleased to introduce a series of progressive symposia including *Interventional Radiology Fellows Symposium: Tips and Tricks for New Practice* and a Symposium on Interventional Techniques, *How I Do It: Top 10 Clinical Pearls You Should Know*. We also encourage attendees to take part in discussions on key topics including Hepatocellular Carcinoma and Colon and Neuroendocrine Liver Metastases. There will be additional tumor boards including audience participation, live cases, a special topics plenary session, and a variety of stimulating workshops.

WCIO 2012 is a truly unique conference developed by an international team of experts from multiple specialties, to further the goal of cross-disciplinary collaboration and education. This is your opportunity to explore new agents, delivery systems, and potential synergies. You will be sure to bring back new insights and strategies for the fight against cancer to your home institution.

Welcome to Chicago! We're happy you're here.

WCIO Program Chairs

Riad Salem, MD
Program Chair
Northwestern University
Chicago, Illinois, USA

Riccardo A. Lencioni, MD
Science & Technology Chair
University of Pisa
Pisa, Italy

William S. Rilling, MD
Workshop Chair
Medical College of Wisconsin
Milwaukee, Wisconsin, USA

WCIO Program Committee:

Thierry de Baere, MD
Institut de Cancérologie Gustave Roussy
Villejuif, France

Stephen Solomon, MD
Memorial Sloan-Kettering Cancer Center
New York, New York, USA

Michael C. Soulen, MD
Hospital of the University of Pennsylvania
Philadelphia, Pennsylvania, USA

WCIO Board of Directors

Michael C. Soulen, MD, Chair
Hospital of the University of Pennsylvania
Philadelphia, Pennsylvania, USA

Riccardo A. Lencioni, MD, Vice Chair
University of Pisa
Pisa, Italy

Michael C. Brunner, MD, Past Chair
Swedish Covenant Hospital
Chicago, Illinois, USA

Thierry de Baere, MD
Institut de Cancérologie Gustave Roussy
Villejuif, France

Gary S. Dorfman, MD
Weill Cornell Medical College
New York, New York, USA

Jeffrey F. Geschwind, MD
Johns Hopkins Hospital
Baltimore, Maryland, USA

David Lu, MD
University of California, Los Angeles
Los Angeles, California, USA

Luigi Solbiati, MD
General Hospital of Busto Arsizio
Buston Arsizio, Italy

Stephen Solomon, MD
Memorial Sloan-Kettering Cancer Center
New York, New York, USA

Ex-Officio Members
Riad Salem, MD, Program Chair
Northwestern University
Chicago, Illinois, USA

Michelle Zinnert, CAE
WCIO Executive Director
Washington, District of Columbia, USA

Introducing...

IO Central

An online network for members of the IO community to engage 24/7, 365 days a year.

Join now for free—www.IO-central.org

Brought to you by
WCIO
Advancing Interventional Oncology

CME Information

Accreditation Statement and Learning Objectives

Overview

The World Conference on Interventional Oncology[SM] is designed to focus on image-guided interventional oncologic therapies and their relationship to other existing and emerging treatments. The course will utilize state-of-the-art lectures, live surgery presentations, hands-on workshops, and invited abstract presentations. WCIO will include presentations of basic, translational, and clinical research in a forum that promotes meaningful discussion as well as open and panel discussions on other available and emerging therapies among experts in Radiology, Medical Oncology, Surgical Oncology, Interventional Oncology, Hepatology, and Radiation Oncology.

Objectives

At the conclusion of this learning activity, the learner will be able to:

- Utilize new technologies presented to help select the appropriate therapies in the treatment of patients
- Integrate multi-disciplinary treatment options into a comprehensive patient care program
- Incorporate international practices presented into their current practice

Who Should Attend

The World Conference on Interventional Oncology[SM] is specifically designed to meet the educational needs of:

- Clinical Researchers
- Medical Oncologists
- Diagnostic Radiologists
- Radiation Oncologists
- Gastroenterologists
- Scientists
- General Surgeons
- Spine Interventionalists
- Hepatologists
- Surgical Oncologists
- Interventional Oncologists
- Thoracic Surgeons
- Interventional Radiologists
- Urologists

Conference Accreditation

This activity has been planned and implemented in accordance with the Essentials and Standards of the Accreditation Council for Continuing Medical Education (ACCME) through joint sponsorship of the Society of Interventional Radiology (SIR) and The World Conference on Interventional Oncology[SM] (WCIO).

SIR is accredited by the ACCME to provide continuing medical education for physicians. SIR designates this live activity for a maximum of 27 *AMA PRA Category 1 Credits*™. Physicians should claim only the credit commensurate with the extent of their participation in the activity.

Acknowledgements

WCIO thanks the following companies* for their support:

Sponsors

AngioDynamics
B. Braun
Biocompatibles, Inc.
Boston Scientific Corporation
BSD Medical Corporation
CeloNova Biosciences, Inc.
Covidien
Delcath Systems, Inc.
Galil Medical
GE Healthcare
Guerbet LLC
HealthTronics/Endocare
iSYS Medizintechnik GmbH
Eli Lilly and Company
Merit Medical/BioSphere Medical
Microsulis Medical Ltd
NeoRad
NeuWave Medical, Inc.
Nordion
Onyx Pharmaceuticals
Philips Healthcare, North America
Siemens Healthcare
Sirtex Medical Inc.
Veran Medical

Exhibitors

Activiews, Inc.
AngioDynamics
AprioMed, Inc
Baylis Medical Company Inc.
Biocompatibles, Inc.
Boston Scientific Corporation
BSD Medical Corporation
CeloNova Biosciences, Inc.
CIVCO Medical Solutions
Cook Medical
Covidien
Delcath Systems, Inc.
DFINE
Elsevier
Galil Medical
Guerbet LLC
HealthTronics/Endocare
HS Medical Inc.
INTIO
iSYS Medizintechnik GmbH
Medwaves, Inc.
Merit Medical/BioSphere Medical
Microsulis Medical Ltd
NeoRad
NeuWave Medical Inc.
Nordion
Onyx Pharmaceuticals
Perfint Healthcare Pvt. Ltd
Philips Healthcare, North America
Sirtex Medical Inc.
Society of Interventional Radiology
Surefire Medical Inc.
Veran Medical

WCIO gratefully acknowledges the participation of its 2012 Corporate Partners:

AngioDynamics
Benvenue Medical
Biocompatibles, Inc.
Guerbet LLC
Merit Medical/BioSphere Medical
Sirtex Medical Inc.

For more information on the WCIO Corporate Partner program, please contact Beverlee Galstan at *bgalstan@wcioonline.org*.

* Current at time of publication.

Industry Symposia Information

Friday, 15 June, 12:30 - 13:30
Industry Symposium presented by Philips Healthcare
Multimodality Image Guidance for Advanced Percutaneous and Transarterial Applications

Saturday, 16 June, 12:30 - 13:30
Industry Symposium presented by Siemens Healthcare
Integrating C-Arm Cone Beam CT as a Routine Part of Imaging During Chemoembolization

Saturday, 16 June, 19:00 - 20:30
Industry Symposium presented by Onyx Pharmaceuticals
Nexavar® (sorafenib) in the Treatment of Patients with Unresectable Hepatocellular Carcinoma (HCC) Open Gallery Reception

General Information

Registration Hours

Registration will take place in the Chicago Ballroom Foyer of the Sheraton Chicago Hotel & Towers during the following times:

Thursday, 14 June 2012	06:30 - 18:00
Friday, 15 June 2012	06:30 - 18:00
Saturday, 16 June 2012	06:30 - 18:00
Sunday, 17 June 2012	06:30 - 10:30

Exhibit Hours

The Exhibit Hall will be located in the Chicago 8-10. All refreshment breaks will take place in the Exhibit Hall. The Exhibit Hall will be open during the following hours:

Thursday, 14 June 2012	18:00 - 19:30
Friday, 15 June 2012	09:00 - 19:00
Saturday, 16 June 2012	09:00 - 14:00

Speaker Ready Room Hours

The Speaker Ready Room will be located in the Missouri Room during the following times:

Thursday, 14 June 2012	06:30 - 18:00
Friday, 15 June 2012	06:30 - 18:00
Saturday, 16 June 2012	06:30 - 18:00
Sunday, 17 June 2012	06:30 - 12:00

WCIO Posters

Posters will be on display from 09:30 on Thursday, 14 June until 17:00 on Saturday, 16 June in the Riverside Exhibition Hall. Please visit these throughout the day and recognize your fellow colleagues for their wonderful work.

Faculty

Yasuaki Arai, MD
National Cancer Center Hospital
Tokyo, Japan

Thierry de Baere, MD
Institut de Cancérologie Gustave Roussy
Villejuif, France

Al B. Benson, III, MD, FACP
Northwestern University
Chicago, Illinois, USA

Daniel B. Brown, MD
Thomas Jefferson University
Philadelphia, Pennsylvania, USA

Karen T. Brown, MD
Memorial Sloan-Kettering Cancer Center
New York, New York, USA

Michael C. Brunner, MD
Swedish Covenant Hospital
Chicago, Illinois, USA

Matthew R. Callstrom, MD, PhD
Mayo Clinic
Rochester, Minnesota, USA

Gary S. Dorfman, MD
Weill Cornell Medical College
New York, New York, USA

Joseph Erinjeri, MD, PhD
Memorial Sloan-Kettering Cancer Center
New York, New York, USA

Giammaria Fiorentini, MD
Azienda Ospedaliera Ospedali Riunti Marche Nord
Pesaro, Italy

Afshin Gangi, MD
University Hospital of Strasbourg
Strasbourg Cedex, France

Christos Georgiades, MD
Johns Hopkins Hospital
Baltimore, Maryland, USA

Debra Gervais, MD
Massachusetts General Hospital
Boston, Massachusetts, USA

Jeffrey F. Geschwind, MD
Johns Hopkins University
Baltimore, Maryland, USA

S. Nahum Goldberg, MD
Hadassah Hebrew University
Medical Center
Jerusalem, Israel

William F. Hartsell, MD
CDH Proton Center
Warrenville, Illinois, USA

Tobias Jakobs, MD
University of Munich
Munich, Germany

Laura Kulik, MD
Northwestern Medical Faculty Foundation
Chicago, Illinois, USA

Andrew C. Larson, PhD
Northwestern University
Chicago, Illinois, USA

Fred T. Lee, MD
University of Wisconsin
Madison, Wisconsin, USA

Riccardo A. Lencioni, MD
University of Pisa
Pisa, Italy

Robert Lewandowski, MD
Northwestern University
Chicago, Illinois, USA

Eric Lis, MD
Memorial Sloan-Kettering Cancer Center
New York, New York, USA

Peter Littrup, MD
Karmanos Cancer Institute
Detroit, Michigan, USA

David Lu, MD
University of California, Los Angeles
Los Angeles, California, USA

David C. Madoff, MD
New York-Presbyterian
Hospital/Weill Cornell Medical Center
New York, New York, USA

Jorge Marrero, MD
University of Michigan
Ann Arbor, Michigan, USA

Shari Meyerson, MD
Northwestern Memorial Hospital
Chicago, Illinois, USA

Frank H. Miller, MD
Northwestern University
Chicago, Illinois, USA

Mary Mulcahy, MD
Northwestern Memorial Hospital
Chicago, Illinois, USA

Govindarajan Narayanan, MD
University of Miami
Miami, Florida, USA

Albert Nemcek, Jr., MD
Northwestern Memorial Hospital
Chicago, Illinois, USA

Charles Nutting, DO
Radiology Imaging Associates, PC
Greenwood Village, Colorado, USA

Reed Omary, MD, MS
Northwestern University
Chicago, Illinois, USA

Franco Orsi, MD
European Institute of Oncology
Milan, Italy

Rod Pommier, MD
Oregon Health and Science University
Portland, Oregon, USA

William S. Rilling, MD
Medical College of Wisconsin
Milwaukee, Wisconsin, USA

Riad Salem, MD
Northwestern University
Chicago, Illinois, USA

Paul B. Shyn, MD
Brigham and Women's Hospital
Boston, Massachusetts, USA

Constantinos T. Sofocleous, MD, PhD
Memorial Sloan-Kettering Cancer Center
New York, New York, USA

Luigi Solbiati, MD
General Hospitals of Busto Arsizio
Busto Arsizio, Italy

Stephen Solomon, MD
Memorial Sloan-Kettering Cancer Center
New York, New York, USA

Michael C. Soulen, MD
Hospital of the University of Pennsylvania
Philadelphia, Pennsylvania, USA

Robert Suh, MD
University of California, Los Angeles
Los Angeles, California, USA

Sean Tutton, MD
Medical College of Wisconsin
Milwaukee, Wisconsin, USA

James Urbanic, MD
Wake Forest School of Medicine
Winston-Salem, North Carolina, USA

Jean-Nicolas Vauthey, MD
The University of Texas MD Anderson Cancer Center
Houston, Texas, USA

Michael Wallace, MD
The University of Texas MD Anderson Cancer Center
Houston, Texas, USA

Bradford Wood, MD
National Institutes of Health
Bethesda, Maryland, USA

Vahid Yaghmai, MD
Northwestern University
Chicago, Illinois, USA

Ren Jie Yang, MD, PhD
Peking University Cancer Hospital
Beijing, China

Francis Yao, MD
University of California San Francisco
San Francisco, California, USA

THURSDAY, 14 JUNE 2012		Room
6:30 - 8:00	**Continental Breakfast**	**Chicago Pre-Function**
8:00 - 9:30	**Concurrent Sessions** **Guidance and Targeting** Moderators: Michael Wallace, MD and Bradford Wood, MD	**Chicago 6**
8:00 - 8:15	**How to Optimize US/CT with Fusion** Luigi Solbiati, MD	
8:15 - 8:30	**CT Navigation** Bradford Wood, MD	
8:30 - 8:45	**Cone Beam CT: Intraprocedural Role** Michael Wallace, MD	
8:45 - 9:00	**Tumor Vessel Tracking in Embolotherapy** Thierry de Baere, MD	
9:00 - 9:15	**Tumor Segmentation and Response** Vahid Yaghmai, MD	
9:15 - 9:30	**PET Guided Ablation: Feasibility** Stephen Solomon, MD	
8:00 - 9:30	**Abstract Presentations - Hepatocellular Carcinoma**	**Chicago 7**
8:00 - 8:08	Paper 1: **Survival in Patients with Hepatocellular Carcinoma: Improvements in Locoregional Therapy and Multidisciplinary Approach Over Two Decades at a Single Institution** **T.O. Lawal,** J.R. Spivey, S.I. Hanish, B.F. El-Rayes, D.A. Kooby, H.S. Kim *Emory University School of Medicine, Atlanta, Georgia, USA*	
8:08 - 8:16	Paper 2: **Review of Unusual Arterial Supply to Liver Tumors and Its Impact on Transarterial Therapies** **P. Dalvie,** O. Ozkan, J. McDermott *University of Wisconsin, Madison, Wisconsin, USA*	
8:16 -8:24	Paper 3: **Comparison of Survival Outcome in Patients with Unresectable Hepatocellular Carcinoma Treated with Triple Drug TACE and TACE with Doxorubicin Loaded LC-Beads** **A.S. Gomes[1],** P.A. Monteleone[1], C.D. Britten[2], R.S. Finn[2], S. Sadeghi[2], J.W. Sayre[1] *[1]UCLA Medical Center, Los Angeles, California, USA, [2]UCLA Medical Center, Santa Monica, California, USA*	
8:24 -8:32	Paper 4: **Contrast Trapping in Hepatocellular Carcinoma on Non-Contrast CT after Chemoembolization with Drug Eluting Beads May Predict Tumor Response** **Y.S. Golowa,** P. Golshani, M. Abrams, M. Jagust, J. Cynamon *Montefiore Medical Center, Bronx, New York, USA*	

THURSDAY, 14 JUNE 2012		Room
8:32 - 8:40	Paper 5: **Efficacy of Radiofrequency Ablation and Drug Eluting Beads Transarterial Chemoembolization in Treating Hepatoma** **G. Narayanan**, S. Naidu, K. Pereira, V. Sarode, K.J. Barbery, T. Froud *University of Miami, Miami, Florida, USA*	
8:40 - 8:48	Paper 6: **Combined Radiofrequency Ablation and Ethanol Injection with a Multi-Pronged Needle for the Treatment of Medium and Large Hepatocelluar Carcinoma** **X. Xie**, M. Kuang, M. Lu *The First Affiliated Hospital of Sun Yat-sen University, Guangzhou, China*	
8:48 - 8:56	Paper 7: **Studies on the Feasibility of Radiofrequency Ablation in Treatment of Advanced Hepatocellular Carcinoma** **M. Chen**, J. Wu, W. Yang, W. Wu, K. Yan *Peking University Cancer Hospital, Beijing, China*	
8:56 - 9:04	Paper 8: **Microwave Ablation of Hepatocellular Carcinoma: Long-Term Results in a Single Center** **M. Kuang,** X. Xie, M. Lin, G. Liu, Z. Xu, M. Lu *The First Affiliated Hospital of Sun Yat-sen University, Guangzhou, China*	
9:04 - 9:12	Paper 9: **Irreversible Electroporation for the Treatment of Early-Stage Hepatocellular Carcinoma: A Prospective Multicenter Phase II Clinical Trial** ***R. Lencioni*[1]**, L. Crocetti[1], F. Izzo[2], V. Vilgrain[3], J. Bruix[4], J. Ricke[5] *[1]University of Pisa School of Medicine, Pisa, Italy, [2]National Cancer Institute, Naples, Italy, [3]Centre Hospitalier Universitaire de Beaujon, Clichy, France, [4]University of Barcelona, Barcelona, Spain, [5]Universitatsklinikum Magdeburg, Magdeburg, Germany*	
9:12 -9:20	Paper 10: **Radiofrequency Ablation Versus Liver Resection for Elderly Patients with Hepatocellular Carcinoma (HCC) within the Milan Criteria** **Z. Peng**, M. Chen *Sun Yat-sen University, Guangzhou, Guangdong, China*	
9:30 - 10:30	**Break in the Poster Hall**	**Riverside B**
10:30 - 10:45	**Opening Remarks**	**Chicago 6/7**
10:45 - 12:30	**Multidisciplinary State-of-the-Art: Hepatocellular Carcinoma 1** Moderator: Laura Kulik, MD	**Chicago 6/7**
10:45 - 10:55	**Diagnosis of HCC: Review of Guidelines** Frank H. Miller, MD	
10:55 - 11:15	**Staging of HCC: Is There One Best System?** Jorge Marrero, MD	

THURSDAY, 14 JUNE 2012		Room
11:15 - 11:35	**Treatment of Small HCC: Should We Replace RFA with Microwave?** Fred T. Lee, MD	
11:35 - 12:05	**Current Status of Liver Transplantation: Downstaging Strategies and Expanded Criteria** Laura Kulik, MD	
12:05 - 12:30	**Audience Q&A/Panel Discussion**	
12:30 - 13:30	**Irreversible Electroporation: An Evolving Treatment Modality for the Interventional Oncologist**	**Chicago 6/7**
12:30-13:00	**Rationale and Clinical Application of IRE in Hepatic and Lung Tumors** Riccardo A. Lencioni, MD	
13:00-13:30	**Novel Applications for IRE** Govindarajan Narayanan, MD	
12:30 - 14:00	**Lunch & Poster Session**	**Riverside B**
14:00 - 16:00	**Multidisciplinary State-of-the-Art: HCC 2** Moderator: Michael C. Brunner, MD	**Chicago 6/7**
14:00 - 14:15	**Bland Embolization: Role in HCC** Karen T. Brown, MD	
14:15 - 14:30	**Conventional TACE: Rationale As Gold Standard** Michael C. Soulen, MD	
14:30 - 14:45	**Drug Loaded Microspheres: Better Than cTACE?** Jeffrey F. Geschwind, MD	
14:45 - 15:00	**Y90 for HCC: Rationale for Integration in Treatment Algorithm** Riad Salem, MD	
15:00 - 15:15	**Combining Locoregional and Systemic Therapies** Riccardo A. Lencioni, MD	
15:15 - 15:30	**Systemic Treatments for HCC: What You Need to Know** Jorge Marrero, MD	
15:30 - 15:45	**Ongoing Clinical Trials in HCC** Riad Salem, MD	
16:00 - 17:00	**Break in the Poster Hall**	**Riverside B**

THURSDAY, 14 JUNE 2012		Room
17:00 - 18:30	**Concurrent Sessions** **HCC Tumor Board and Live Case from Northwestern University** Moderator: Riad Salem, MD Speakers: Karen T. Brown, MD, Jeffrey F. Geschwind, MD, Laura Kulik, MD, Fred T. Lee, MD, Jorge Marrero, MD, Michael C. Soulen, MD	**Chicago 6**
17:00 - 18:30	**Abstract Presentations - New Developments and Clinical Advances**	**Chicago 7**
17:00-17:08	Paper 11: **Therapeutic Lymphangiography by Lymph Node Injection in the Treatment of Lymphatic Leak Secondary to Nephrectomy and Radical Lymphadenectomy: Preliminary Experience** **E. Santos**[1], K. McCluskey[1], R. Bandi[1], C. Friend[1], A. Zajko[1], F. Gomez[2] *[1]Univiersity of Pittsburgh Medical Center, Pittsburgh, PA, USA,* *[2]Hospital La Fe, Valencia, Spain*	
17:08 - 17:16	Paper 12: **US-Guided Fiducial Placement Before Targeted Radiation Therapy for Prostate Cancer** **J. Rosenbaum**, W. Chong, M. Kably, J. Salsamendi, G. Narayanan *University of Miami, Miami, Florida, USA*	
17:16 - 17:24	Paper 13: **Result of Treatment Painful Bone Metastases with Magnetic Resonance Guided Focused Ultrasound** **V.G. Turkevich**, V.V. Savelyeva, I.V. Dunaevsky, P.I. Krzhivitsky, S.V. Kanaev *Petrov Research Institute of Oncology, Saint-Petersburg, Russian Federation*	
17:24 - 17:32	Paper 14: **Image Guided Displacement of Organs at Risk Prior to Stereotactic Body Radiation Therapy Minimizes Toxicity and Facilitates Dose Escalation** **M. Maybody**, J.P. Erinjeri, W. Alago, R.H. Thornton, S. Solomon, Y. Yamada *Memorial Sloan-Kettering Cancer Center, New York, New York, USA*	
17:32 - 17:40	Paper 15: **Trans Arterial Irinotecan Chemoembolization (IRI TACE) for Symptomatic and Intractable Colorectal Cancer (CC)** **R. Bini**, R. Leli, S. Comelli, F.A. Valle, D. Savio, G.P. Vaudano *SG Bosco Hospital, Turin, Italy*	
17:40 - 17:48	Paper 16: **Radical Treatment of Stage IV Pancreatic Cancer by the Combination of Cryosurgery and Iodine-125 Seed Implantation** J. Chen, J. Li, **L. Niu**, K. Xu *Guangzhou Fuda Cancer Hospital, Guangzhou, China*	
17:48 - 17:56	Paper 17: **PLGA Microspheres for Image-Guided Transcatheter Delivery of Sorafenib to Liver Tumors** **J. Chen**, L. Shea, A.Y. Sheu, R.A. Omary, A.C. Larson *Northwestern University, Chicago, Illinois, USA*	

THURSDAY, 14 JUNE 2012		Room
17:56 - 18:04	Paper 18: **Microwave Ablation Energy Delivery: Power Pulsing May Improve Ablation Zone Size and Reduce Treatment Time** **M. Bedoya**, C. Brace *University of Wisconsin-Madison, Madison, Wisconsin, USA*	
18:04 - 18:12	Paper 19: **Irreversible Electroporation (IRE) Ablation of the Lumbar Vertebrae in a Porcine Model** **M. Abdelsalam**, K. Dixon , A. McWatters., J. Miller, A. Tam, M. Gagea *The University of Texas MD Anderson Cancer Center , Houston, Texas, USA*	
18:12: - 18:20	Paper 20: **Percutaneous Cryoablation and 125I Seeds Implantation Combined with Chemotherapy for the Treatment of Advanced Pancreatic Cancer: Reports of 96 Cases** **L. Niu**, L. He, L. Zhou, B. Wu, J. Zuo, K. Xu *GIHB Affiliated Fuda Hospital Oncology,Chinese Academy of Sciences, Guangzhou, China*	
18:30 - 19:30	**Welcome Reception in Exhibit Hall**	**Chicago 8-10**

FRIDAY, 15 JUNE 2012		Room
6:30 - 8:00	**Continental Breakfast**	**Chicago Pre-Function**
7:00 - 8:00	**Concurrent Workshop 1: Y90** Speakers: Robert Lewandowski, MD, Charles Nutting, DO, and Tobias Jakobs, MD	**Chicago 6**
	Concurrent Workshop 2: Guidance and Targeting Workshop (Non-CME) Speakers: Bradford Wood, MD, Luigi Solbiati, MD, and Thierry de Baere, MD	**Superior**
8:00 - 9:30	**Concurrent Sessions** **New Devices** Moderators: Gary S. Dorfman, MD and Govindarajan Narayanan, MD	**Chicago 6**
8:00 - 8:15	**Current Status of Irreversible Electroporation: What's Next?** Govindarajan Narayanan, MD	
8:15 - 8:30	**Cryoablation: Novel Applications** Peter Littrup, MD	
8:30 - 8:45	**HIFU: Ready for Prime Time?** Franco Orsi, MD	
8:45 - 9:00	**Improving the Local Effect of Ablation** S. Nahum Goldberg, MD	

FRIDAY, 15 JUNE 2012		Room
9:00 - 9:15	**Microwave: Better than RFA?** David Lu, MD	
9:15 - 9:30	**Bronchial Stenting for Lung Cancer** Ren-Jie Yang, MD	
8:00 - 9:30	**Abstract Presentations - Imaging Guidance and Assessment**	**Chicago 7**
8:00 -8:08	Paper 21: **Post-TACE DynaCT Attenuation Value as Predictor of Treatment Response in HCC.** **J. Wan**, D. Klass, S.G. Ho, D. Liu, A. Weiss, A. Buczkowski *Vancouver General Hospital, Vancouver, British Columbia, Canada*	
8:08 - 8:16	Paper 22: **A Precise Safety Margin of 1.0 cm is Required for Best Local Efficacy of Radiofrequency Ablation of Hepatocellular Carcinoma: Assessment with a Novel Three Dimensional Reconstruction Software** **M. Kuang**, Y. Wang, C. Jiang, X. Xie, M. Lu *The First Affiliated Hospital of Sun Yat-sen University, Guangzhou, Guangdong, China*	
8:16 - 8:24	Paper 23: **Tumor Response Assessment in Hepatocellular Carcinoma: Efficacy of Segmentation and Automated Volumetric Measurements Using Triple-Phase Contrast-Enhanced Computed Tomography Scans Before and After Loco-Regional Therapy** **K. Memon[1]**, R. Salem[1], D. Cioni, R.A. Lencioni[2], L. Zhang[3], D.E. Gustafson[3] *[1]Northwestern University, Chicago, IL, USA, [2]Pisa University, Pisa, Italy, [3]Intio Inc, Broomfield, Colorado, USA*	
8:24 - 8:32	Paper 24: **Contrast-Enhanced Ultrasound for Accurate Measurement Tumor Size in Colorectal Liver Metastases** **J. Wu**, M. Chen, S. Yin, K. Yan, W. Wu, Y. Shi *Peking University Cancer Hospital & Institute, Beijing, China*	
8:32 - 8:40	Paper 25: **Percutaneous Ultrasound-Guided Ablation for Liver Tumor with Artificial Pleural Effusion or Ascites** **X. Xie[1]**, M. Kuang[1], M. Lu[1], H. Xu[2] *[1]The First Affiliated Hospital, Sun Yat-sen University, Guangzhou, China, [2]Shanghai Tenth People's Hospital and the Tenth People's Hospital of Tongji University, Shanghai, China*	
8:40 - 8:48	Paper 26: **Safe Percutaneous Thermal Ablation of Poorly Accessible High Dome Liver Lesions Using One-Lung Ventilation Technique: Preliminary Experience** **N. Yu**, K. Dittmar, C. Frenette, H. Monsour, S. Gordon-Burroughs, R. Ghobrial *The Methodist Hospital, Houston, Texas, USA*	

FRIDAY, 15 JUNE 2012		Room
8:48 - 8:56	Paper 27: **Pre-Clinical and Phase I Studies Using the MAXIO System for CT Guided Probe Placement** **F.M. Moeslein**[1], A.K. Chaturvedi[2] [1]University of Maryland School of Medicine, Baltimore, MD, USA, [2]*Rajiv Gandhi Cancer Institute & Research Center, New Delhi, India*	
8:56 – 9:04	Paper 28: **Initial Assessment of Semi-Automated Vessel Segmentation Software as a Potential Application for Guidance during Chemoembolization Procedures** **M. Wallace**[1], G. Chintalapani[2], P. Chinna Durai[2] [1]*The University of Texas M.D. Anderson Cancer Center, Houston, Texas, USA,* [2]*Siemens Medical Solutions USA, Inc., Hoffman Estates, Illinois, USA*	
9:04 - 9:12	Paper 29: **Magnetic Resonance Imaging Detection of Targeted Intrarterial Delivery of Iron Oxide Nanoparticles to the Liver Tumors in the Rabbit Cancer Model** **V. Prieto**, T.O. Lawal, L. Wang, H. Mao, H.S. Kim *Emory University School of Medicine, Atlanta, Georgia, USA*	
9:12 - 9:20	Paper 30: **MRI-Monitored Transcatheter Intra-Arterial Delivery of Spio-Labeled Natural Killer Cells to Hepatocellular Carcinoma** **A.Y. Sheu**, Z. Zhang, R.A. Omary, A.C. Larson *Northwestern University, Chicago, Illinois, USA*	
9:20 - 9:28	Paper 31: **7T MRI Accurately Quantifies Intratumoral Uptake of Nanotherapeutics in a Rat Model of Liver Cancer** **P. Tyler**, A.Y. Sheu, D. Procissi, R.J. Lewandowski, A.C. Larson, R.A. Omary *Northwestern University, Chicago, Illinois, USA*	
9:30 - 10:30	**Break in the Exhibit Hall**	**Chicago 8-10**
10:30 - 12:30	**Multidisciplinary State-of-the-Art: Liver Metastases (Colon)** Moderator: Constantinos T. Sofocleous, MD, PhD	**Chicago 6/7**
10:30 - 10:45	**Modern Chemotherapy for CRC** Mary Mulcahy, MD	
10:45 - 11:00	**Intra-arterial Ports for Chemoinfusion** Yasuaki Arai, MD	
11:00 - 11:15	**Combining Resection with Chemotherapy** Jean-Nicholas Vauthey, MD	
11:15 - 11:30	**Portal Vein Embolization** David C. Madoff, MD	
11:30 - 11:45	**Ablation for Liver Metastases: Should it Replace Resection?** Luigi Solbiati, MD	

FRIDAY, 15 JUNE 2012		Room
11:45 - 12:00	**Radioembolization for Liver Metastases** Constantinos T. Sofocleous, MD, PhD	
12:00 - 12:15	**Drug Eluting Beads for Colon Metastases** Giammaria Fiorentini, MD	
12:15 - 12:30	**Audience Q&A/Panel Discussion**	
12:30 - 13:30	**Industry Symposium supported by Philips Healthcare (Non-CME)**	**Chicago 6/7**
12:30 - 14:00	**Lunch & Exhibits**	**Chicago 8-10**
14:00 - 16:00	**Multidisciplinary State-of-the-Art: Musculoskeletal** Moderator: Christos Georgiades, MD	**Chicago 6/7**
14:00 - 14:15	**Ablation for Soft Tissue Sarcomas** Joseph Erinjeri, MD, PhD	
14:15 - 14:30	**Ablation for Bone Metastases** Matthew R. Callstrom, MD	
14:30 - 14:45	**Spinal Intervention** Afshin Gangi, MD	
14:45 - 15:00	**Radiotherapy for Bone Metastases** William F. Hartsell, MD	
15:00 - 15:15	**Novel Bone Interventions (Including Vertebroplasty)** Sean Tutton, MD	
15:15 - 16:00	**MSK Tumor Board** Moderators: Matthew R. Callstrom, MD and Afshin Gangi, MD Speakers: Joseph Erinjeri, MD, PhD, William F. Hartsell, MD, Sean Tutton, MD	
16:00 - 17:00	**Break in the Exhibit Hall**	**Chicago 8-10**
17:00 - 18:30	**Concurrent Sessions**	
	Liver Metastases (Colon) Tumor Board and Live Case from the Medical College of Wisconsin Moderators: Daniel B. Brown, MD and Michael C. Soulen, MD Speakers: Giammaria Fiorentini, MD, David C. Madoff, MD, Mary Mulcahy, MD, Constantinos T. Sofocleous, MD, PhD, Luigi Solbiati, MD, Speaker TBD	**Chicago 6**

FRIDAY, 15 JUNE 2012		Room
17:00 - 18:30	**Abstract Presentations - Basic Science and Technology**	**Chicago 7**
17:00 - 17:08	Paper 32: **Intravenous Vasopressin for the Prevention of Non-Target Gastrointestinal Embolization During Liver Directed Cancer Treatment: Experimental Study in a Porcine Model** **J.C. Durack**[1], T.A. Hope[2], M.W. Wilson[2], M. Saeed[2], R.K. Kerlan[2], E.J. Ring[2] *[1]Memorial Sloan-Kettering Cancer Center, New York, New York, USA, [2]University of California, San Francisco, San Francisco, California, USA*	
17:08 - 17:16	Paper 33: **Percutaneous Cryoablation for Pancreatic Cancer: Feasibility and Safety Assessment** **L. Niu**, L. He, L. Zhou, B. Wu, J. Zuo, K. Xu *GIHB Affiliated Fuda Hospital Oncology, Chinese Academy of Sciences, Guangzhou, China*	
17:16 - 17:24	Paper 34: **A Novel Method for Bone Tumor Radiofrequency Ablation** **M. Gofeld**[1], A. Yee[2] , J. Woo[3], C. Whyne[3], M. Akins[3] *[1]University of Washington, Seattle, Washington, USA, [2]University of Toronto, Toronto , Ontario, Canada, [3]Orthopaedic Biomechanics Laboratory, Sunnybrook Research Institute, Toronto , Ontario, Canada*	
17:24 – 17:32	Paper 35: **Effect of Irreversible Electroporation (IRE) on Bile Ducts Following Treatment of Primary and Metastatic Liver Tumors – A Single Center Retrospective Analysis** G. Narayanan, V. Sarode, K.J. Barbery, G. Guerrero, **G. Mohin** *University of Miami, Miami, Florida, USA*	
17:32 - 17:40	Paper 36: **Anti-vascular Ultrasound: Validation of Treatment Effects with Contrast-enhanced Ultrasound, Dynamic Contrast-enhanced Magnetic Resonance Imaging and Histopathology** **S. Hunt**, M.C. Soulen, C. Sehgal *Hospital of the University of Pennsylvania, Philadelphia, Pennsylvania, USA*	
17:40 - 17:48	Paper 37: **The Impact of Variation in Portal Venous Blood Flow on the Size of the Radiofrequency and Microwave Ablation Lesions in In-Vitro Blood Perfused Bovine Livers** **G.D. Dodd**, N.A. Dodd, A.C. Lanctot *UCDenver HSC SOM , Aurora, Colorado, USA*	
17:48 - 17:56	Paper 38: **Cooled Dual-Slot Microwave Antenna Optimization to Create More Spherical Ablation Zones** **J. Chiang**, K. Hynes, M. Bedoya, C. Brace *University of Wisconsin, Madison, Wisconsin, USA*	

17:56 - 18:04	Paper 39: **Tumor Volume Comparison Between Semi-Automatic Tumor Segmentations on CBCT and MDCT, and Pathologic VX2 Rabbit Hepatic Tumor Model** **O. Pellerin**, M. Lin, N. Bhagat, J.H. Geschwind *Johns Hopkins Hospital, Baltimore, Maryland, USA*	
18:04 - 18:12	Paper 40: **Pathologic Cancer Staging by Measuring Cell Growth Energy** **E.Y. Moawad** *Ain -Shams University Graduated, Cairo, Egypt*	
18:12 - 18:20	Paper 41: **ZBP-89 is Required for p21Waf1-Mediated Apoptosis in Hepatocellular Carcinoma** **G.G. Chen**, C.Z. Zhang, S. Chun, P.B. Lai *The Chinese University of Hong Kong, Hong Kong*	
18:20 - 18:28	Paper 42: **Nanocytomics-Based Assessment of Transcriptional Activity of Malignant/Premalignant Cells** **A.K. Tiwari**[1], H. Roy[2], H. Subramanian[3], V. Backman[3] *[1]Michigan State University, East Lansing, Michigan, USA, [2]NorthShore University HealthSystem, Evanston, Illinois, USA, [3]Northwestern University, Evanston, Illinois, USA*	
18:30 - 19:30	**Poster Hall Reception**	**Riverside B**
18:30 - 20:00	**Medical Student/Resident Symposium: Introduction to Interventional Oncology** Moderator: Robert Lewandowski, MD Speakers: Daniel B. Brown, MD, William S. Rilling, MD	**Chicago 7**
18:30 - 20:00	**Interventional Radiology Fellows Symposium: Tips and Tricks for New Practice Development**	**Chicago 6**

Ablation/Microwave/IRE for Liver/Lung/Renal Cancers
Riccardo A. Lencioni, MD

Conventional and Drug Loaded Chemoembolization
Jeffrey F. Geschwind, MD

Adding Y90 to the Treatment Algorithm
Riad Salem, MD

Clinical Service: Putting it All Together
Michael C. Soulen, MD

SATURDAY, 16 JUNE 2012		Room
6:30 - 8:00	**Continental Breakfast**	**Chicago Pre-Function**
7:00 - 8:00	**Concurrent Workshop 1: Lung Tumor Ablation Workshop** Speakers: Robert Suh, MD and Thierry de Baere, MD	**Chicago 6**
7:00 - 8:00	**Concurrent Workshop 2: Drug Eluting Beads** Speakers: Govindarajan Narayanan, MD, Jeff Geschwind, MD, and Peter Littrup, MD	**Chicago 7**
8:00 - 9:30	**Concurrent Sessions** **Synergies** Moderator: Reed Omary, MD, MS	**Chicago 6**
8:00 - 8:15	**Isolated Liver Perfusion: Ready for Prime Time?** Bradford Wood, MD	
8:15 - 8:30	**Immunoembolization: Better than Chemo or Radioembolization for Melanoma?** Daniel B. Brown, MD	
8:30 - 8:45	**Ablation and Drugs** Riccardo A. Lencioni, MD	
8:45 - 9:00	**Combining Y90 with Sorafenib in HCC** Laura Kulik, MD	
9:00 - 9:15	**Nanotechnology** Andrew C. Larson, PhD	
9:15 - 9:30	**Kyphoplasty and Radiation** Eric Lis, MD	
8:00 - 9:30	**Abstract Presentations - Liver Metastases and Colangiocarcinoma**	**Chicago 7**
8:00 - 8:08	Paper 43: **Trans Arterial Hepatic Embolization (TACE) Adopting Polyvinal Alcohol Microspheres Preloaded with Irinotecan (DEBIRI) versus Systemic Therapy (FOLFIRI) for Liver Metastases (LM) from Colorectal Cancer (CRC): A Randomized Study of Efficacy, Toxicity and Quality of Life** **G. Fiorentini**[1], P. Coschiera[1], L. Mulazzani[1], V. Catalano[1], C. Aliberti[2], M. Cantore[3] *[1]Azienda Ospedaliera Ospedali Riuniti Marche Nord, Pesaro, Marche/PU, Italy, [2]Istituto Oncologico Veneto IRCCS, Padova, Veneto/PD, Italy, [3]ASL 1 Massa Carrara, Carrara, Toscana/MS, Italy;*	
8:08 - 8:16	Paper 44: **Transarterial Chemoembolization for Metastatic Colorectal Liver Metastases Using M1 DC Beads®: Initial Experience** **A. Farghal**, T. Cabrera, D. Valenti, *McGill University, Montreal, Quebec, Canada*	

8:16 - 8:24 Paper 45: **The Use of Therasphere in Metastatic Liver Tumors: Risk Factors Associated with Poor Prognosis**
D. Conners, J. Zechlinski, S.B. White, R.A. Hieb, P.J. Patel, W.S. Rilling
Medical College of Wisconsin, Milwaukee, Wisconsin, USA

8:24 - 8:32 Paper 46: **Percutaneous Microwave Ablation with High-Powered, Gas-Cooled Antennas: Short-Term Results in 52 Patients**
T. Ziemlewicz, J. Hinshaw, M. Lubner, C. Brace, S. Wells, F.T. Lee
University of Wisconsin, Madison, Wisconsin, USA

8:32 - 8:40 Paper 47: **Phase II Clinical Trail of Yttrium-90 Resin Microspheres for the Treatment of Metastatic Neuroendocrine Tumor**
J.H. McElmurray, P.R. Bream, E. Grzeszczak, S.G. Meranze, I.D. Feurer, J.D. Berlin
Vanderbilt University Medical Center, Nashville, Tennessee, USA

8:40 - 8:48 Paper 48: **Differential Response to Radioembolization for Colorectal Cancer Metastases to the Liver in KRAS Mutant Patients**
D. Coldwell, **M. Schacht**, V. Sharma
University of Louisville, Louisville, Kentucky, USA

8:48 - 8:56 Paper 49: **Prognostic Factors of Resin-Based Yttrium-90 Radioembolization for Unresectable Metastatic Neuroendocrine Tumors**
E.B. McIntosh, H.J. Prajapati, T.O. Lawal, H.S. Kim, B.F. El-Rayes, J.S. Kauh
Emory University School of Medicine, Atlanta, Georgia, USA

8:56 - 9:04 Paper 50: **Single Center Experience with GlassBbased Yttrium 90 Embolization in Neuroendocrine Liver Metastases**
B. Arslan[1], A. Sardari[2], J. Sweeney[2], B. Biebel[2], J. Choi[2], R. Shridhar[2]
[1]Rush University Medical Center, Chicago, IL, USA, [2]Moffitt Cancer Center, Tampa, Florida, USA

9:04 - 9:12 Paper 51: **Local Control of Focal Hepatic Malignancies Treated with Microwave Ablation with a High-Power Applicator System in 165 Patients**
T. Tondolo[1], L. Cova[1], G. Mauri[1], T. Ierace[1], **L. Solbiati[1],** S. Goldberg[2]
[1]General Hospital of Busto Arsizio, Busto Arsizio, Italy, [2]GHadassah University Hospital, Jerusalem, Israel

9:12 - 9:20 Paper 52: **Yttrium-90 Radioembolization for Intrahepatic Cholangiocarcinoma**
S. Mouli, K. Memon, A. Riaz, R.K. Ryu, R. Salem, R.J. Lewandowski
Northwestern University Feinberg School of Medicine, Chicago, Illinois, USA

SATURDAY, 16 JUNE 2012		Room
9:20 - 9:28	Paper 53: **Yttrium-90 Radioembolization for Chemorefractory Unresectable Intrahepatic Cholangiocarcinoma (ICC): Survivals and Prognostic Factors** **H.J. Prajapati**, T.O. Lawal, E.B. McIntosh, H.S. Kim, B.F. El-Rayes, J.S. Kauh *Emory University School of Medicine, Atlanta, Georgia, USA*	
9:30 - 10:30	**Break in the Exhibit Hall**	**Chicago 8-10**
10:30 - 12:30	**Multidisciplinary State-of-the-Art: Liver Metastases (Neuroendocrine)** Moderator: Thierry de Baere, MD	**Chicago 6/7**
10:30 - 10:45	**Surgery and Ablation for NET** Rod Pommier, MD	
10:45 - 11:00	**Chemoembolization/Drug Eluting Beads** Thierry de Baere, MD	
11:00 - 11:15	**Y90 in NET** William S. Rilling, MD	
11:15 - 11:30	**Systemic Treatment for NET** Al B. Benson, III, MD, FACP	
11:30 - 12:30	**NET Tumor Board** Moderator: William S. Rilling, MD Speakers: Al B. Benson, III, MD, FACP, Thierry de Baere, MD	
12:30 - 14:00	**Lunch & Exhibits**	**Chicago 8-10**
12:30 - 13:30	**Integrated C-Arm Come Beam CT as a Routine Part of Imaging During Chemoembolization** **Industry Symposium supported by Siemens Healthcare (Non-CME)**	**Chicago 6/7**
14:00 - 16:00	**Multidisciplinary State-of-the-Art: Thoracic** Moderator: Stephen Solomon, MD and Robert Suh, MD	**Chicago 6/7**
14:00 - 14:15	**Surgical Treatment of Lung Cancer** Shari Meyerson, MD	
14:15 - 14:30	**Review of Chemotherapy for Lung Cancer** Speaker TBD	
14:30 - 14:45	**Ablation: What's New?** Robert Suh, MD	
14:45 - 15:00	**Radiotherapy: Competing or Complementary to Surgery** James Urbanic, MD	

SATURDAY, 16 JUNE 2012		Room
15:00 - 16:00	**Lung Tumor Board and Live Case from Memorial Sloan-Kettering Cancer Center** Moderator: Stephen Solomon, MD and Robert Suh, MD Speakers: Shari Meyerson, MD, James Urbanic, MD	**Chicago 6/7**
16:00 - 17:00	**Break**	**Chicago Pre-Function**
17:00 - 18:30	**Concurrent Sessions**	
	Special Topics Moderator: Debra Gervais, MD and Albert Nemcek, MD	**Chicago 6**
17:00 - 17:15	**Pleurex Catheter Placement (Abdominal/Thoracic)** Albert Nemcek, MD	
17:15 - 17:30	**Pain Management** Afshin Gangi, MD	
17:30 - 17:45	**Renal Ablation** Debra Gervais, MD	
17:45 - 18:00	**Treatment Options for Cholangiocarcinoma** Robert Lewandowski, MD	
18:00 - 18:15	**PET Guided Ablation** Paul Shyn, MD	
18:15 - 18:30	**Role of Temporary Filters in the Oncology Patient** Robert Lewandowski, MD	
18:30 – 18:45	**Academic Corner: Top 10 Recent Manuscripts All Interventional Oncologists Should Know** Reed Omary, MD, MS	
17:00 - 18:30	**Abstract Presentations - Genitourinary, Thoracic, and Novel Clinical Applications**	**Chicago 7**
17:00 - 17:08	Paper 54: **Long-Term Outcomes of Thermal Ablation for Metastatic Tumors in the Lung** **J. Meyer[1]**, J.A. Requarth[1], D. Childs[1], H. Clark[1], J.J. Urbanic[2], B. Steadman[3] *[1]Wake Forest School of Medicine, Winston Salem, NC, USA, [2]Wake Forest University Baptist Medical Center, Winston-Salem, North Carolina, USA, [3]West Virginia University, Morgantown, West Virginia, USA*	
17:08 - 17:16	Paper 55: **Factors that Influence Pneuthorax and Chest Tube Placement Following Microwave Ablation of Lung Malignancy** S. Kishore, **J.P. Erinjeri**, E. Petre, C. Sofocleous, M. Maybody, S. Solomon *Memorial Sloan-Kettering Cancer Center, New York, New York, USA*	

SATURDAY, 16 JUNE 2012		Room
17:16 - 17:24	Paper 56: **Irreversible Electroporation of Lung Metastases: Initial Experience** **T. de Baere**, J. Joskin, F. Deschamps, G. Farouil *Institut Gustave Roussy, Villejuif, France*	
17:24 - 17:32	Paper 57: **Percutaneous Irreversible Electroporation of Renal Lesions in 10 Patients** S. Barry, C. Shaw, **J.D. Meler** *Baylor University Medical Center, Dallas, Texas, USA*	
17:32 - 17:40	Paper 58: **Histological Determination of Non-Lethal Margins during Renal Cryoablation** C. Georgiades, **E.M. Azene**, C.R. Weiss, R. Rodriguez, A. Chaux, G. Netto *Johns Hopkins, Baltimore, Maryland, USA*	
17:40 - 17:48	Paper 59: **Ultrasound-Guided Percutaneous Microwave Ablation of Renal Cell Carcinoma: Intermediate-Term Results** **P. Liang** *Chinese PLA General Hospital, Beijing, China*	
17:48 - 17:56	Paper 60: **Percutaneous Cryoablation as a Follow-Up Modality for Locally Progressive RCC after Laparoscopic Partial Nephrectomy** M. Morgan, E.J. Trabulsi, C.D. Lallas, L. Pino, **D.B. Brown** *Thomas Jefferson University, Philadelphia, Pennslyvania, USA*	
17:56 - 18:04	Paper 61: **Preliminary Clinical Experience with the Use of the ExAblate® Magnetic Resonance Guided Focused Ultrasound Surgery (MRgFUS) System for Focal Treatment of Organ-Confined Low-Risk Prostate Cancer** **V.G. Turkevich**, A.K. Nosov, A.V. Mishchenko, S.A. Rozengard, S.V. Kanaev, M.S. Molchanov *Research Institute of Oncology, Saint-Petersburg, Russian Federation*	
18:04 - 18:12	Paper 62: **Percutaneous US-Guided Interstitial Laser Ablation of Metastatic Lymph Nodes in the Neck from Papillary Thyroid Carcinoma following Thyroidectomy and Lymphadenectomy** **G. Mauri**, L. Cova, T. Ierace, T. Tondolo, L. Solbiati *General Hospital of Busto Arsizio, Busto Arsizio, Varese, Italy*	
19:00 - 20:30	**Nexacar® (sorafenib) in the Treatment of Patients with Unresectable Hepatocellular Carcinoma (HCC) Open Gallery Reception** **Industry Symposium supported by Onyx Pharmaceuticals (Non-CME)**	**Superior**

SUNDAY, 17 JUNE 2012		Room
6:30 - 8:00	**Continental Breakfast**	**Chicago Pre-Function**
8:00 - 9:00	**Hands-On Workshop: Tumor Ablation (Non-CME)** Speakers: Riccardo Lencioni, MD and Debra Gervais, MD	**Superior**
9:00 - 1:00	**Symposium on Interventional Techniques, How I Do it: Top 10 Clinical Pearls You Should Know**	**Chicago 6/7**
9:00 - 9:20	**Lung Ablation** Stephen Solomon, MD	
9:20 - 9:40	**Liver Ablation** Riccardo A. Lencioni, MD	
9:40 - 10:00	**Renal Ablation** Debra Gervais, MD	
10:00 - 10:20	**Chemoembolization** William S. Rilling, MD	
10:20 - 10:40	**Drug Loaded Microspheres** Jeffrey F. Geschwind, MD	
10:40 - 11:00	**Radioembolization** Riad Salem, MD	
11:00 - 11:20	**Bone Intervention** Sean Tutton, MD	
11:20 - 11:40	**Hepatic Port Placement for Infusional Therapy** Thierry de Baere, MD	
11:40 - 12:00	**Bland Embolization** Karen T. Brown, MD	
12:00 - 12:20	**Clinical Management of the Oncology Patient: General Principles** Michael C. Soulen, MD	

Exhibitors

Activiews, Inc.
591 North Ave
Wakefield, Massachusetts 01880, USA
www.activiews.com

AngioDynamics
14 Plaza Drive
Latham, New York 12110, USA
www.angiodynamics.com

AprioMed, Inc
2 Palmer Drive Suite #1
Londonderry, New Hampshire 03053, USA
www.apriomed.com

Baylis Medical Company Inc.
5959 Transcanada Highway
St-Laurent, Quebec, H4T 1A1, CANADA
www.baylismedical.com

Biocompatibles, Inc.
115 Hurley Road, Building 3
Oxford, Connecticut, 06478, USA
www.biocompatibles.com

Boston Scientific Corporation
One Boston Scientific Place
Natick, Massachusetts 01760, USA
www.bostonscientific.com

BSD Medical Corporation
2188 West 2200 South
Salt Lake City, Utah 84119, USA
www.bsdmedical.com

CeloNova Biosciences Inc.
18615 Tuscany Stone Ste 100
San Antonio, Texas 78258, USA
www.celonova.com

CIVCO Medical Solutions
102 1st St. South
Kalona, Iowa 52247, USA
www.civco.com

Cook Medical
750 Daniels Way
Bloomington, Indiana 47404, USA
www.cookmedical.com

Covidien
5920 Longbow Drive
Boulder, Colorado 80301, USA
www.covidien.com

Delcath Systems, Inc.
810 Seventh Avenue, Suite 3500
New York, New York 10019, USA
www.delcath.com

DFINE
3047 Orchard Parkway
San Jose, California 95134, USA
www.dfineinc.com

Elsevier
1600 John F. Kennedy Boulevard
Philadelphia, Pennsylvania 19103, USA
www.us.elsevierhealth.com

Galil Medical
4364 Round Lake Road West
Arden Hills, Minnesota 55112, USA
www.galilmedical.com

Guerbet LLC
1185 W 2nd St
Bloomington, Indiana 47403, USA
www. guerbet.com

HealthTronics/Endocare
9825 Spectrum Drive, Bldg. 3
Austin, Texas 78717, USA
www.healthtronics.com

HS Medical Inc.
4521 N Dixie Hwy
Boca Raton, Florida 33432, USA
www.hsmedicalinc.com

INTIO
325 Interlocken Parkway, Building C
Broomfield, Colorado 80021, USA
www.intio.us

iSYS Medizintechnik GmbH
Bergwerksweg 21
Kitzbuhel, 6370, AUSTRIA
www.isys.co.at

MedWaves, Inc.
16760 W Bernardo Drive
San Diego, California 92127, USA
www.medwaves.com

Merit Medical/BioSphere Medical
1600 West Merit Parkway
South Jordan, Utah 84095, USA
www.merit.com

Exhibitors

Microsulis Medical Ltd
Units 1-2 Parklands Business Park, Denmead
Portsmouth, P076XP, UNITED KINGDOM
www.microsulis.com

NeoRad
Parkview 53B
Oslo NORWAY 0256
www.neorad.no

NeuWave Medical, Inc.
3529 Anderson Street
Madison, Wisconsin 53704, USA
www.neuwavemedical.com

Nordion
447 March Rd.
Ottawa, Ontario K2K 1X8, CANADA
www.therasphere.com

Onyx Pharmaceuticals
249 E. Grand Avenue
South San Francisco, California 94080, USA
www.onyx.com

Perfint Healthcare Pvt. Ltd
M2D2 Center 600, Suffolk Street, I Floor
Lowell, Massachusetts 01854, USA
www.perfinttech.com

Philips Healthcare, North America
22100 Bothell Everett Highway
Bothell, Washington 98021, USA
www.healthcare.philips.com

Sirtex Medical Inc.
300 Unicorn Park Drive
Woburn, Massachusetts 01801, USA
www.sirtex.com
www.facebook.com/SIRSpheresmicrosphere

Society of Interventional Radiology
3975 Fair Ridge Drive, Suite 400N
Fairfax, Virginia 22033, USA
www.SIRweb.org

Surefire Medical Inc.
8601 Turnpike Drive, Suite 206
Westminster, Colorado 80031, USA
www.surefiremedical.com

Veran Medical
1908 Innerbelt Business Center Drive
St. Louis, Missouri 63114, USA
www.veranmedical.com

SAVE THE DATES

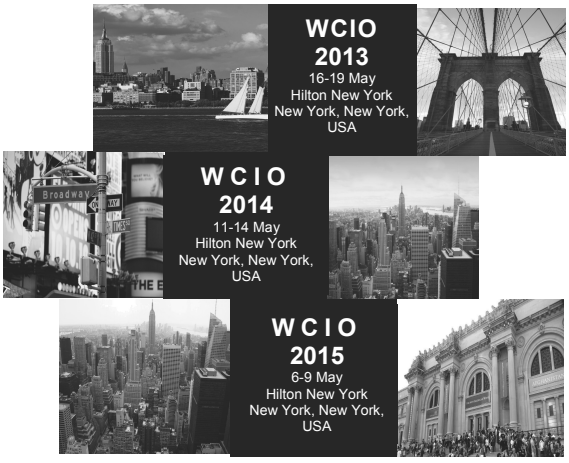

Thank you for joining us at WCIO 2012. We look forward to seeing you at these upcoming WCIO meetings!

Exhibitor Booths

Exhibitor	Booth #
Activiews, Inc.	219
AngioDynamics	206
AprioMed, Inc	312
Baylis Medical Company Inc.	113
Biocompatibles, Inc.	115
Boston Scientific Corporation	221
BSD Medical Corporation	216
CeloNova Biosciences, Inc.	103
CIVCO Medical Solutions	203
Cook Medical	217
Covidien	119
Delcath Systems, Inc.	101
DFINE	105
Elsevier	314
Galil Medical	214
Guerbet LLC	308
HealthTronics/Endocare	209
HS Medical Inc.	205
INTIO	215
iSYS Medizintecnik GmbH	213
Medwaves, Inc.	218
Merit Medical/BioSphere Medical	109
Microsulis Medical Ltd	202
NeoRad	304
NeuWave Medical, Inc.	201
Nordion	208
Onyx Pharmaceuticals	200
Perfint Healthcare Pvt. Ltd	207
Philips Healthcare, North America	212
Sirtex Medical Inc.	220
Society of Interventional Radiology	306
Surefire Medical Inc.	107
Veran Medical	302

Exhibit Hall Map

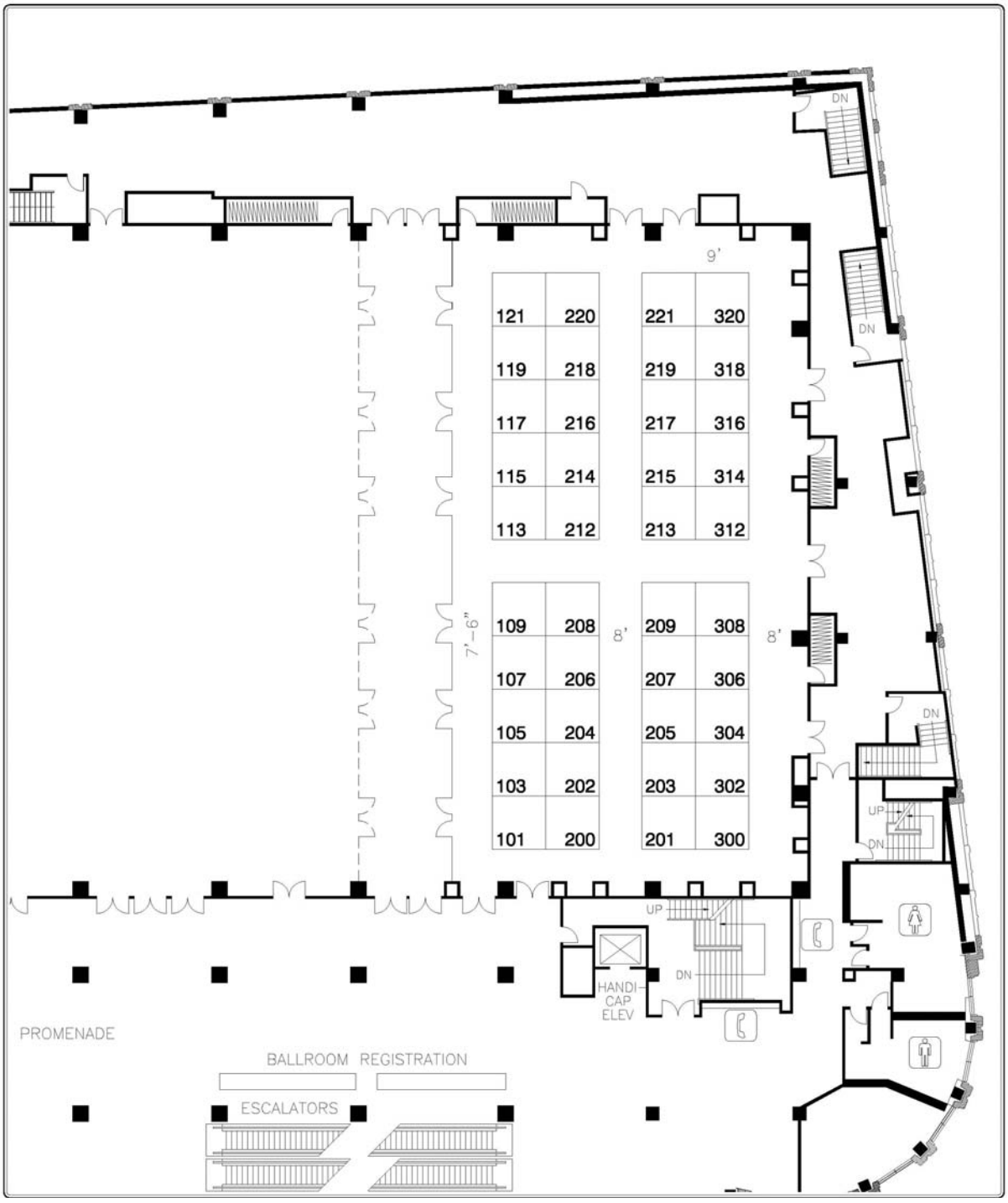

World Conference on Interventional Oncology (WCIO) 2012

June 14-17, 2012, Chicago, Illinois

Paper 1: Survival in Patients with Hepatocellular Carcinoma: Improvements in Locoregional Therapy and Multidisciplinary Approach Over Two Decades at a Single Institution

T.O. Lawal, J.R. Spivey, S.I. Hanish, B.F. El-Rayes, D.A. Kooby, H.S. Kim

Objectives: This study explores the therapy trends and effect multidisciplinary approach to hepatocellular carcinoma (HCC). Furthermore, the utilization and survival outcomes of locoregional therapy (LRT) as a first-course treatment for HCC over a span of 2 decades at a single academic tertiary cancer center are investigated.
Methods: Patients diagnosed with HCC who received first-course cancer treatment at a single institution between 1991 and 2010 were included in the study. The hospital-wide cancer registry was used to collect first-course treatment plan along with laboratory and clinical data. Patients were divided into 2 groups based on the year of diagnosis (Group 1: 1991-2000 and Group 2: 2001-2010). Kaplan Meier method was used for survival analysis, and survival curves were compared using the log rank test.
Results: A total of 961 patients were included in the study period. 74% were male, 68% were white, and the mean age at diagnosis was 60 ±11.3 years. Group 1 (1991-2000) consisted of 265 patients, and Group 2 (2001-2010) consisted of 696 patients. The median overall survival of Group 1 was 7 months compared to 26 months in Group 2 ($p<0.0001$). The percentage of patients receiving first-course LRT increased 6-fold between the 2 decades (4 vs 36% in Groups 1 and 2, respectively). Other treatments were as follows: radiation (2 vs 1%), chemotherapy (16 vs 3%), resection (20% vs 17%), and transplantation (3 vs 19%), respectively. 55% and 24% of the patients in Groups 1 and 2 received no identifiable treatment at our institution. The median overall survival of patients receiving LRT increased by 14 months (12 vs 26 months in Groups 1 and 2, respectively; $p<0.0001$). Other survival changes were as follows: radiation (7 vs 7 months), chemotherapy (7 vs 8 months), and resection (33 vs 44 months) ($p<0.0001$). The median survival for patients receiving no identifiable treatment was 4 months in Group 1 vs 5 months in Group 2. The median survival for transplantation could not be calculated as greater than 50% of the patients are still living.
Conclusions: There has been a significant increase in HCC patients' overall survival within the last 2 decades. Additionally, there has been an increase in the utilization of LRT as the first-course treatment for HCC and a corresponding improvement in survival when compared to changes seen in other cancer therapies. These measures both reflect a shift to a multidisciplinary liver cancer approach and advances in therapeutic and technical delivery of LRT over the previous 2 decades.

Paper 2: Review of Unusual Arterial Supply to Liver Tumors and its Impact on Transarterial Therapies

P. Dalvie, O. Ozkan, J. McDermott

Objectives: 1. To review normal and variant hepatic arterial supply and its impact on trans-arterial therapies. 2. To demonstrate treatment options in tumors with extra-hepatic arterial supply. 3. Discuss management of challenging vascular cases (such as celiac stenosis, large arterio-venous shunts, etc.) encountered during trans-arterial treatments.
Methods: Case studies are used along with a literature review to demonstrate techniques for safely performing trans-arterial chemotherapy and radio-embolization in patients with primary and secondary liver tumors with variant arterial supply, parasitization of extra-hepatic supply by liver tumors and challenging acquired vascular problems. Techniques described include superselective treatments using a hybrid CT/angiographic suite, redistribution of blood flow by arterial embolization and treatment through collateral pathways.
Results: Transarterial chemotherapy and radioembolization are safe and viable treatment options in patients with non standard arterial supply with the use of modified angiographic techniques.
Conclusions: With an increasing incidence of primary and secondary liver tumors, more challenging cases will be encountered for loco-regional treatments. A good knowledge of variant supply, extra hepatic arterial supply and collateral pathways along with options for modifying treatment strategies in this subgroup of patients is critical for ensuring safe and effective treatment.

Paper 3: Comparison of Survival Outcome in Patients with Unresectable Hepatocellular Carcinoma Treated with Triple Drug TACE and TACE with Doxorubicin Loaded LC-Beads

A.S. Gomes, C.D. Britten, R.S. Finn, S. Sadeghi, P.A. Monteleone, J.W. Sayre

Objectives: The purpose of this study is to describe overall survival outcome in patients with unresectable HCC treated with two different transcatheter arterial chemoembolization (TACE) regimens.
Methods: One group (N=113) was treated with Doxorubicin loaded LC beads and their survival outcome compared to a second group of historical controls (N=124) treated with triple drug therapy using doxorubicin-ethiodol, cisplatin and mitomycin, and particulate embolic (Avitene or Embospheres). The patients represent a single center experience from 1994-2009, with implementation of a single drug regimen employing doxorubicin loaded LC beads in 2005. The patient selection criteria for TACE were uniform over this period. All patients were followed for a minimum of 12 months in the LC Bead group and for a minimum of 48 months in the Triple Drug group. Kaplan-Meier survival curves were used with the log rank (Mantel Cox) test for differences.
Results: In the Triple Drug TACE group mean survival at 60 months was 22.17 + 2.07 mos (SE) median survival 15.75 + 4.11 mos. In the single drug doxorubicin loaded LC Beads group, mean survival was 19.46 + 1.96 mos. and median survival 13.6 + 2.18 mos. There was no significant difference in survival between the two groups at 60 months ($p=0.78$). Complications occurred in 12.9% of the Triple Drug group and 7.6% of the doxorubicin loaded LC Bead group. Thirty day mortality was 2.4% in the Triple Drug group and 1.8% in the LC Bead group.
Conclusions: In this interim analysis there is no significant difference in overall survival in patients with unresectable HCC treated with triple drug TACE as compared to treatment with single drug doxorubicin loaded LC beads.

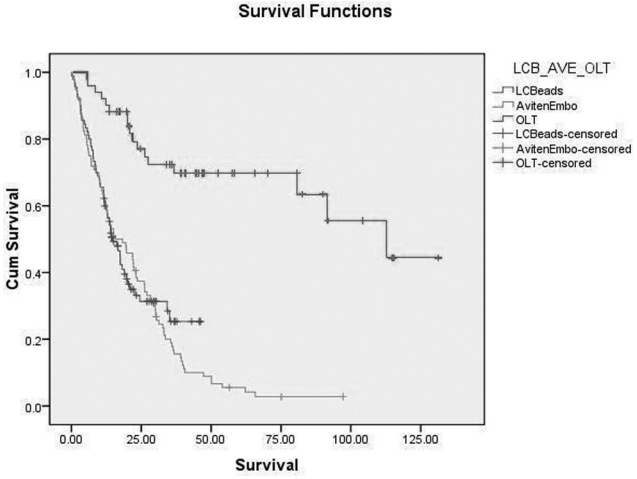

Paper 4: Contrast Trapping in Hepatocellular Carcinoma on Non-Contrast CT after Chemoembolization with Drug Eluting Beads May Predict Tumor Response

Y.S. Golowa, P. Golshani, M. Abrams, M. Jagust, J. Cynamon

Objectives: To correlate the amount of contrast trapping seen on non-contrast CT performed immediately after chemoembolization of HCC with DEB with the amount of tumor coagulation necrosis on follow up imaging.
Methods: 30 patients with 46 previously untreated lesions which were diagnosed as HCC using AASLD criteria were treated with chemoembolization with DEB (LC beads mixed with doxorubacin and iodinated contrast). CT was performed in immediately post procedure (within 1 to two hours) to assess for trapping of contrast within the targeted lesion. Contrast trapping pattern on post procedure CT was classified as completely dense (CD), partially dense (PD) or not dense (ND) by correlating enhancement of tumor on pre-procedure imaging with trapping of contrast in the lesion on post-procedure non-contrast CT. If more than 70% of the lesion trapped contrast, it was graded as CD; less than 70%, then PD; and if the lesion did not trap contrast, then ND. Post procedure CT was compared with follow up imaging to assess for the amount of tumor coagulation necrosis after chemoembolization. Follow up imaging was graded as complete necrosis (CN) if there was less than 30% residual enhancing tissue compared with pre procedure imaging, partial necrosis (PN) if 30% or more of the lesion demonstrates enhancement and no necrosis (NN) if there is persistent complete enhancement of the lesion on follow up imaging.
Results: On post chemoembolization CT, of the 46 lesions embolized, 28 were CD, 14 were PD and 4 were ND. Of the CD 89.3% (n=25) had CN; 7.1% (n=2) had PN and 3.6% (n=1) had NN. Of the PD 7.1% (n=1) had CN 78.6% (n=11) had PN and 14.3% (n=2) had NN. Of the NR lesions, 0% had CN; 0% had PN and 100% had NN.
Conclusions: Focal trapped contrast is seen in HCC on non-contrast CT performed immediately after chemoembolization with DEB while sparing normal liver. Contrast is likely trapped within the tumor by DEB which is injected at the same time. Retained contrast on CT may serve as a surrogate marker of DEB within the targeted tumor. In this cohort, the amount of contrast trapped in the lesion as seen on post-procedure CT correlates with tumor coagulation necrosis on follow up imaging. The observation of contrast trapping on post chemoembolization CT may help predict effectiveness of therapy immediately after procedure. Further study with a larger cohort would be necessary to confirm this preliminary finding.

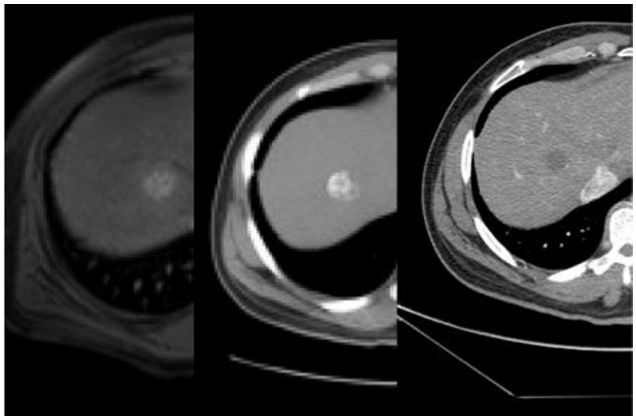

From left to right; Imaging before chemoembolization shows enhancing lesion, non-contrast CT after chemoembolization with DEB shows trapped contrast in lesion in complete dense pattern, follow up imaging shows complete necrosis.

	Complete dense (CD) n=28	Partial Dense (PD) n=14	Not Dense (ND) n=4
Complete Necrosis (CN)	25	1	0
Partial Necrosis (PN)	2	11	0
No Necrosis (NN)	1	2	4

Paper 5: Efficacy of Radiofrequency Ablation and Drug Eluting Beads Transarterial Chemoembolization in Treating Hepatoma

G. Narayanan, S. Naidu, K. Pereira, V. Sarode, K.J. Barbery, T. Froud

Objectives: To retrospectively evaluate the safety and efficacy of combination treatment of hepatocellular carcinoma (HCC) using radiofrequency ablation (RFA) followed with Drug Eluting Beads Transarterial Chemoembolization (DEBTACE) within 24 hours.
Methods: Between May 2008 and November 2011, 17 patients (2F, 15M) with 20 lesions underwent the combination treatment. Results were analyzed retrospectively in this HIPAA compliant study. Percutaneous RFA was performed under general anesthesia with CT guidance, using Leveen probes. DEBTACE was performed using 100-300 micron and 300-500 micron LC beads for a total doxorubicin dose of 150mg. Mean patient age 63 ± 8 yrs (range 47-81). Mean tumor size was 4.2 cm (range 1.7-7.0). Mean duration of follow up was 336 days (range 14-838). Safety was evaluated with tolerance of the procedure and frequency of complications during the first 30 days post procedure including liver function. Efficacy was evaluated using mRECIST criteria on triple phase CT. Tumor burden was also assessed using Alpha fetoprotein (AFP) levels.
Results: The combination treatment was tolerated by all patients. Procedure related complications included local pain (n=3), bleed (n=1). All lesions were successfully treated, complete response n=17, partial response n=3 at 30 days post procedure (n=20). Three patients were down-staged to transplant. During follow up, 4 patients demonstrated local recurrence, mean time to recurrence 248 days (range 28-81. Progressive disease was seen in 6 patients, mean time to progression 259 days (range 30-838). 13/17 patients (76.4%) demonstrated AFP reduction, mean 70% (range 15-99), 4/17 patients (23.5%) demonstrated AFP elevation mean 44% (range 15-97). One patient died 40 days post procedure.
Conclusions: Combination treatment with RFA/DEBTACE is a safe and effective method of treating hepatocellular carcinoma and may be a means of treating patients with larger lesions that cannot be effectively treated with either modality alone. Randomized trials are required to further validate results.

Paper 6: Combined Radiofrequency Ablation and Ethanol Injection with a Multi-Pronged Needle for the Treatment of Medium and Large Hepatocelluar Carcinoma

X. Xie, M. Kuang, M. Lu

Objectives: To evaluate the efficacy and safety of combined radiofrequency ablation (RFA) and ethanol injection with a multi-pronged needle in the treatment of medium (3.1-5.0 cm) and large (5.1-7.0 cm) hepatocellular carcinoma (HCC).
Methods: 50 patients (mean age, 55.3 years; age range, 30-81 years) with a total of 52 (3.1-7.0 cm) HCC nodules were enrolled in this prospective study. The longest and shortest diameter of the tumors was 3.8 ± 0.8 cm and 3.1 ± 0.7 cm. All of them received the treatment of combined RFA and ethanol injection with a multipronged needle percutaneously. Initial tumor response was assessed on 1-month CT scans by using modified Response Evaluation Criteria in Solid Tumors (mRECIST) for HCC. Follow-up protocol included imaging examinations at 3-month intervals.
Results: The average volume of injected ethanol was 14.4 ± 4.3 ml (range, 9-30 ml). The average number of RFA electrode insertions was 1.8 ± 0.8 (range, 1-4). The mean size of the ablation zone was 5.1 ± 0.9 cm (range, 2.9 - 6.7 cm) × 4.2 ± 0.8 cm (range, 3.6 - 8.6 cm). The rate of initial local complete response (CR) according to mRECIST was 94.2% (49/52). After additional treatment, technical success was achieved in all (100%) HCC nodules. After a mean follow-up period of 15.6 ± 5.3 months (range, 6.5-25.0 months), local tumor progression was observed in 7 (13.5%) of the 52 tumor nodules with CR. Therefore, the rate of sustained local CR was 86.5% (45/52). Distant recurrence developed in 38% (n=19) of patients. There were no treatment-related deaths, and the major complications were observed in 3 (6%) patients (1 liver abscess, 1 massive hemoperitoneum, 1 masssive ascites due to liver function damage). Minor complication included asymptomatic intraabdominal hemorrhage (n = 4), pleural effusion (n = 1), and bilomas secondary to bile duct damage (n = 2). The 1-year and 2-year survival rates were 90.8% and 88.1%, respectively.
Conclusions: The combination of RFA and ethanol injection with a multipronged needle in the treatment of medium and large HCC is safe and effective. It can provide a high rate of local tumor control for the treatment of patients with medium and large size HCC.

Paper 7: Studies on the Feasibility of Radiofrequency Ablation in Treatment of Advanced Hepatocellular Carcinoma

M. Chen, J. Wu, W. Yang, W. Wu, K. Yan

Objectives: To investigate the feasibility of radiofrequency ablation (RFA) in treating with advanced hepatocellular carcinoma (HCC) by applying standard treatment strategies in the ultrasound-guided percutaneous RFA.
Methods: 655 patients with unresectablely advanced HCC underwent percuatenous RFA therapy and 92 patients with 136 tumors among them were enrolled into the study. According to the 6th UICC/AJCC-TNM system, 82 patients with 126 tumors and 10 patients with 10 tumors were in stage III and IV, respectively. The tumor size ranged from 1.5 to 8.0 cm (Average, 4.5 cm). 59 patients had solitary tumor and the remaining 33 patients had multiple tumors (2-4 tumors). The Child-Pugh classification of A, B and C were 58,32 and 2 patients, respectively. Contrast-enhanced ultrasound (CEUS) was performed in 51 patients (55.4 %) before RFA. The standard treatment using optimal strategies were applied in 67 patients (72.8 %). The established strategies included: (1) select RFA indications based on the CEUS results; (2) design radical protocols based on invasive range showed by CEUS; (3) multiple overlapping ablations based on mathematical protocols; (4) two or three bipolar RFA electrodes with three dimensional localization; (5) color US guided percutaneous ablation of tumor feeding artery (PAA)/transcatheter arterial chemoembolization (TACE) + RFA for HCC with rich supply.The patients underwent follow-up using enhanced CT at one month, and then every

three months after RFA. The ablation was considered a success if no abnormal enhancement or wash-out was detected in the treated area on the CT scan at one month. All patients after RFA received liver protection treatments. Chi square test or Fisher's exact test were used to compare with the early complete tumor necrosis rates and the local recurrence rates. Survival was estimated by Kaplan-Meier analysis and Log-rank test. P<0.05 was considered as a statistically significant difference.

Results: Early complete tumor necrosis rate after initial RFA was 90.4% (123/136 tumors). Serious complications were developed in two patients (2.2%) and no treatment-related death occurred. 3~132 months were followed up. Local recurrence rate was 15.4% (21/136 tumors). The 1-, 3-, 5-year overall survival rates were 83.3%, 48.3%, 21.9%, respectively, and the median survival time was 35 months. By further stratified analysis, the early complete tumor necrosis rate was higher in groups of Child-Pugh A, applying CEUS and standard treatment (98.3%, 98.0% and 97.0%, respectively). And the local recurrence rate was lower in groups of applying CEUS and standard treatment (11.8% and 16.4%, respectively). 5-year survival was improved in patients with Child-Pugh A, tumors less than 3.0 cm, applying CEUS and standard treatment (P<0.05).

Conclusions: RFA treatment in advanced HCC proved to be feasible. Paying attention to apply treatment strategies and liver protection therapies in RFA can improve the survival.

Paper 8: Microwave Ablation of Hepatocellular Carcinoma: Long-Term Results in a Single Center

M. Kuang, X. Xie, M. Lin, G. Liu, Z. Xu, M. Lu

Objectives: In this single-center study, we assessed the long-term treatment results in patients with primary hepatocellular carcinoma (pHCC) and recurrent HCC (rHCC), who undergone microwave ablation (MWA).

Methods: The study was approved by the ethics committee of the hospital and all patients signed informed consent. From August 1997 to November 2006, a total of 171 patients with HCC were treated with microwave ablation. Sixty-nine patients with 99 pHCC nodules received MWA as the first-choice treatment, and 102 patients with 165 recurrent tumors after initial treatment underwent MWA. The mean diameter was 3.0±1.5 cm (range, 0.9-9.5 cm) in pHCCs and 2.6±1.5 cm (0.8-8.1 cm) in rHCCs. MWA were performed percutaneously under real-time ultrasound guidance and a 0.5 to 1 cm of safety margin was achieved. Treatment efficacy was evaluated according to the standardization terminology and reporting criteria of image-guided tumor ablation.

Results: Complete ablation was achieved in 94 (94/99, 94.9%) pHCCs and in 149 (149/165, 90.3%) rHCCs after the first-time MWA. Major complications occurred in 11 patients (6.4%), no treatment-related death was observed. Local tumor progression rates were 12% (12/99) in pHCCs and 10.3% (17/165) in rHCCs, after an average follow-up time of 53 months. The 3-year, 5-year, and 7-year disease-free survival rates were 42%, 33%, and 33% in patients with pHCC, and 16%, 13%, and 13% in patients with rHCC, respectively. Overall 3-year, 5-year, and 7-year survival rates were 58%, 45%, and 40% in patients with pHCC, and 36%, 25%, and 20% in patients with rHCC, respectively.

Conclusions: MWA is an effective treatment for HCC and could be used as an initial treatment option for pHCC.

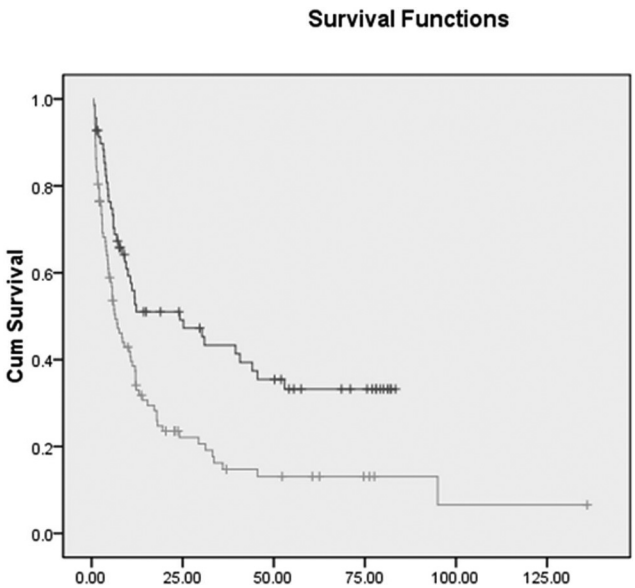

Disease-free survival curves in patients with pHCC(blue dots) and rHCC(green dots). Significant differences (P<0.05) were found between two groups.

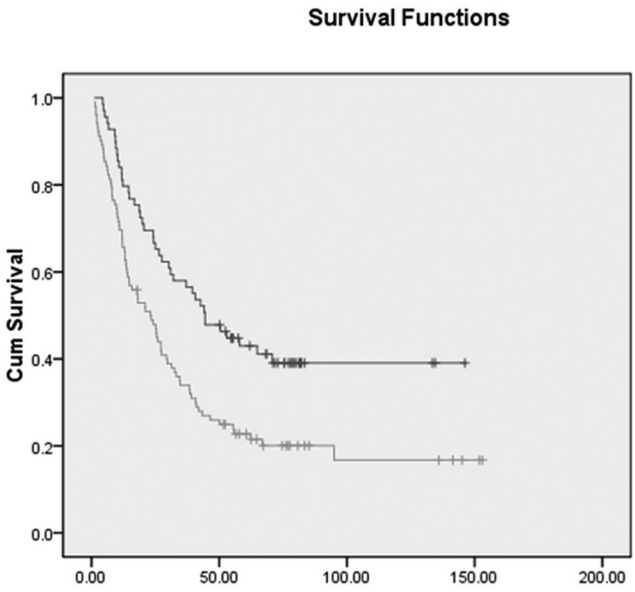

The differences in overall survivals between pHCC(blue dots) and rHCC(green dots) were significant (P<0.05).

Paper 9: Irreversible Electroporation for the Treatment of Early-Stage Hepatocellular Carcinoma: A Prospective Multicenter Phase II Clinical Trial

R. Lencioni, F. Izzo, V. Vilgrain, L. Crocetti, J. Ricke, J. Bruix

Objectives: Radiofrequency ablation (RFA) is the standard treatment for nonsurgical patients with early-stage hepatocellular carcinoma (HCC). However, its ability to achieve complete tumor eradication is dependent on tumor size and location. Irreversible electroporation (IRE) is a novel, non-thermal ablation technique that uses high-voltage DC current to induce irreversible disruption of cell membrane integrity. We conducted a phase II prospective, multicenter clinical study to evaluate the efficacy and safety of IRE as first-line nonsurgical treatment for early-stage HCC. This trial is registered with ClinicalTrials.gov, number NCT01078415.

Methods: Patients were eligible if they had Child class A cirrhosis; ECOG performance status of 0; ASA score ≤ 3; prothrombin time ratio > 50%; platelet count > 50,000 / ml; and 1- 3 HCC tumors 3 cm or less in longest diameter. Exclusion criteria included eligibility for surgical resection or transplantation; presence of vascular invasion or extrahepatic metastases; Child class B or C; and cardiac insufficiency, ongoing coronary artery disease, or arrhythmia. Eligible patients were scheduled to receive IRE as the sole anticancer therapy. The primary study endpoint was tumor response according to modified Response Evaluation Criteria In Solid Tumors (mRECIST) — as assessed by independent, central, blinded review. Secondary endpoints were safety, overall survival, and local tumor recurrence.

Results: Twenty-six patients with 29 tumors were included in the study. All patients had biopsy-proven HCC. One-month overall patient response as assessed by central readers was CR in 20/26 (77%), PR in 4/26 (15%), SD in 1/26 (4%), and PD in 1/26 (4%). On a lesion-by-lesion basis, 23 of 29 tumors (79%) were scored as having undergone CR. No 30-day mortality occurred. Major complications included hemothorax due to needle puncture of an intercostal artery and requiring drainage (n =1) and transient hepatic decompensation undergoing spontaneous resolution (n =1).

Conclusions: Early efficacy and safety data collected in the first prospective multicenter study on the use of IRE in cancer treatment are promising and suggest that IRE can be a valuable new option for unresectable HCC.

Paper 10: Radiofrequency Ablation versus Liver Resection for Elderly Patients with Hepatocellular Carcinoma (HCC) within the Milan Criteria

Z. Peng, M. Chen

Objectives: To compare the safety and efficacy of radiofrequency ablation (RFA) with liver resection (LR) in elderly patients with hepatocellular carcinoma (HCC) within the Milan criteria.

Methods: From January 2003 to January 2007, 180 elderly patients (age>65 years) with HCC within the Milan criteria were studied. As an initial treatment, 89 patients were treated by RFA and 91 patients by LR.

Results: The complication rates were significantly higher in the LR group (p<0.001). The 1-, 3-, 5- year overall survival for the RFA and LR groups were 93.2%, 71.1%, 55.2% and 88.8%, 62.8%, 51.9%, respectively (p=0.305). The 1-, 3-, 5- year recurrence-free survival for the RFA and LR groups were 84.1%, 62.7%, 35.5% and 76.7%,

39.3%, 33.1%, respectively (p=0.035). On subgroup analysis for tumor ≤3 cm, the 1-, 3-, 5- year overall survival for the RFA and LR groups were 94.2%, 82.6%, 67.5% and 90.1%, 65.0%, 55.1%, respectively (p=0.038). The corresponding recurrence-free survivals for the 2 groups were 85.5%, 69.1%, 40.7% and 82.2%, 40.1%, 31.8%, respectively (p=0.049). For tumor >3cm, the 1-, 3-, 5- year overall survival for the RFA and LR groups were 91.7%, 53.9%, 36.6% and 87.1%, 58.8%, 47.0%, respectively (p=0.543). The corresponding recurrence-free survivals for the 2 groups were 79.4%, 51.8%, 30.0% and 62.1%, 38.4%, 28.8%, respectively (p=0.356). A multivariate regression analysis showed that tumor size was a significant prognostic factor for overall survival (p=0.007).
Conclusions: RFA had better efficacy and safety than LR for elderly patients with HCC ≤3 cm.

Paper 11: Therapeutic Lymphangiography by Lymph Node Injection in the Treatment of Lymphatic Leak Secondary to Nephrectomy and Radical Lymphadenectomy: Preliminary Experience

E. Santos, K. McCluskey, F. Gomez, R. Bandi, C. Friend, A. Zajko

Objectives: To present the efficacy of therapeutic lymphangiography via a groin lymph node injection to treat lymphatic leakage after radical nephrectomy with retroperitoneal lymphadenectomy when conservative treatment has failed.
Methods: Two female patients (56 and 79 year old), one with metastatic breast carcinoma and one with a left renal cell carcinoma, underwent left radical nephrectomy associated with lymphadenectomy. After the sugery, both patients developed a high output chylous leak, one patient developed a left chylothorax with a small retroperitoneal collection and the other patient had a large left retroperitoneal lymphatic collection. One patient was treated with bowel rest and both patients a catheter drainage was placed within the chyolus collections. After 2 weeks and 9 months, respectively, of failed conservative treatment, the patients underwent therapeutic lymphangiography by lymph node injection. Under ultrasound guidance, a 25 gauge needle was inserted within the hilum of a left groin lymph node and 6-9 ml of lipiodol was injected. Fluoroscopy was used to track the filling of the pelvic lymph nodes and identify the level of the leak. A CT scan of the abdomen was also performed to confirm the leak. Therapeutic success was considered when the catheter drainage output was less than 20 cc in 24 hours.
Results: The procedure was succesfully performed in both patients. In one patient the level of the leak was not visualized. In the other patient, the leak was identified at the left para aortic region. Lipiodol extravasation was seen within the retroperitoneal collection at the L3-L4 intervertebral disc space. The lymphatic leaks were progressively diminishing and the drainage catheters were removed after 8 and 24 days of the lymphangiography, respectively, when the output was less than 20 cc per day.
Conclusions: Therapeutic lymphangiography by lymph node injection is an effective technique in the treatment of lymphatic leaks secondary to radical nephrectomy associated with lymphadenectomy. Lymphangiography through a lymph node can avoid the traditional pedal lymphangiography.

Paper 12: US-Guided Fiducial Placement before Targeted Radiation Therapy for Prostate Cancer

J. Rosenbaum, W. Chong, M. Kably, J. Salsamendi, G. Narayanan

Objectives: To determine the technical feasibility and safety profile of implanting fiducial markers in the prostate under trans-rectal ultrasound guidance before undergoing IMRT.
Methods: We performed a retrospective review of 35 patients (mean age= 61.9 ± 6.7) from 2010 to 2012 who underwent fiducial marker placement under trans-rectal ultrasound guidance. We evaluated patient demographics, immediate and delayed outcomes, correct placement of markers and complications from the procedure. An ultrasound transducer fitted with a needle driver was used for insertion of gold markers into the prostate.
Results: We successfully implanted four fiducial markers in all patients, with one requiring an extra marker due to asymmetrical enlargement of the prostate. Two patients had the fiducial markers implanted in the prostatic bed due to previous prostatectomy. One patient had prior cryosurgery. There were only two complications: one patient had a small hemorrhage within the prostate and another experienced nausea. Subsequent imaging showed that none of the patients had migration of the markers. All patients successfully underwent radiation therapy.
Conclusions: Trans-rectal ultrasound guided implantation of fiducial markers is a technically feasible method for marker placement within the prostate. The procedure was well tolerated and demonstrated a good safety profile. Our experience can serve as guide to interventional radiologists for performing this relatively simple procedure in an efficacious manner.

Paper 13: Result of Treatment Painful Bone Metastases with Magnetic Resonance Guided Focused Ultrasound

V.G. Turkevich, V.V. Savelyeva, I.V. Dunaevsky, P.I. Krzhivitsky, S.V. Kanaev

Objectives: Magnetic Resonance guided Focused Ultrasound Surgery (MRgFUS) is an innovative technology combining non-invasive deposition of high intensity focused ultrasound energy into a specified target inside the body, with high-resolution Magnetic Resonance Imaging (MRI) guidance and real-time thermal feedback. This unique combination enables precise treatment planning, targeting, and conduction with continuous control for case-specific customization. We present the results of a clinical trial conducted in our facility. The main objective of the trial was to evaluate safety and effectiveness of MRgFUS treatment of pain caused by bone metastases.
Methods: 31 patients with painful bone metastases were treated with MRgFUS by the ExAblate® system (InSightec, Haifa, Israel) at Petrov Research Institute of Oncology, St. Petersburg, Russia. Immediately after procedure patients were examined for any adverse events and after a brief recovery discharged. Patients were followed up on 1 and 3 days, 1 and 2 weeks, 1, 2 and 3 months post treatment. During each visit, treatment safety was evaluated by recording and assessment of device or procedure related adverse events. Effectiveness of palliation was evaluated using the standard pain scale (0-no pain/10-worst pain imaginable) and by monitoring changes in the intake of pain-relieving medications. A reduction of 2 points or more on pain scale was considered a significant response to treatment. 17 patients were male and 14 female. Mean age was 55 years old (19-76). The primary cancers were: 19 breast, 4 stomach, 2 bronchus, 2 bladder, 4 other. Targeted lesions were 14 osteolytic, 8 osteoblastic and 9 mixed. 23 were pelvis metastases, 4 were located in the humerus bone and 4 were located in the ribs.
Results: No significant device or procedure related adverse events were recorded. 3 patients died during the follow-up period due to disease progression, thus 3 months follow-up data includes only results of 28 patients. All patients reported significant improvement in pain with no change in their medication intake. Mean worst pain score at baseline, 1 day, 3 days, 1 week, 2 weeks, 1, 2 and 3 months post-treatment was 6.9, 6.1, 5.1, 3.5, 2.6, 1.8, 1.2 and 0.9, respectively.
Conclusions: MRgFUS can provide effective, safe and noninvasive palliative therapy for patients suffering from painful bone metastases. The ability to achieve rapid pain relief after only one treatment session, combined with the high safety profile of the procedure implies that MRgFUS has a significant potential for patients suffering from painful bone metastases.

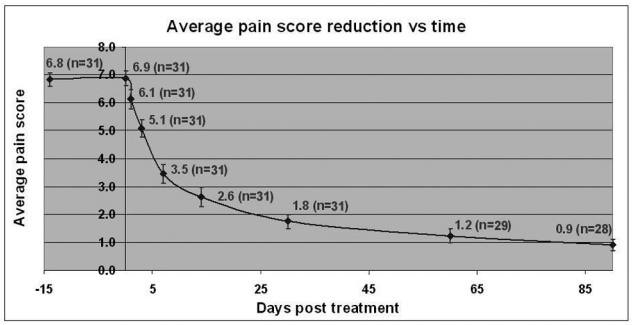

Paper 14: Image Guided Displacement of Organs at Risk Prior to Stereotactic Body Radiation Therapy Minimizes Toxicity and Facilitates Dose Escalation

M. Maybody, Y. Yamada, J.P. Erinjeri, W. Alago, R.H. Thornton, S. Solomon

Objectives: Several techniques such as inverse treatment planning, image guidance and reproducible patient immobilization have dramatically improved safe delivery of high dose stereotactic body radiotherapy (SBRT). However, the anatomic proximity of critical organs at risk (OAR) remains a significant challenge to effective dose delivery to the planning target volume (PTV). In tumor ablation studies, several techniques such as injection of buffers and utilization of drainage catheters and balloons have been successfully used to displace non-target organs in order to prevent thermal injury. We applied these organ displacement techniques to OAR during SBRT to minimize toxicity and facilitate dose escalation. The feasibility of achieving the desired displacement and quantification of dosimetric benefits were evaluated.
Methods: Between February 2010 and August 2011, 10 patients underwent 11 image-guided displacement of OAR (rectum n=6, kidney n=4, stomach n=1). All cases were performed with conscious sedation. Under image guidance (CT and fluoroscopy n=6, CT n=5), an all-purpose drainage catheter (APD) (8.5-10.2 F) was inserted in the potential space between the OAR and PTV (n=8). One patient received two APDs and one patient underwent exchange of an occluded APD with a balloon on the day of treat-

ment. Displacement was not technically possible in one patient. Iohexol 140 diluted with normal saline (100-1000 mL, Mean: 269 mL, Median: 140 mL) was injected via the APD and minimum displacement was verified by CT imaging. The duration of procedure ranged 60-150 minutes (mean: 85.9 minutes, median: 70 minutes). Simulation was done immediately after displacement. Displacement was repeated on the day of SBRT. The median prescribed dose was 2400cGy in a single fraction (2000cGy/1 - 3000cGy/3). The APD was removed afterwards. To determine the degree of OAR displacement, the pre-displacement CT was fused with the post displacement planning simulation CT. OARs were contoured and planned with the same stereotactic dose constraints to OARs while maintaining the same PTV coverage. Dmax, D(5cc), and Dmean for critical OAR were calculated. Pairwise comparison was performed with 2-tailed t-test.

Results: Technical success was 91% (10/11 interventions). Minimum displacement achieved at the time of catheter placement ranged 7-31 mm (Mean: 15.1 mm; Median: 14 mm). Displacement decreased the Dmax from 2245cGy to 1737cGy (93% to 71%, p=0).135; D(5cc) from 1884cGy to 1226cGy (78% to 50%, p=0.041); and Dmean from 856cGy to 528cGy (35% to 22%, p=0.049). In general the dose to OAR was reduced by 13%-28%. Displacement was well tolerated and there were no complications associated with the procedure.

Conclusions: Image guided displacement of organs at risk prior to image guided stereotactic body radiation therapy is safe and feasible. It minimizes toxicity and facilitates dose escalation.

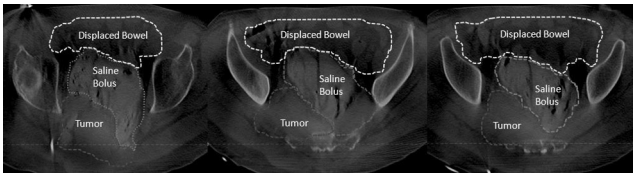

Cone beam CT images at the time of simulation show displacement of OAR (bowels) from PTV (sacral tumor) by instillation of dilute contrast via an APD placed percutaneously.

Paper 15: Trans Arterial Irinotecan Chemoembolization (IRI TACE) for Symptomatic and Intractable Colorectal Cancer (CC)

R. Bini, S. Comelli, F.A. Valle, D. Savio, G.P. Vaudano, R. Leli

Objectives: Inoperable, recurrent or not responder to treatment CC patients are at risk to develop symptoms such as bleeding (BL), intestinal obstruction (OS) and pain. The aim of the study was to assess feasibility, safety and efficacy of trans arterial chemoembolization using Irinotecan loaded micro-particles (IRI TACE) for treatment of such complications in patients treated on a compassionate use basis.

Methods: According to Institutional Guidelines, we enrolled patients admitted for intestinal OS and/or rectal BL and pain due to CC. A colostomy was performed to manage the obstruction. A multidisciplinary evaluation excluded in 7 patients (pt) (mean age 79yo) the indication for conventional treatment such as radical surgery, chemotherapy (cht) or radiotherapy (rt) for the presence of severe comorbidities thus we performed ultra-selective rectal TACE by femoral access. RECIST criteria (partial response ≥ 30%) were used to compare 48h and 4 week results after the procedure. One single IRI TACE with a drug dose of 30mg/m2 each, was performed for each patient.

Results: 2/7 patients had an isolated pelvic recurrence after surgical resection and cht; 3/7 were primary inoperable, not eligibly for rt or cht for severe comorbidities and the last 2 were already treated with rt (54Gy) for a locally advanced cancer in progression despite the treatment. Relieve of BL occurred in 100% of the patients and the pain was significantly reduced also. After 4 weeks, in 5 pt CT revealed that the mean volume lesion (MVL) reduction was 26±5%. 2 patients have shown unexpected more than 50% MVL, probably due to the main rectal lesion vessel supply embolization. One patient developed mild fever which was associated to necrosis of his rectal lesion. All patients were alive and asymptomatic after at a mean follow up of 2 months.

Conclusions: Ultra-selective IRI TACE for symptomatic inoperable CC not otherwise treatable is safe and well tolerated in patients with severe comorbidities. Its efficacy not only to relieve symptoms, but also to induce CC cytoreduction and reach the value of partial response by RECIST criteria.

Paper 16: Radical Treatment of Stage IV Pancreatic Cancer by the Combination of Cryosurgery and Iodine-125 Seed Implantation

J. Chen, J. Li, L. Niu, K. Xu

Objectives: To assess the therapeutic effect of radical treatment (cryoablation and iodine-125 seed implantation (C&S) for intrapancreatic and extrapancreatic tumors) and palliative treatment (seed implantation for intrapancreatic tumor, C&S treatment for extrapancreatic tumors) in stage IV pancreatic cancer patients.

Methods: There were 81 patients enrolled in the study. Radical treatments were performed on 51 patients, and 30 patients were under palliative treatment. The procedural safety and interval survival for stage IV pancreatic cancer (IS-IV) were assessed by follow-up in 2.5 years. The IS-IV of patients under two kinds of treatment and the effects of treatment timing and frequency on IS-IV were compared.

Results: The IS-IV of patients who received radical treatment was significantly longer than those received palliative treatment (P<0.001). The IS-IV of patients who received delayed radical or palliative treatment was longer than those received accordingly timely treatment (P=0.0034 and 0.0415, respectively). Multiple treatment can play important roles in improving the IS-IV of patients who received radical treatment (P=0.0389), but not for those received palliative treatment (P=0.99).

Conclusions: In the aspects of enlarging the IS-IV of patients, the effect of radical treatment was significantly obvious than that of palliative treatment, and multiple radical treatment may contribute more to IS-IV of patients than single radical treatment.

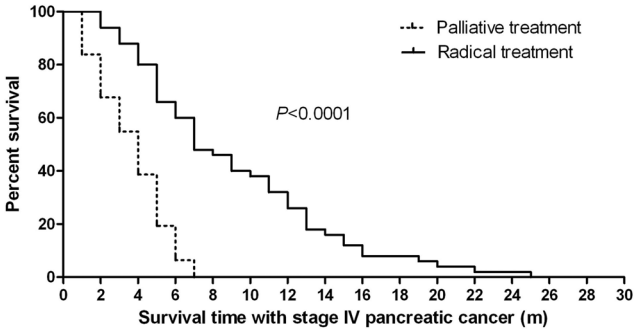

Figure 1. IS-IV of patients under radical or palliative treatment. All 81 patients had suffered from stage IV pancreatic cancer and died before October of 2011. There were 51 patients in radical treatment group, and 30 patients in palliative treatment group. The median follow-up period was 8 months. The IS-IV of patients were accumulated from the early diagnosis of stage IV pancreatic cancer in another or our hospital.

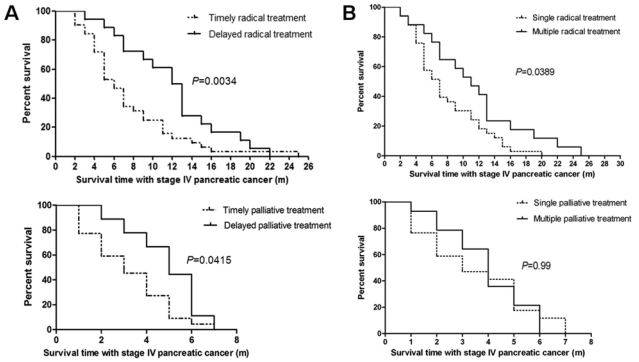

Figure 2. IS-IV of patients under different treatment conditions. (A) IS-IV of patients under timely or delayed treatment; (B) IS-IV of patients under different treatment frequecny.

Paper 17: PLGA Microspheres for Image-Guided Transcatheter Delivery of Sorafenib to Liver Tumors

J. Chen, A.Y. Sheu, R.A. Omary, L. Shea, A.C. Larson

Objectives: Sorafenib is a multi-kinase inhibitor used as a targeted therapy against angiogenesis for the treatment of hepatocellular carcinoma (HCC). Unfortunately, the current formulation for oral administration results in highly non-specific delivery of the drug and consequently many patients cannot tolerate the resulting side effects such as hand-foot syndrome and cardiac ischemia. Local transcatheter, intra-arterial delivery of polymer microspheres containing sorafenib should improve patient tolerance and increase the dose ultimately reaching the tumors. The purpose of this study was to develop this much needed drug delivery system and show that we can feasibly deliver the microspheres to McA-RH7777 rat hepatoma cells implanted in the livers of Sprague Dawley rats.

Methods: Polylactide-co-glycolide (PLGA) microspheres co-encapsulating sorafenib and an iron-oxide ferrofluid were synthesized via a double emulsion solvent evaporation method. The microspheres were characterized using microscopy for size and morphology, high performance liquid chromatography (HPLC) for sorafenib content, and inductively coupled plasma mass spectrometry (ICP-MS) for ferrofluid content. Additionally, two male Sprague Dawley rats were implanted with McA-RH777 rat hepatoma cells and later infused transcatheter with 4 mgs of the microspheres via the proper hepatic artery and then imaged with a 7 Tesla Magnetic Resonance Imaging (MRI) magnet (Bruker Clinscan, Billerica, MA) to visualize the biodistribution of the

microspheres. Histology using Prussian blue staining for iron was used to verify the presence of microspheres in the tumor and normal hepatic tissue.

Results: The characterization studies indicated that the microspheres had an average diameter of 12.2 μm and included 18.7% (w/w) sorafenib and 0.54% (w/w) ferrofluid. For the rat studies, the intra-hepatic distribution of the microspheres, specifically in the tumor, was clearly depicted in follow-up T2-weighted MRI images. Prussian blue staining confirmed successful hepatic microsphere delivery to the tumor.

Conclusions: The developed PLGA microspheres co-encapsulating sorafenib and ferrofluid allowed for local delivery of treatment to rat liver tumors as well as visualization of the resulting microsphere distribution using MRI. Current studies are being performed to evaluate therapy response in the tumors after delivery of the microspheres

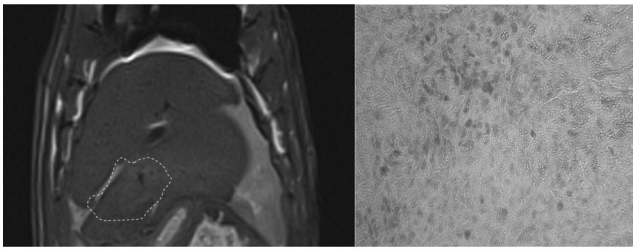

Fig. 1: Post microsphere infusion image (left) of the tumor (indicated by yellow dashes) and histology of the tumor tissue (right) using Prussian blue staining for iron in the microspheres indicates the successful delivery of the microspheres to the tumor.

Paper 18: Microwave Ablation Energy Delivery: Power Pulsing May Improve Ablation Zone Size and Reduce Treatment Time

M. Bedoya, C. Brace

Objectives: Microwave ablation is an emerging tumor ablation modality that has demonstrated great clinical promise in early studies. Microwave systems may create faster heating, larger ablations, and more consistent results than predicate RF ablation systems. However, as microwave technologies are still evolving, optimized methods for power delivery have yet to be realized. The purpose of this study was to compare the impact of continuous and pulsed energy delivery on microwave ablation growth and final geometry in ex vivo and in vivo liver models.

Methods: A total of 15kJ at 2.45GHz was applied to ex vivo liver using one of five delivery methods: 25W for 10min, 50W for 5min, 100W for 2.5min, 100W pulsed over 10min (30s on, 90s off), and 100W pulsed over 5min (50s on, 50s off). Temperatures were monitored 5-20mm from the monopole antenna by fiber optic probes. A total of 30kJ was applied to swine livers in vivo using delivery methods similar to the ex vivo study, but with twice the total ablation time due to perfusion effects, and 75s on/off times substituted for 50s on/off times. Ablation zones were sliced along the antenna tract and analyzed for transverse diameter, length, volume, and circularity. Comparisons of size and shape were made between groups based on total energy delivery, average power applied, and peak power.

Results: No significant differences were noted in the ablation sizes or circularities between pulsed and continuous groups ex vivo. The maximum percent difference between measurements was less than 10% (Table 1). Temperature curves in pulsed ablations showed rapidly increased heating rates at all points, suggesting the possibility to overcome blood perfusion and coagulate tissues more readily than lower continuous powers. Indeed, differences in ablation size and shape were noted in vivo despite equivalent total energy delivery among all groups. Overall, the largest ablations were produced with 100W for 5min, but the most circular ablations were produced with 25W for 20min (Table 1). When comparing 25W average power, pulsed ablations were significantly greater. It almost doubled in diameter and length, with reduced circularity. Continuous delivery of 25W was not sufficient to overcome perfusion. When comparing 50W average power groups, no differences in size were noted, but pulsed ablations were again slightly less circular. Therefore, it appears that at least 50W average power is needed to produce reasonable ablations in vivo.

Conclusions: Changing energy delivery did not impact results ex vivo, but substantial differences were observed in vivo. Pulsed delivery creates larger ablation zones in less time than continuous delivery of the same average power and total energy. Pulsed ablations were also slightly more elongated. Improved energy delivery may be possible with higher powers and shorter treatment times; however, a more complete study of pulsing parameters is needed to optimize power delivery for microwave ablation.

Table 1

	Group	Input Power (W)	Time On (s)	Time Off (s)	DC	Tot Time (min)	Ave Power (W)	Ave Energy (KJ)	Ave Length (cm)	Ave Diameter (cm)	Diameter / Length	Vol (cm^3)
EX-VIVO	1	25	600		100%	10	25	15	4.90 ± 0.44	3.00 ± 0.20	0.61 ± 0.02	184.73
	2	100	30	90	25%	10	25	15	5.10 ± 0.26	2.93 ± 0.06	0.58 ± 0.02	183.82
	3	50	300		100%	5	50	15	5.07 ± 0.12	2.83 ± 0.35	0.56 ± 0.06	170.38
	4	100	50	50	50%	5	50	15	5.13 ± 0.32	3.07 ± 0.45	0.60 ± 0.12	202.22
	5	100	150		100%	2.5	100	15	4.93 ± 0.55	2.90 ± 0.46	0.59 ± 0.09	173.79
IN-VIVO	1	25	1200		100%	20	25	30	1.55 ± 0.30	0.88 ± 0.06	0.57 ± 0.09	5.03
	2	100	30	90	25%	20	25	30	3.31 ± 1.44	1.47 ± 0.36	0.44 ± 0.13	29.85
	3	50	600		100%	10	50	30	4.09 ± 1.02	2.32 ± 0.83	0.57 ± 0.09	92.08
	4	100	75	75	50%	10	50	30	5.03 ± 1.56	2.38 ± 0.72	0.47 ± 0.05	119.66
	5	100	300		100%	5	100	30	5.11 ± 0.89	2.49 ± 0.88	0.49 ± 0.14	132.93

Paper 19: Irreversible Electroporation (IRE) Ablation of the Lumbar Vertebrae in a Porcine Model

M. Abdelsalam, M. Gagea, K. Dixon, A. McWatters., J. Miller, A. Tam

Objectives: The use of thermal ablation in the vertebral body has been limited because of the potential for damage to critical neural structures. This pilot study evaluates the feasibility and safety of IRE ablation in lumbar vertebrae using a porcine model.

Methods: Sixteen CT-guided IRE ablations were performed in the lumbar vertebrae of 4 pigs. Ablations were performed either in the transpedicular (n=8 vertebral bodies) location or directly over the posterior cortex (n=8 vertebral bodies). Animals were euthanized at 4-hours, 6-hours, 24-hours and 7-days post-ablation. Magnetic resonance imaging (MRI) was obtained immediately after ablation and prior to euthanasia. Clinical, imaging and histopathological data were analyzed.

Results: The technical success rate for IRE probe placement and ablation was 100%. The mean distances from the IRE probe to the posterior wall of vertebral body or the exiting nerve root were 2.68 ± 1.19 mm and 7.7 ± 2.61 mm, respectively. The two pigs euthanized at 24-hours and 7-days post-ablation had no clinical signs of paraplegia or paresis. There were no MRI findings of focal myelopathy or radiculopathy immediately following ablation or on follow-up MRI. A small retroperitoneal hematoma developed in one of the animals euthanized immediately post-ablation. Histopathologic examination revealed acute bone marrow and bone tissue necrosis extending radially from the probe for 2-5mm, and acute degeneration and necrosis of skeletal muscle adjacent to the vertebral body. Similar lesions associated with fibroplasia and tissue repair changes were present in the 7-day post-ablation animal. No significant histologic changes of the spinal cord, nerve roots or ganglia were observed in any pig.

Conclusions: IRE ablation of the vertebrae in a porcine model is feasible. Histopathological changes of the bone marrow & bone tissue necrosis of the vertebral body are detected. IRE in the porcine spine does not appear to be associated with paraplegia or radiculopathy.

Paper 20: Percutaneous Cryoablation and 125I Seeds Implantation Combined with Chemotherapy for the Treatment of Advanced Pancreatic Cancer: Reports of 96 Cases

L. Niu, L. He, L. Zhou, B. Wu, J. Zuo, K. Xu

Objectives: To assess the efficacy and the safety of percutaneous cryoablation (PCC) and 125I seeds implantation combined with chemotherapy in the treatment of advanced pancreatic cancer.

Methods: Ninety-six patients with advanced pancreatic cancer underwent PCC and 125I seeds implantation combined with concomitant chemotherapy were analyzed.

Results: Eighty-seven patients were followed up successfully. Median survival was 10.5, and 6-month and 1-year survival was 69.6% and 43.1%, respectively. The maximum survival reached 47 months. CR, PR and SD were achieved in 9, 26 and 53 patients, respectively. 70.8% of CBR and significant increase of KPS ($P<0.05$) were achieved. No serious therapy-related complications except pancreatic fistula accompanied abdominal hemorrhage, bile leakage, acute pancreatitis and 125I seeds leaved over in needle track occurred in 1, 1, 2 and 1 case, respectively.

Conclusions: PCC and 125I seeds implantation combined with chemotherapy are effective and safe for the treatment of advanced pancreatic cancer.

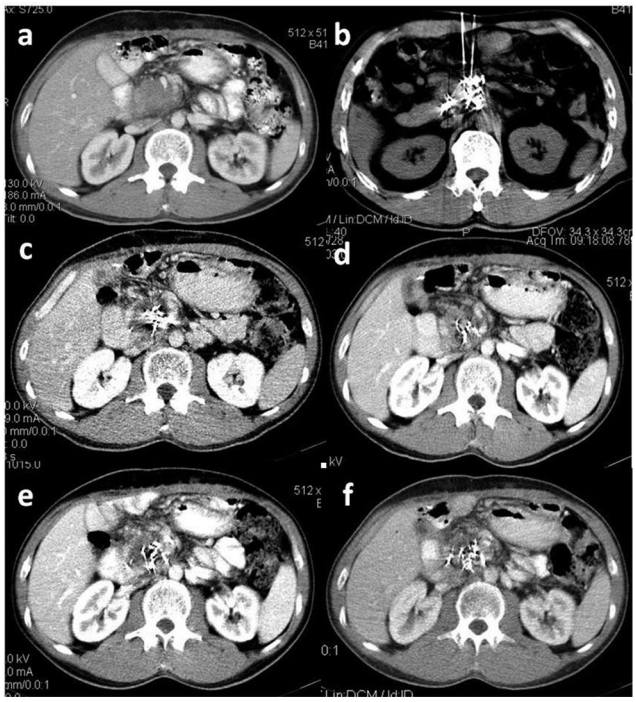

Comparison of computed tomography prior, during and after percutaneous cryoablation and 125I seeds implantation on a patient with pancreatic cancer (male, 40y, stage IV, pancreatic head cancer with liver metastasis, diameter of primary mass 5.8 cm×4.6 cm×3.1 cm (a)). Cryoablation and 125I seeds implantation were performed with percutaneous approach through left lobe of liver under ultrasonography and computed tomography guidance (b). Mass in pancreas necrosed gradually without enhancement on computed tomography in 2 months (c), 4 months (d), 5 months (e) and 6 months (f).

Table1 Influencing factors of percutaneous cryoablation and 125I seeds implantation combined with chemotherapy on pancreatic patients

Characteristics	n	CBR	P-value	1-year-survival (%)	P-value
Age, years					
Average 56.9(Rang, 30-82)					
≤55	40	80.6	0.255	50.6	0.002
>55	56	75.9		26.7	
Sex					
Male	58	83.4	0.778	48.9	0.718
Female	38	77.2		35.9	
Pancreas tumor location					
Head of pancreas	55	75.1	0.206	36.7	0.574
Body and/or tail of pancreas	41	89.3		47.0	
Max diameter of tumor, cm					
>2, <5	55	76.8	0.833	37.8	0.259
≥5	41	79.4		43.6	
Stage					
III	16	97.8	0.207	50.0	0.952
IV	80	76.3		40.1	
Metastasis					
Liver	71	80.7	0.146	41.9	0.508
Others	25	89.6		33.3	
Metastasis number					
Single	61	92.4	0.000	42.4	0.050
Multiple	35	33.8		13.6	

Paper 21: Post-TACE DynaCT Attenuation Value as Predictor of Treatment Response in HCC

J. Wan, D. Klass, S.G. Ho, A. Weiss, A. Buczkowski, D. Liu

Objectives: To determine if attenuation value of lesions on immediate post-Trans Arterial Chemoembolization (TACE) non contrast (NC) DynaCT can predict 1-month treatment response in HCC.

Methods: 16 patients (16 males, median age 69, range 53-84 years) with 27 lesions (1-9.7cm) underwent TACE (lipiodol/doxorubicin) from 2009-2011. Patients with immediate post-TACE NC DynaCT, pre-/1-month post treatment imaging and lesions ≥1cm were included for evaluation. The attenuation of lesions was measured by placing a Houndsfield region of interest (ROI) over reconstructed axial images, with concurrent Houndsfield measurement of adjacent liver parenchyma on the most representative axial image.

Results: Using mRECIST criteria, 19 of 27 lesions demonstrated 100% response at 1 month, defined by the absence of enhancement on triphasic CT, despite little/no change in size. 3 lesions demonstrated partial response (63-85%), and 5 lesions no (0%) response. Lesions with no response had mean attenuation 57.8HU (Range 1-88HU), and mean attenuation ratio between lesion and adjacent parenchyma 1.3 (Range 0.02-2.6). Lesions with 100% response had mean attenuation 554.9HU (Range 89-1057HU), and mean ratio of attenuation between lesion and adjacent parenchyma 11.6 (Range 3.4-57). The 3 lesions with partial response had mean attenuation 331.1HU (Range 326-341HU) and mean ratio of attenuation between lesion and adjacent parenchyma 11.8 (Range 4.4-24.3). ROC analysis using 19 lesions with 100% and 5 lesions with 0% response to determine ideal cut-off ratio of attenuation between lesion and adjacent parenchyma yielded 3.4, with AUROC=1 (95% Confidence Interval 1-1).

Conclusions: A ratio of >3.4 between the target lesion and adjacent parenchyma on immediate post-TACE NC DynaCT is a strong predictor of good response for HCCs treated with lipiodol-based TACE, while a ratio of <3.4 is a strong predictor of poor response at 1 month. Larger studies are needed in order to evaluate this potentially valuable imaging tool further.

Paper 22: A Precise Safety Margin of 1.0 cm is Required for Best Local Efficacy of Radiofrequency Ablation of Hepatocellular Carcinoma: Assessment with a Novel Three Dimensional Reconstruction Software

M. Kuang, Y. Wang, C. Jiang, X. Xie, M. Lu

Objectives: To analyze the relationship between safety margin and local tumor control of radiofrequency (RF) ablation in treatment of small hepatocellular carcinoma by reconstructing and fusing 3-D images of tumor zones and ablation zones with a three dimensional reconstruction software.

Methods: From March 2011 to December 2011, 69 patients (10 female and 59 male) with 95 hepatocellular carcinoma nodules less than 5 cm admitted to the Division of Interventional Ultrasound, The First Affiliated Hospital of Sun Yat-sen University were enrolled in the study. The study was approved by the Ethics Committee of the hospital and informed consent was signed by all patients. All nodules were treated by RF ablation with curative intention. 64-row Enhanced CT scan was performed before and 1 month after treatment. CT data were processed with three dimensional reconstruction software. Three dimensional tumor and ablation zones were reconstructed into 3-D images and fused to show the safety margins for accurate measurement. Ablation margin, tumor size, tumor volume and heat sink effect due to adjacent hepatic vessels were assessed by multivariate analysis.

Results: Follow up was conducted on all patients for 6.3 months (2.0-10.9 months). The reconstructed ablation zone covers the original tumor zone completely each tumor nodule, but the safety margins vary in all directions. The complete ablation rate was 97% (92/95). LTP was found in 4.2% (4/95) nodules. A safety margin of 5.5±2.0 mm (0.9-8.0 mm) was found at where incomplete ablation or LTP happened. Safety margin < 1 cm is the sole significant factor related with insufficient local efficacy.

Conclusions: The use of three dimensional reconstruction software makes it possible for calculating precise safety margin of RF ablation. To achieve the best local efficacy, a safety margin of at least 1.0 cm is necessary.

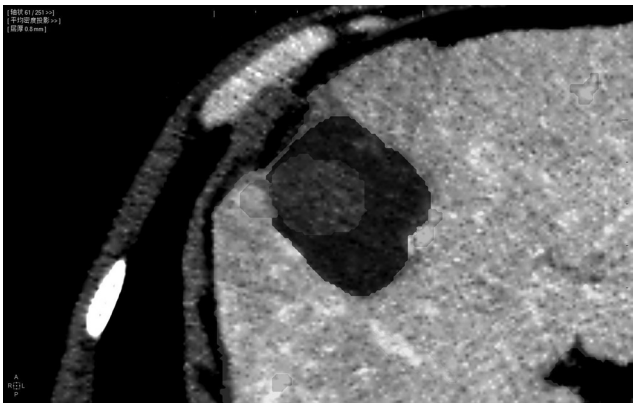

Fig 1. Local tumor progression 1 month after ablation with a minimal ablation margin of 1.4mm.

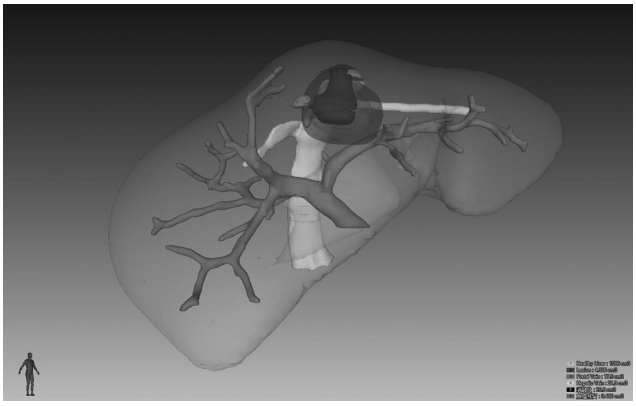

Fig 2. 3-D fusing image of the primary tumor, ablation zone and local recurrent tumors.

Paper 23: Tumor Response Assessment in Hepatocellular Carcinoma: Efficacy of Segmentation and Automated Volumetric Measurements using Triple-Phase Contrast-Enhanced Computed Tomography Scans Before and After Loco-Regional Therapy

K. Memon, R. Salem, D. Cioni, L. Zhang, D.E. Gustafson, R.A. Lencioni

Objectives: Previous work including imaging-pathology correlation has shown that SVM (INTIO, Broomfield, Colorado), a semi-automated segmentation method, enables accurate determination of tumor volume in patients with hepatocellular carcinoma using triple-phase contrast-enhanced computed tomography (CT). The purpose of this study is to assess whether SVM can be used to assess HCC response to loco-regional treatments, using semi-automated segmentation and automated measurement technique.

Methods: Twenty patients with HCC diagnosed according to noninvasive imaging criteria or biopsy underwent loco-regional treatment with drug-eluting bead chemoembolization or radiofrequency ablation. All patients had pre-treatment and post-treatment triple-phase contrast-enhanced CT. Post-treatment scans were obtained 4-8 weeks after therapy. Images were reviewed blindly by two independent radiologists according to standard Response Evaluation Criteria In Solid Tumor (RECIST), modified RECIST (mRECIST), and volumetric mRECIST (Vol-mRECIST). Vol-mRECIST criteria were derived from mRECIST criteria, assuming equivalent spherical lesions wherein a decrease in viable tumor of 30% or more in longest diameter or 66% or more in volume represents partial response (PR), an increase of 20% or more in longest diameter or 73% or more in volumes is progressive disease (PD), and changes within these limits represent stable disease (SD). Complete Response (CR) is the defined as the complete absence of viable tumor following therapy.

Results: Response classification performed by using Vol-mRECIST showed an absolute correlation between the two readers (20 of 20 subjects), with 12 patients classified as CR, 2 as PR, 5 as SD, and 1 as PD. By using manual determinations of viable diameter according to mRECIST, agreement between the two observers in response determination was seen in 19 of 20 subjects (Spearman correlation (ρ): 0.981; 1 case was classified as SD by reader 1 and as PD by reader 2). Of importance, response assessment between Vol-mRECIST and conventional mRECIST was coincidental in 19 of 20 patients ($\rho = 0.991$). In contrast, standard RECIST showed poor correlation with either mRECIST ($\rho = -0.072$)or Vol-mRECIST ($\rho = -0.096$), with no subject classified as CR and only 1 as PR.

Conclusions: Tumor response assessment by Vol-mRECIST showed absolute inter-observer agreement and excellent correlation with mRECIST. The development of a validated semi-automated segmentation and 3D measurement algorithm able to differentiate viable vs necrotic tumor is an important step toward 3D quantitative assessment of tumor response.

Paper 24: Contrast-Enhanced Ultrasound for Accurate Measurement Tumor Size in Colorectal Liver Metastases

J. Wu, M. Chen, S. Yin, Y. Shi, K. Yan, W. Wu

Objectives: Accurate assessment of tumor size is important for making treatment protocols, especially for local therapeutic treatment. The purpose of the study was to evaluate tumor size in colorectal liver metastasis using baseline ultrasonography (US) and contrast-enhanced ultrasonography (CEUS) compared with histopathological tumor size.

Methods: 40 consecutive patients with colorectal liver metastasis were prospectively examined at US and CEUS with contrast agent SonoVue. 46 metastases in 40 patients with complete data were recruited for the study. The largest diameters of 46 metastases were measured at US, CEUS and POST-CEUS, respectively. Three CEUS measurements were made: at CEUS-vascular phase (VP) measuring the maximum enhanced tumor size (hyperechoic area), at CEUS-portal venous phase (PVP) and late phase (LP) measuring the maximum clearance tumor size (hypoechoic area), respectively. Measurements were compared with histopathological tumor sizes (the largest diameters of the surgical gross specimens plus the largest distances of the micrometastases from the margin of the gross specimens under microscopy). Factors of micrometastases and tumor size (≤2 cm and >2 cm) were further analyzed, respectively. Bland-Altman analysis and independent t test were used in overall and stratified analysis to examine the measurements differences.

Results: Micrometastases were found in 24 (52.2 %) of 46 tumors, with a distance of 0.05~0.50 cm (mean±SD, 0.19±0.11 cm) from the margin of the main tumors. By overall analysis, Bland–Altman plots showed the most accurate measurement method was POST-CEUS, while CEUS-PVP was the poorest. For tumors with micrometastases and tumors larger than 2 cm, CEUS-VP performed the best size estimation with a mean difference of 0.01cm. While other methods all underestimated the tumor size, CEUS-PVP was the poorest.

Conclusions: CEUS-VP could more accurately to assess the histopathological tumor size for tumors with micrometastase and tumors larger than 2 cm.

Paper 25: Percutaneous Ultrasound-Guided Ablation for Liver Tumor with Artificial Pleural Effusion or Ascites

X. Xie, H. Xu, M. Kuang, M. Lu

Objectives: This study used artificial pleural effusion or ascites to extend the indications of ablation for liver tumor, and assessed the feasibility, safety and availability of artificial pleural effusion or ascites in percutaneous ablation procedure.

Methods: Artificial pleural effusion was performed in 25 difficult cases (30 lesions) before percutaneous ultrasound-guided ablation procedures. Criteria for inducing artificial pleural effusion were as follows: lesions were not clearly revealed since they were located in the hepatic dome; no proper puncture path was identified since it was blocked by major vessels or gallbladder. Artificial ascites was performed in 61 difficult cases (70 lesions) before percutaneous ultrasound-guided thermal ablation procedures.

Results: 1. The artificial pleural effusion technical success rate was 96% (24/25), the achieved purpose rates was 100% for artificial pleural effusion successfully instilled. The use of artificial pleural effusion makes 28 lesions in the S7.8 of the liver near the hepatic dome clearly visualized, which were partially or completely sheltered by gas-containing pulmonary tissue previously. 4 lesions surrounded by major vessels or gallbladder have got a safe puncture path via the pleural cavity. Coughing, subcutaneous effusion and pneumothorax were observed in three patients after the technique of artificial pleural effusion. No major complications and procedure-related death occurred. The complete ablation rates was 84% (21/25)at the first ablation, and 92% (23/25) after the second supplementary ablation. 2. The artificial ascites technical success rate was 100% (61/61). 73.7% (42/57) lesions are separated successfully from the gastrointestinal track after induction of artificial ascites, which were close to the gastrointestinal track; 66.7% (6/9) lesions are clearly revealed, which were adjacent to the diaphragm and could not be completely revealed before; 88.2% (15/17)lesions adjacent to the abdominal wall were separated successfully ; one lesion which was surrounded by major vessels without safe puncture path, has got a safe puncture path after instilling; but no lesions close to the gallbladder are separated successfully. Coughing (1 case) and the pleural effusion of the right pleural cavity (5 cases) were observed after the technique of artificial ascites. No major complications and procedure-related death occurred. The complete ablation rate was 90% (44/49)at the first ablation, and 96% (47/49) after the second supplementary ablation.

Conclusions: The use of artificial pleural effusion or ascites expand the indications of thermal ablation and offers opportunities of treatment for some difficult cases. Artificial pleural effusion and ascites are safe, feasible, and they should be spread and be used in large clinical population.

Paper 26: Safe Percutaneous Thermal Ablation of Poorly Accessible High Dome Liver Lesions using One-Lung Ventilation Technique: Preliminary Experience

N. Yu, K. Dittmar, C. Frenette, H. Monsour, S. Gordon-Burroughs, R. Ghobrial

Objectives: Percutaneous access for ablation of high dome lesions in the liver is usually problematic due to overlying lung and may require additional invasive steps (artificial pleural effusion or pneumothorax) or a cumbersome guidance approach (e.g., multiplanar MRI). We evaluated the feasibility of one-lung (left) ventilation to deflate the right lung thereby providing an extrapulmonary window for safe and simple probe placement under conventional US or CT guidance.

Methods: From September 2011 to February 2012, five consecutive patients (all male, mean age 59) referred for radiofrequency ablation of liver masses in the dome, with tumor visualization precluded on pre-procedural US due to overlying lung and without an adequate cardiophrenic fat window for safe axial CT guidance, were included in this study. Six lesions were treated in total (5 hepatoma, 1 colorectal metastasis), ranging from 2.0-5.5 cm (mean 3.6 cm). General anesthesia was performed with

use of a double-lumen endotracheal tube. After confirming lack of access window on targeted US and CT at the beginning of the procedure, the anesthesiologist performed selective left lung ventilation by clamping the right bronchial limb with the bronchial cuff inflated and port open to air. D5W artificial ascites was created in 4 patients for diaphragmatic protection. Then the ablation procedure proceeded under US/CT guidance and monitoring using internally-cooled RF probes. Chest radiograph was obtained 6-18 hours post-procedure.

Results: In all five patients, one-lung ventilation resulted in sufficient retraction of the right (contralateral) lung to expose a transdiaphragmatic but extrapulmonary window for sonographic tumor visualization and probe placement. In one patient, axial CT guidance was used since anterior approach through the costochondral junction, also made possible by one-lung ventilation, was favored based on tumor location/geometry. Primary intercostal US guidance was used for all others. Intra-procedural cardiopulmonary status was stable and anesthesia uneventful for all patients. No immediate or delayed complications were encountered. Post-procedurally, no patient reported respiratory symptoms, and chest radiograph confirmed re-expansion of the right lung and absence of pneumothorax. Short-term CT or MRI follow-up to this point has demonstrated complete ablation in all lesions except for the largest (5.5 cm) HCC which locally recurred at 5 months.

Conclusions: One-lung ventilation using a double-lumen endotracheal tube seems to be a safe and effective technique to permit percutaneous thermal ablation of poorly accessible hepatic dome tumors, obviating the need for more invasive and time-consuming alternative approaches.

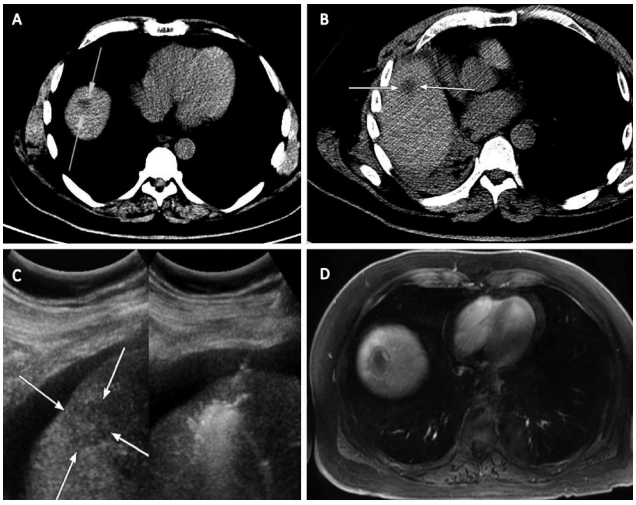

A 2 cm colorectal metastasis at the liver dome (A) was not visible on pre-procedural targeted US. After initiation of one-lung ventilation, the right lung retracted from over the anterolateral dome (B), and the lesion was well exposed for US guided ablation (C). Ablation defect with no local recurrence was demonstrated on follow-up MRI (D).

Paper 27: Pre-Clinical and Phase I Studies Using the MAXIO System for CT Guided Probe Placement

F.M. Moeslein, A.K. Chaturvedi

Objectives: International multicenter pre-clinical and early Phase I studies to assess accuracy, feasibility and safety of the MAXIO system for CT guided probe placement.

Methods: The described work was performed at institutions in the USA, Italy and India. The MAXIO system is a novel targeting software/hardware package that allows precise probe guidance using non-contrast CT imaging. Initially, a lab study was conducted to verify the targeting accuracy of the system and the targeting accuracy was found to be 1.90+/-1.92 (Mean +/- SD). Preclinical work using the MAXIO system was performed using a phantom to verify the targeting capabilities of the software and hardware package. In this portion of the study, a junior resident and a senior faculty member each performed 15 CT guided needle placements into various targets within a phantom using either free-hand CT fluoroscopic guidance or the MAXIO system. Accuracy, radiation exposure and time to needle placement were tracked. Subsequently, a 30 patient Phase I clinical study was performed using the MAXIO planning software and hardware for probe placement. In this study, patients with solitary tumors less than 3 cm in the chest, abdomen and pelvis were recruited. The single arm trial was designed to test the safety and feasibility of the MAXIO system for targeting, target path determination, accuracy of probe placement, requirement (and number) of probe repositions, radiation exposure, probe placement verification, as well as adverse event monitoring.

Results: The pre-clinical study demonstrates that the average time per needle placement is decreased, both for experienced and inexperienced operators, when using MAXIO vs. CT fluoroscopy. The accuracy of needle placement using the MAXIO system is at least as accurate as free-hand biopsy using CT fluoroscopy. Importantly, there is marked radiation savings to both the patient and the operator using the MAXIO system as compared to CT fluoroscopy. The final data analysis of the Phase I trial is ongoing and should be complete by the time of data presentation, but the preliminary analysis demonstrates the MAXIO system to be safe, with no increased morbidity or mortality associated with the targeting system. Pre-operative analysis and planning is improved when using the MAXIO software system. The final accuracy and efficacy data will be presented at the meeting.

Conclusions: In the pre-clinical trial, the MAXIO targeting system significantly improves targeting time and decreases radiation exposure during CT guided probe placements. Importantly, the MAXIO system is at least as accurate as an experienced Interventionalist for CT guided targeting. While the final data analysis is not yet complete (it will be in time for the final presentation), the early results demonstrate MAXIO to be a safe alternative to conventional CT targeting. The clinical Phase I data coupled with the pre-clinical data demonstrate that the MAXIO system offers operators the potential for rapid probe placement, with reduced radiation exposure to both patient and operator. The MAXIO system also simplifies even complex probe targeting. Moreover, the system will allow efficient targeting of lesions that are not readily detectable with non-contrast CT alone. The early data is compelling, and further studies, including a randomized comparative trial are warranted.

Paper 28: Initial Assessment of Semi-Automated Vessel Segmentation Software as a Potential Application for Guidance during Chemoembolization Procedures

M. Wallace, G. Chintalapani, P. Chinna Durai

Objectives: To evaluate the accuracy of C-arm cone beam CT (C-arm CBCT) based semi-automated vessel segmentation software as applied to patients who underwent hepatic chemoembolization.

Methods: Commercially available software (syngo Embolization Guidance; syngo XWP VB20C, Siemens AG Healthcare Sector, Germany) was applied to 15 consecutive patients who underwent chemoembolization between July 2011 and October 2011 in whom contrast enhanced C-arm CBCT was obtained. All imaging studies were evaluated retrospectively and all segmentations were performed offline. Seed points were manually placed on the distal aspect of the desired vessel(s) with a mean diameter of 1.51 mm (range .75 - 2.19 mm), at a mean distance of 2.95 mm (max 9.1 mm) from the target lesion. The vessel segmentation tool was then engaged and a graphic centerline was automatically generated and displayed on the desired vessels within the C-arm CBCT dataset. The following variables were recorded for each study: the number of lesions, target vessels selected, success of vessel segmentation on first attempt, and the time required to process and review the results of segmentation.

Results: A total of 49 arteries for 23 lesions were identified for analysis and segmentation. The success of segmentation on first attempt was accomplished in 44/49 (90%) arteries. With minor seed point manipulation, success rate increased to 96%. Two errors that could not be corrected by seed point manipulation resulted from direct contact between arterial segments. One error related to the presence of a hairpin turn in the same vessel creating a shortcut. The second error occurred when two distinct vessels crossed each other resulting in an aberrant path. The average time required to preview the C-arm CBCT, apply the segmentation software and review the results was 3.2 minutes (1-5 minutes).

Conclusions: Semi-automated vessel segmentation and centerline extraction is a quick and reliable method of extracting the path from small vessels adjacent to the target lesion back to the catheter tip. Leveraging this information during real-time catheter manipulations, as a graphic overlay, could enhance the operator's ability to achieve higher orders of catheterization.

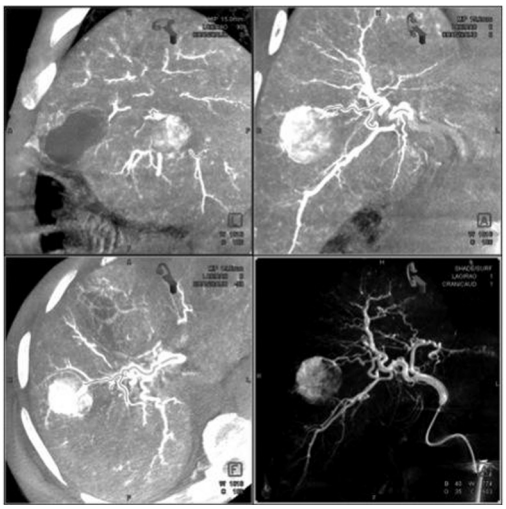

Paper 29: Magnetic Resonance Imaging Detection of Targeted Intrarterial Delivery of Iron Oxide Nanoparticles to the Liver Tumors in the Rabbit Cancer Model

V. Prieto, T.O. Lawal, L. Wang, H. Mao, H.S. Kim

Objectives: To develop novel magnetic iron oxide nanoparticles as a delivery vehicle for intrarterial (IA) administration of chemotherapy and to assess in vivo iron concentration and distribution by magnetic resonance imaging (MRI) after targeted IA administration to liver tumors in a rabbit model.

Methods: VX2 liver tumors were induced in the left lobe of rabbits (N=5). After growing for 2 weeks to a size of 2.0 cm measured by MRI, tumors were subsequently treated with the 4-5mg Fe/kg of the suspension of magnetic iron oxide (IO) nanoparticles (2 mg Fe/mL with core and hydrodynamic sizes of 10 nm and 23 nm, respectively) loaded with 20% doxorubincin (per mg Fe) via left hepatic artery under fluoroscopy. Animals were imaged before and 24 hours after treatment using a 3T MRI scanner using T1, T2 weighted MRI. The mean signal intensities (SI) from selected regions of interest (ROI) in the following areas: central tumor, peritumoral within the tumor, periliver contiguous to the tumor, left lobe, and right lobe, were measured on T2-weighted MRI; decreases in signal intensity corresponded to increasing Fe concentration (1). SI values were obtained in quadruplicate ROIs (an area of 136 mm2) using imaging analysis software, ImageJ (NIH).

Results: The SI values in ROIs with the tumor decreased significantly for all animals 24 hours after IA administration of iron oxide nanoparticles compared to SI values of the same ROIs before treatment. More specifically, the signal changes were seen in peritumoral, periliver, left lobe, and the right lobe areas (i.e. 248 vs 215, 126.8 vs 52.9, 105.2 vs 50.5, 103.2 vs 48.1, p=0.002, respectively). However, SI did not decrease significantly in the central tumoral areas after treatment (248.2 vs 248.4 p=0.967). Furthermore, post-treatment peri-liver SI was significantly less when compared to peritumoral areas (52.9 vs 215.8 p<0.0001).

Conclusions: Targeted IA administration of novel iron-oxide nanoparticles is preferentially delivered to the liver peritumoral areas and can also be localized and quantified by T2-weighted MRI, making this a promising tool for imaging guided drug delivery and cancer therapy.

Paper 30: MRI-Monitored Transcatheter Intra-Arterial Delivery of Spio-Labeled Natural Killer Cells to Hepatocellular Carcinoma

A.Y. Sheu, Z. Zhang, R.A. Omary, A.C. Larson

Objectives: Adoptive immunotherapy with natural killer (NK) lymphocytes is a promising approach for treatment of HCC; however, intravenous (IV) infusion may lead to insufficient NK dose delivery to tumors. Also, quantification of intra-tumoral NK delivery may be crucial to optimize therapy or to predict response. We hypothesize that: a) transcatheter intra-arterial (IA) infusion allows for targeted delivery of NK cells to HCC, and b) iron oxide labeling methods allow for visualization of IA NK delivery with MRI.

Methods: 4.0×10^6 NK-92 MI cells (ATCC) were incubated overnight with 30 pg/cell of Texas Red iron oxide nanoparticles (GENOVIS AB) using 4.5 μg/ml protamine sulfate as a transfection agent. Cell viability was measured using a cell counter, and labeling efficacy was measured by fluorescence microscopy with DAPI. With IACUC approval, 6 Sprague-Dawley rats were implanted with 4.0×10^6 McA-RH7777 HCC cells divided between the left lateral and median lobes to simulate a metastatic tumor. After 8 days of tumor growth, a 24G catheter (Terumo Medical) was placed in the proper hepatic artery via laparotomy, and digital subtraction angiography (DSA) confirmed placement. 7.0T MRI scanner (Bruker) was used for T2*-weighted scans pre- and post-NK infusion. T2* measurements in tumor and normal liver were compared pre- and post-infusion by t-test. Prussian blue iron staining confirmed NK delivery histologically; percentage of cells in a high-powered (20×) field identified as labeled NKs (%HPF) were compared between tumor and normal tissues by t-test.

Results: NK cell viability was >90% before and after labeling. Labeling efficacy was 88.0±3.0%. Transcatheter NK infusions led to significant reductions in T2* values for the tumor (mean±SD: pre 20.9±5.1 msec, post 12.4±1.2 msec, p<0.01) and normal liver (pre 11.8±0.5 msec, post 7.5±1.2 msec, p<0.01) during intra-procedural MRI scans (Fig. 1); however, tumor T2* values decreased significantly more than those of the normal liver (p=0.04). Histologic %HPF measurements were significantly higher in tumor (1.25%) than surrounding normal liver tissues (0.29%) (p<0.01) (Fig. 2).

Conclusions: Transcatheter infusion permitted selective delivery of NK cells to HCC. The intra-hepatic distribution of iron oxide labeled NK cells was quantitatively visualized with MRI. Future studies will assess relationships between therapeutic outcomes and the delivered NK dose, comparing IV and IA administration routes. Clinicians could one day use these methods to adjust patient-specific therapeutic regimens during adoptive immunotherapies for the treatment of HCC.

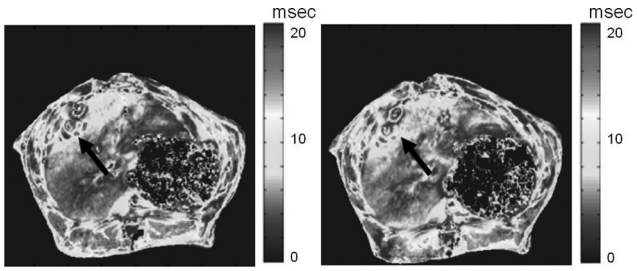

Fig. 1. T2* maps demonstrated decreased relaxation times in the tumor after infusion of labeled NKs.

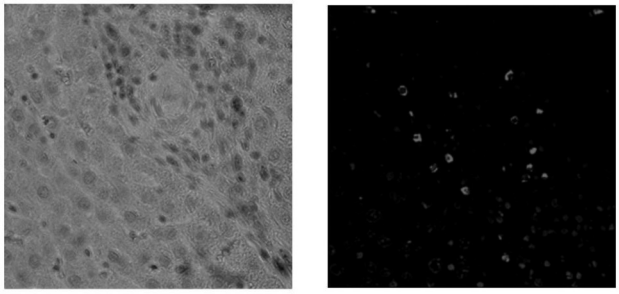

Fig. 2. Prussian blue iron staining and fluorescence microscopy confirmed selective delivery of labeled NKs to the tumor but not to normal liver.

Paper 31: 7T MRI Accurately Quantifies Intratumoral Uptake of Nanotherapeutics in a Rat Model of Liver Cancer

P. Tyler, A.Y. Sheu, D. Procissi, R.J. Lewandowski, A.C. Larson, R.A. Omary

Objectives: Interventional oncologists require animal models of hepatocellular carcinoma (HCC) to develop and test innovative therapies. An ideal animal model would show histological and physiological similarity to HCC, with blood vessels large enough to permit IV or IA delivery of therapies. The McA-RH7777 (McA) tumor model in Buffalo rats is both hypervascular and resembles HCC histologically; however, the rats' small anatomy limits utility for investigating IO procedures. The larger Sprague-Dawley (SD) rat provides more favorable anatomy, but its native N1S1 tumor is less vascular than HCC. In this study, we aimed to test the hypotheses that: a) McA tumors can be grown in SD rats; and b) high-field MRI can enable quantification of intra-tumoral uptake of doxorubicin-loaded iron oxide nanoparticles (Dox-SPIOs).

Methods: To test the hypothesis that the McA tumor could be implanted in SD rats, we injected 1x10^6 McA cells into the left lobe of the liver in SD rats (n=14) using a previously described subcapsular implantation technique. MRI scans were taken 14d post-implantation, and tumor dimensions were characterized using descriptive statistics. To test the hypothesis that this model could be used for drug uptake studies, therapies were administered on day 14 after implant. We delivered Dox-SPIOs IV via the femoral vein (n=7) or IA via the proper hepatic artery (n=1). McA tumor controls (n=2) were infused with saline. We obtained pre- and post-treatment R2*-weighted images (Fig 1) using a 7T Bruker MRI scanner. After euthanasia, we used trace metal-grade nitric acid to dissolve the tumors. We measured tumor iron concentration ([Fe]), an indicator of Dox-SPIO uptake, using inductively-coupled plasma mass spectroscopy (ICPMS). We used Jim software (Xinapse, UK) to analyze images. Mean signal intensities, weighted by area, were averaged across five tumor slices for each pre- and post-treatment image to obtain ΔR2*. Three identical sets of nanoparticle phantoms were used to validate image analysis methods. We calculated the Pearson coefficient (r) to assess linear correlation between ΔR2* and [Fe], in phantoms and in vivo.

Results: Tumors grew successfully in 10/14 implanted rats (success rate = 71%). Maximum tumor diameter (Dmax) ranged from 0.65-1.2 cm. Mean Dmax was 0.92+/-0.14. Phantom studies revealed a strong positive correlation between ΔR2* and [Fe], with r=0.99 (p<0.01). In vivo drug uptake studies showed significant positive correlation between ΔR2* and [Fe], with r=0.70 (p=0.015).

Conclusions: McA tumors can successfully be grown in SD rats. This animal model is of a suitable size that the hepatic artery can be catheterized for drug delivery and the tumors can be identified with MRI. MRI quantification of intra-tumoral uptake strongly correlated with Dox-SPIO concentrations in pathological specimens. This finding suggests that imaging may be used to estimate the uptake of iron-oxide nanotherapeutics. In the future, these imaging methods could potentially be used as a tool to quantify drug delivery in patients.

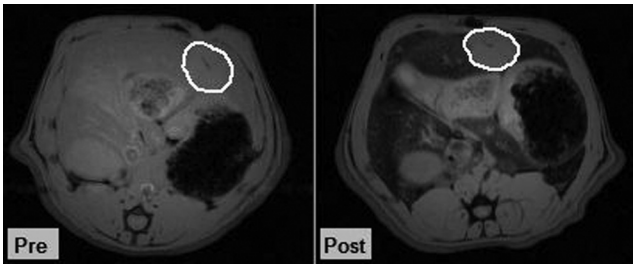

Fig 1. Pre-treatment (left) and post-treatment (right) T2* weighted images acquired using a gradient echo pulse sequence showing loss of signal intensity in the hepatic parenchyma and the tumor (white boundary). In the post-treatment scan, the liver has relatively greater signal loss than the tumor due to increased uptake of the Dox-SPIOs within the normal liver's Kupffer cells.

Paper 32: Intravenous Vasopressin for the Prevention of Non-Target Gastrointestinal Embolization During Liver Directed Cancer Treatment: Experimental Study in a Porcine Model

J.C. Durack, T.A. Hope, M.W. Wilson, M. Saeed, R.K. Kerlan, E.J. Ring

Objectives: Previous studies have demonstrated a relative redistribution of hepatic arterial blood flow to liver tumors after administration of vasoconstricting agents such as epinephrine, angiotensin II or vasopressin. Our objective was to determine whether vasopressin may also reduce the risk of non-target gastrointestinal embolization during transcatheter liver directed cancer treatment in a porcine model.
Methods: An angiographic catheter was used to select the celiac or common hepatic arteries under fluoroscopic guidance in six anesthetized healthy pigs. After angiography of hepatic and splanchnic territories was performed, 99mTc-MAA was injected through the catheter. Serial arteriograms were obtained while 0.4 units per minute of vasopressin were infused through a peripheral vein. After 10 minutes of infusion, 111In-MAA was injected through the arterial catheter. Changes in arterial blood flow before and after vasopressin infusion were evaluated by contrast angiography and dual isotope SPECT/CT imaging. Quantitative comparisons of liver activity and gastrointestinal activity within regions of interest on SPECT/CT imaging were performed.
Results: Catheter angiography demonstrated markedly reduced blood flow to the splanchnic vasculature while maintaining blood flow in the hepatic arteries during vasopressin infusion. Angiographic findings correlated with the relative distribution of 99mTc-MAA (pre-vasopressin) and 111In-MAA (post-vasopressin) on SPECT/CT. An increase in the ratio of liver to gastrointestinal tract activity before vasopressin and during the administration of vasopressin was statistically significant (6.2 to 11.4 respectively, p=0.018).
Conclusions: In this pre-clinical study, we obtained pharmacoangiographic and nuclear imaging evidence that intravenous vasopressin reduces arterial blood flow to the splanchnic vasculature while preserving hepatic arterial blood flow. Vasopressin may be clinically beneficial for prevention of unintended bland embolic, chemoembolic or radioembolic agent delivery into gastrointestinal vascular territories during liver-directed endovascular cancer treatment.

Paper 33: Percutaneous Cryoablation for Pancreatic Cancer: Feasibility and Safety Assessment

L. Niu, L. He, L. Zhou, B. Wu, J. Zuo, K. Xu

Objectives: To describe the preliminary experience of percutaneous cryoablation for pancreatic cancer using ultrasonography (US) and computed tomography (CT) guidance, and to assess the feasibility and safety of the procedure.
Methods: Thirty-three pancreatic tumors in 32 patients were treated with 52 times of percutaneous cryoablations guided by US and CT; cryoprobes were percutaneously placed with real-time monitoring. Subsequent cryosurgeries or brachytherapies were performed for residual lesions. Clinical signs and symptoms were assessed 1-3 months after cryoablation.
Results: No serious complications occurred in these patients. Six tumors were successfully ablated at the first session of cryoablation, and the remainders were controlled using percutaneous cryoablation combined with brachytherapy during subsequent sessions. Twenty-seven patients experienced a ≥50% reduction in pain score, 22 experienced a 50% decrease in analgesic consumption and 16 experienced an ≥20 increase in KPS Score. Partial response, stable disease and progressive disease turned up in 9, 21 and 2 patients, respectively, with mean and median survival of 15.9 and 12.6 months, respectively. The 6 -, 12- and 24-month survival rates were 82.8%, 54.7% and 27.3%, respectively.
Conclusions: US and CT guided percutaneous cryoablation is a safe and promising local treatment for pancreatic tumors.

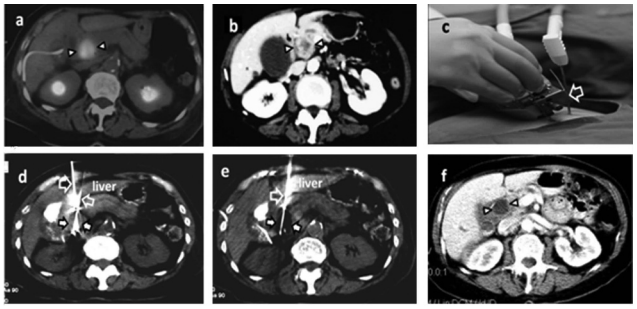

FIGURE 1. Therapeutic data of a 74-year-old female patient who suffered from adenocarcinoma on pancreatic head. The tumor (arrow head) was 3.7×3.6×3.1 cm, stage IIa, detected by PET-CT (a) or CT (b). The procedure was performed with a cryoprobe (hollow arrow) approaching through the left liver lobe (c) and the center of the mass to the inner border of the mass (d), and two freeze-thaw cycles gradually enlarged the ice ball (arrow) until it completely covered the mass (e). A contrast enhanced CT image 3 months after cryoablation (f) depicts non-enhancement in the site of the tumor (arrow head).

Patients' Characteristics

Characteristics	N	Survival (%)		P-value
		6-months	12-months	
Age, years				
Median	62 (Rang, 30-77)			
<62	15	12/14 (85.7)	7/14 (50.0)	0.857
≥62	17	12/15 (80.0)	6/11 (63.6)	
Sex				
Male	18	13/15 (86.7)	8/13 (64.6)	0.272
Female	14	11/14 (78.6)	5/12 (44.2)	
Pancreas tumor location				
Head of pancreas	13	10/12 (83.3)	6/10 (64.3)	0.133
Body and/or tail of pancreas	19	14/17 (82.4)	7/15 (48.4)	
Max diameter of tumor, cm				
Mean (mean ± SE)	5.2 ± 0.3 (Rang, 2.0-11.0)			
>2, ≤5	16	13/15 (86.7)	6/11 (60.5)	0.671
>5	16	11/14 (78.6)	7/14 (50.0)	
Stage				
II	3	2/2 (100.0)	1/1 (100.0)	0.973
III	11	8/10 (80.0)	4/9 (46.7)	
IV	1	14/17 (82.4)	8/15 (56.1)	

Paper 34: A Novel Method for Bone Tumor Radiofrequency Ablation

M. Gofeld, A. Yee, J. Woo, C. Whyne, M. Akins

Objectives: Radiofrequency ablation (RFA) is a percutaneous technique utilizing high frequency oscillating electrical current emitted from a specially designed canulla, which generates heat in the surrounding tissue leading to cell death. RFA of the bone tumors has been challenging because bone is less thermally and electrically conductive than soft tissue. Furthermore, due to the large size and high vascularity of tumors, it is difficult to generate sufficient heat to effectively treat anatomically relevant volumes with currently marketed RF technologies. A new internally cooled bipolar probe design allows creation of large lesions in heterogeneous bone tumor tissues in a consistent and controlled manner.
Methods: The efficacy of the bipolar RF ablation system was evaluated in a VX-2 metastatic carcinoma rabbit model. To evaluate the pre-clinical safety of the RFA system, RF lesioning was performed in a scale-up healthy porcine model with vertebral dimensions more relevant for potential human applications. First human cases were done under either general or local anesthesia, with or without subsequent vertebral augmentation.
Results: All RFA procedures in the rabbit femurs produced the desired controlled temperature response, demonstrating the ability of the RF system to generate tissue heating in bone tumors. MRI analysis of the treated femurs showed uniform ellipsoid lesions of 3cm x 2cm, while histology revealed corresponding tumor cell death (Figure 1). The RF system also effectively created precise lesions in porcine vertebrae. Follow-up MRI revealed clinically and anatomically relevant lesions spanning half the vertebrae (average 2.5cm x 1.3cm). All animals demonstrated normal behavior during neurological assessment following the procedure. The system (Osteocool, Baylis Medical, Canada) was approved by FDA for palliative symptom control related to vertebral metastases. FDA 510k for tumor destruction is pending Human cases were technically and clinically successful. The device placement was straightforward and performance of Baylis RF Generator was according to methodological profile (Figure 2). Patients tolerated procedure well under local anesthesia and sedation.
Conclusions: Osteocool is the first FDA-approved RF system for palliation of metastatic vertebral malignancies which utilizes an internally cooled technology incorporated into a single electrode with bipolar contacts. Other currently available devices are either off-labelled or monopolar and often requires multiple placements or number

of probes to complete planned procedure. Minimally-invasive, quick and reliable method to ablate large tumors located in a high-resistance bone tissue is particularly desirable to achieve symptom control in these medically and antomically complicated patients. This novel internally cooled bipolar probe design has proven to be effective at creating lesions in diseased and healthy bone that are anatomically relevant in size and shape.

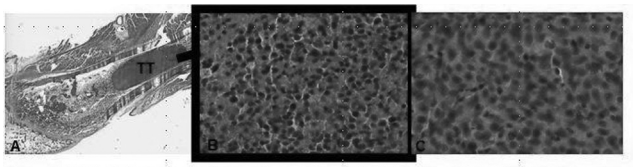

Figure 1. H&E staining showing treated tumor (TT) region in the femur (A). RF ablated tumor cells in the treated tumor (B) is shown in contrast to untreated tumor cells (C).

Figure 2. Computed tomography guided radiofrequency ablation of metastatic tumor of the L3 vertebral body

Paper 35: Effect of Irreversible Electroporation (IRE) on Bile Ducts Following Treatment of Primary and Metastatic Liver Tumors – A Single Center Retrospective Analysis

G. Narayanan, V. Sarode, K.J. Barbery, G. Guerrero, G. Mohin

Objectives: IRE is a non thermal ablative modality that uses high voltage DC current to ablate tissue. Animal studies have demonstrated that bile ducts to be more resistant to the effects of IRE along with the lack of the heat sink effect coomonly seen with thermal ablative techniques. The purpose of this HIPAA compliant retrospective study was to evaluate the effects of IRE on bile ducts in humans, following treatment of hepatocellular carcinoma (HCC) and metastatic liver tumors.
Methods: Between January 2010 and December 2011, 76 patients with primary and metastatic tumors involving the liver had 114 IRE treatments with the Nanoknife (Angiodynamics, NY). All procedures were performed with CAT scan (CT) guidance under general anesthesia and complete muscle relaxation. Thirty-six patients had primary HCC and 40 patients had metastatic disease involving the liver. Patients' age ranged between 40 – 83 years, with a mean of 61 yrs. Forty-seven males and 29 females were treated. Forty-five patients had one treatment, 26 patients had 2 treatments, 3 patients had 3 treatments and 2 patients had 4 treatments. All patients had at least a one month follow up imaging post treatment. Follow up range was between 1-24 months. The appearance of bile ducts in close proximity to the treatment zone, was evaluated prior to, and after IRE treatment with CT and/or Magnetic Resonance imaging. Close proximity was defined as ducts within 0.5 – 1cm from the treatment zone. Bilirubin, AST (Aspartate aminotransferase), ALT (Alanine transaminase) and Alkaline Phosphatase levels pre and post procedure, were analyzed in patients who demonstrated anatomic changes in the bile ducts post IRE.
Results: Mild biliary dilatation was seen in 4/79 (5%). We did not identify strictures or stenosis involving the bile ducts in these patients. Three of the 4 had an increase in the total bilirubin, of which 2 were still within the normal range. One had an increase of bilirubin from 0.7 to 1.9 mg/dl, which dropped to 1.6 mg/dl a month later. Mean increase in bilirubin was 0.6 mg/dl. Two out of the 4 patients had an increase in alkaline phosphtase levels and 2 had a decrease post procedure. None of the patients had bile duct related complications such as fistula or leaks. Five patients had mild dilatation prior to the treatment, which was unchanged post IRE in follow up imaging.
Conclusions: IRE treatment in the liver is well tolerated and does not seem to impact the bile ducts in a significant manner, similar to the results observed in animal studies.

Paper 36: Anti-vascular Ultrasound: Validation of Treatment Effects with Contrast-enhanced Ultrasound, Dynamic Contrast-enhanced Magnetic Resonance Imaging and Histopathology

S. Hunt, M.C. Soulen, C. Sehgal

Objectives: To validate the treatment effects of anti-vascular ultrasound (AVUS) with dynamic contrast-enhanced magnetic resonance (DCE-MR) and ultrasound (CE-US) imaging and histopathology in a murine melanoma model.
Methods: Subcutaneous K1735 murine melanoma tumors were grown in syngeneic C3H/HeN mice to approximately 1 cm maximal diameter. Quantitative tumor perfusion characteristics were measured immediately prior to treatment with both high-resolution CE-US and DCE-MR at 9.4 tesla. Tumors were subsequently treated with 1 or 3 minutes of continuous low-intensity ultrasound (2.3 W/cm2) at 3 MHz frequency after intravenous administration of Definity ultrasound contrast. Controls received 3 minutes sonication in the absence of Definity. Immediate and delayed anti-vascular effects were subsequently re-assessed by quantitative CE-US, DCE-MR, and histopathology.
Results: Low-intensity AVUS treatment results in potent qualitative and quantitative reduction in tumor perfusion as assessed by both CE-US and DCE-MR imaging. After treatment, tumors develop regions of T1 shortening with delayed enhancement and washout kinetics consistent with an antivascular effect. The effect was significantly enhanced at 3 minute vs 1 minute AVUS. These regions correlate with intratumoral hemorrhage on gross pathology. Histologic findings include dilatation of tumor capillaries, intratumoral edema and perivascular hemorrhage, the extent of which correlates with length of treatment. Non-hemorrhagic portions of treated tumors demonstrate apoptotic changes, presumably due to secondary ischemia. Low-intensity sonication in the absence of microbubbles did not demonstrate measurable effects on tumor perfusion kinetics or histopathology.
Conclusions: Contrast-enhanced ultrasound holds great promise for both diagnostic and therapeutic applications in oncology. AVUS treatment effects are exposure-dependent, and correlate well across imaging modalities and histopathology. Immediate effects on tumor vascularity and perfusion characteristics correlate with intratumoral hemorrhage and translate into delayed effects on tumor necrosis. Sonication in the absence of contrast microbubbles fails to replicate the treatment effects, demonstrating the importance of microbubbles in generating the local therapeutic effects.

Paper 37: The Impact of Variation in Portal Venous Blood Flow on the Size of the Radiofrequency and Microwave Ablation Lesions in In-Vitro Blood Perfused Bovine Livers

G.D. Dodd, N.A. Dodd, A.C. Lanctot

Objectives: To assess the impact of variation in portal venous flow on the size of radiofrequency (RF) and microwave (MW) ablation lesions in in-vitro blood perfused bovine livers.
Methods: 60 ablations (2 MW and 2 RF ablations/liver) were performed in 15 bovine livers perfused with autologous blood via the portal vein at 60, 70, 80, 90, and 100 ml/min/100g liver (3 livers/flow rate). Length, width, and volume were measured/calculated for each ablation lesion.
Results: The mean ablation volumes for the 5 flow rates (low to high) were 12.54, 8.00, 5.41, 5.31, and 3.72 for RF, and 22.00, 21.30, 22.37, 22.61, and 21.66 for MW, respectively. The slopes were -0.204 ± 0.03 ($S_{y.x} = 2.23$, $F = 50.54$, $p < 0.0001$) for RF, and 0.006± 0.018 ($S_{y.x} = 1.397$, $F = 0.11$, $p = 0.75$) for MW.
Conclusions: The size of RF ablation lesions is highly variable with a statistically significant inverse relationship to the rate of portal venous blood flow; conversely, the size of MW ablation lesions is unperturbed by changes in portal venous blood flow. The consistency of the size of MW ablation lesions could translate into a higher local tumor eradication rate than reported with RF ablation.

Paper 38: Cooled Dual-Slot Microwave Antenna Optimization to Create More Spherical Ablation Zones

J. Chiang, K. Hynes, M. Bedoya, C. Brace

Objectives: Long treatment times and higher applied powers can lead to elongated ablation zones with many microwave systems. The elongated ablation zone can extend across healthy tissue and may preclude the use of such high-powered ablation systems. A dual-slot antenna has been previously described to reduce ablation length but the bare coaxial geometry was not suitable for percutaneous use. Here, we present a clinically-viable, cooled, dual-slot antenna design that can create a spherical ablation zone and decrease the risk for unnecessary tissue damage.

Methods: The dual-slot antenna geometry was modified to incorporate a cooling chamber and rigid tip into a 17-gauge profile. A numerical study was performed to optimize slot widths/spacing, feed spacing/location and ceramic tip dimensions. A cost function selected the antenna with maximal energy delivery efficiency and minimal heating pattern elongation. This cooled dual-slot antenna was fabricated and applied to ex-vivo bovine liver tissue at 50 and 100 watts for 2 and 5 minutes. A cooled monopole antenna was used as a control to compare ablation size (diameter and length) as well as the aspect ratio, defined as the ablation diameter divided by length.
Results: The optimal antenna design utilized the coaxial cable as a feeding port into the ceramic, which acted as the radiating structure. When applied at 50 W for 2 and 5 minutes, the cooled dual-slot design produced ablation zones that were significantly shorter in length ($p<0.02$) compared to those created by a cooled monopole antenna. As a result, the dual-slot antenna produced ablations with a significantly greater aspect ratio than the monopole antenna ($p<0.05$), suggesting a more spherical ablation zone. At a higher power setting of 100 W, the dual-slot antenna produced a significantly greater ablation diameter at 2 minutes ($p<0.05$) compared to the cooled monopole, again leading to a significantly greater aspect ratio ($p<0.01$). However, at 5 minutes, the ablation dimensions were not significantly different.
Conclusions: The cooled dual-slot antenna created ablation zones that were significantly more spherical than the monopole antennas. Differences were more pronounced when using lower powers and shorter ablation times; therefore, more control over the ablation zone may be achieved by using shorter times or limited powers. Better cooling and fabrication methods can potentially extend the benefits of the cooled dual-slot antenna to higher powers and longer treatment periods.

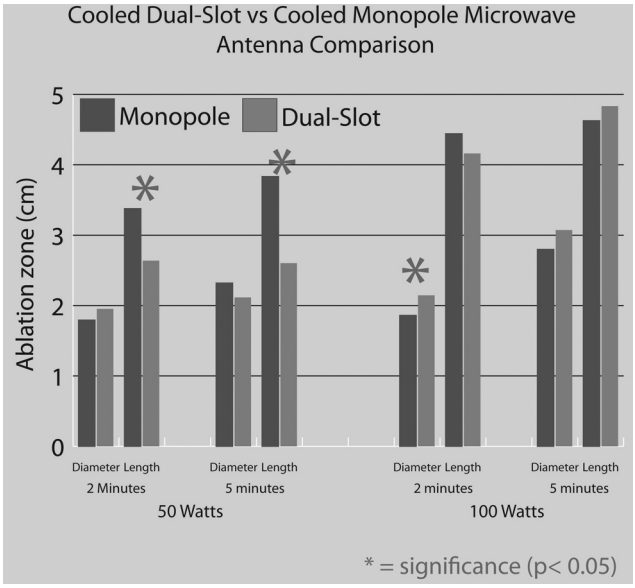

Ablation of cooled dual-slot antenna (left) and monopole antenna (right) at 50 W, 5 minutes

Paper 39: Tumor Volume Comparison Between Semi-Automatic Tumor Segmentations on CBCT and MDCT, and Pathologic VX2 Rabbit Hepatic Tumor Model

O. Pellerin, M. Lin, N. Bhagat, J.H. Geschwind

Objectives: The purpose of this study is to compare the tumor volume in a VX2 rabbit model as calculated by semi-automatic tumor segmentation from C-arm cone-beam CT (CBCT) and multi-detector CT (MDCT) images to the actual tumor volume.
Methods: 20 VX2 tumors in 20 adult male New Zealand rabbits (1 tumor per rabbit) were imaged with CBCT (using an intra-arterial contrast medium injection) and MDCT (using intra-venous contrast injection). All tumor volumes were measured by using a semi-automatic 3D volumetric segmentation software. The software uses a region-growing method employing non-Euclidean radial basis functions. After imaging, the tumors were excised for pathologic volume measurement. The imaging based tumor volume measurements were compared to the pathologic volumes using linear regression, with Pearson test, and correlated with Bland–Altman analysis.
Results: Average tumor volumes were 3.53cm3±1.57 [1.36–7.20] on pathology examination; 3.80cm3±1.58 [1.32–7.26] on CBCT; and 3.90cm3±1.59 [1.76–7.53] on MDCT ($p<0.001$). A strong correlation between pathology and CBCT and also with MDCT volumes was observed (Pearson correlation=0.993; and 0.996, $p < 0.001$, for CBCT and MDCT, respectively). The Bland–Altman analysis showed that MDCT scans tended to overestimate tumor volume, and there was a stronger agreement between CBCT and pathology tumor volume than with MDCT, possibly due to the intra-arterial contrast injection.
Conclusions: The tumor volume as measured by the semi-automatic tumor segmentation software showed a strong correlation with the "real volume" measured on pathology. Use of the segmentation software on CBCT and MDCT can be a useful tool for volumetric hepatic tumor assessment.

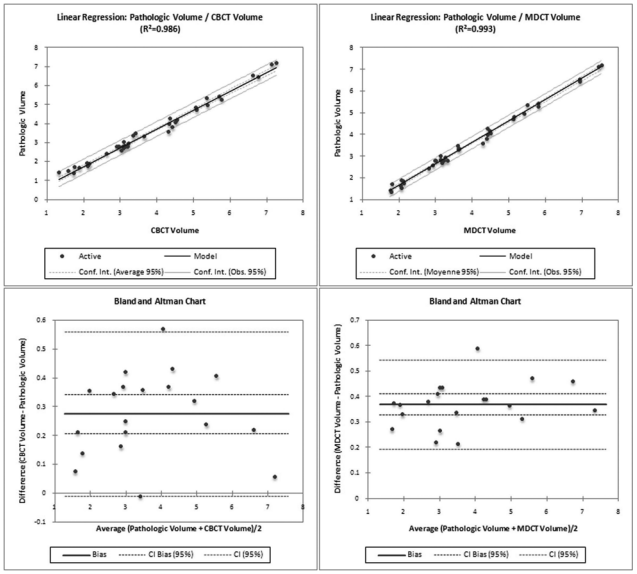

Linear regression curves for tumor volume resulting from CBCT (A) and from MDCT (B). The dotted line represents the ideal situation of absolute agreement between the two modalities. Bland- Altman Plots showing the difference against mean for the two images modalities (C)-CBCT, and (D)-MDCT. The red dotted lines represent the confidence interval around the mean difference, making the level of agreement between the different image modalities.

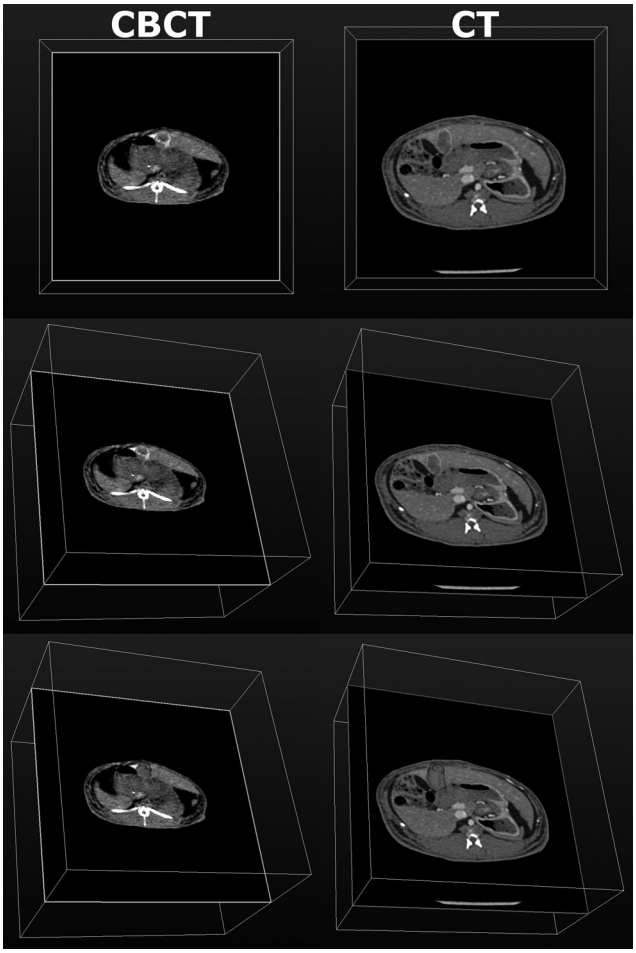

CBCT (right column) and MDCT (left column), image after tumor segmentation. Two first row shows a two different level the tumor segmented by the "elastic band." The third row, shows the 3D projected volume on a single axial slice. Note that the tumor position on CBCT (right column) and MDCT (left column) look slightly different. This is due to liver sliding when positioning the rabbit on two different position on the examination table.

Paper 40: Pathologic Cancer Staging by Measuring Cell Growth Energy

E.Y. Moawad

Objectives: Establishment of a pathologic cancer staging by measuring Cell Growth Energy (CGE) contributes to treatment management and helps to administer the appropriate low-waste dose for all cancer therapies.

Methods: Regarding cancer as a result of energy balances; Nitrogen-containing bisphosphonates (NBPs) alendronate (ALN) of different concentrations were added to samples of Normal Human Epidermal Keratinocytes (NHEKs) (20,000Cell /sample) to inhibit their growth rate to model cancer effects on normal cells, [C-14] thymidine was added at 0.5 Micro Ci/ml to each of control sample and those of cell cycle arrest (with NBPs) to monitor the Cell Growth Energy (CGE) which expresses all aberrant activations of cell that lead to cancer development and simply describes the cancer stage of the cell. Radioactivity incorporated (% of control) at 37°C was determined as a measure of cell rate of growth at 24-h intervals for 3 days using a Top Count NTX micro plate scintillation counter.

Results: NHEKs rate of growth for sample with NBPs of concentration 10 M ALN was the closest to that of induced carcinomas, equivalent to 87% of that of the normal counterpart as measured by [C-14] thymidine incorporation. As inhibition to rate of growth of this sample was 13% compared to the control, cell doubling time was increased consequently to 1.13 times that of cells at the stage of the control sample. Equalizing sample growth energy gained due to cell cycle arrest to the energy of the induced inhibition to [C-14] thymidine incorporation, CGE of this sample was 4,862 MeV =0.21 Emad, which corresponds to cell doubling time according to Emad formula equivalent to 1.12 times that of cells at the stage of Natural Background Radiation which is 99% identical to what has been measured experimentally at 1.13 times that of control cells to confirm and to provide a clear-cut criterion for accepting the CGE test for cancer staging.

Conclusions: Validity of staging classification of CGE as a diagnostic tool recommends to be considered as more reliable test with promising efficacy and low costs to obtain a more accurate assessment as to whether cancer is present, besides to staging as well. Staging of CGE provides the possibility to investigate effects of the human-caused background radiation, and that of all cancer causes.

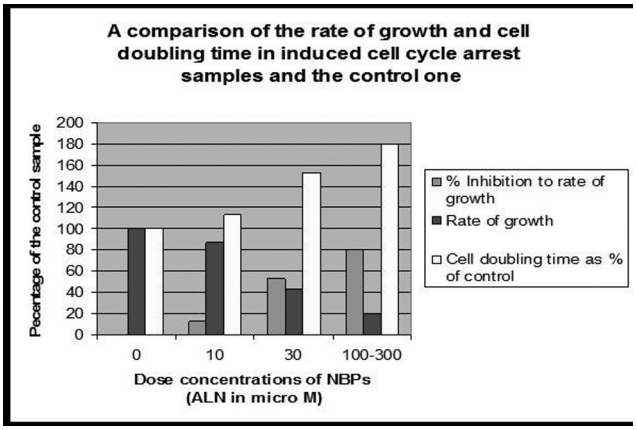

Figure 1. shows a comparison of the rate of growth and cell doubling time in induced cell cycle arrest samples and the control one.

Paper 41: ZBP-89 is Required for p21Waf1-Mediated Apoptosis in Hepatocellular Carcinoma

G.G. Chen, C.Z. Zhang, S. Chun, P.B. Lai

Objectives: p21Waf1 (p21) is often considered as a tumor suppressor in cancer as it promotes the apoptosis in tumor cells via interacting with p53. The inhibitory effect of ZBP-89 is executed through binding to GC-rich elements of gene promoters. Interestingly, the p21 promoter is rich in GC, suggesting that the expression of p21 may be regulated by ZBP-89 in HCC cells. The aim of this study was to examine the role of ZBP-89 in the interaction between p21 and p53 in human hepatocellular carcinoma (HCC) treated with histone deacetylases inhibitors (HDACi).

Methods: HCC cells were treated with HDACi Trichostatin A (TSA) or Sodium butyrate (NaB). Immunofluorescence, immunoprecipitation, immunohistochemistry, immunoblotting, RT-PCR, RNA interference and TUNEL assays were employed to study the ZBP-89, p21, p53 and apoptosis.

Results: Our result showed that NaB or TSA treatment caused more apoptosis in PLC/PRF/5 cells with p53R249S mutant but less apoptosis in HepG2 cells with wild-type (WT) p53. The inhibitory effect of NaB or TSA was associated with an increase in p21. ZBP-89 siRNAs effectively abolished NaB-induced expression of p21 and prevented apoptosis induced, indicating that ZBP-89 is required for NaB/TSA-mediated p21 induction. By analyzing HCC cells with p53 mutants, p53G245D and p53R273C, we found that p53G245D but not p53R273C, abrogated NaB-mediated induction of p21 by directly binding to ZBP-89 and preventing its translocation from the cytoplasm to the nucleus. Functionally, the cytoplasmic import of ZBP-89 by p53G245D significantly protected cells from the death caused by HDACi.

Conclusions: In conclusion, our data have demonstrated that p21 plays a critical role in HDACi-mediated apoptosis of HCC cells, and that ZBP-89 is required in p21-mediated apoptosis. Our findings also indicate that some p53 mutants can abrogate the ZBP-89- and p21-mediated death pathway in HCC cells. The results of our findings may suggest a novel approach to optimize anti-HCC treatment by checking the state of p53 which may interfere with the ZBP-89 and p21 pathway.

Paper 42: Nanocytomics-Based Assessment of Transcriptional Activity of Malignant/Premalignant Cells

A.K. Tiwari, H. Subramanian, V. Backman, H. Roy

Objectives: Perturbation of the transcriptional status of a cell is a hallmark feature of all biological processes. An ability to assess perturbation in the transcriptional activity of cells could easily translate into a useful tool for cancer risk-stratification and drug-responsiveness of cells. However, assessing the overall transcriptional activity has been incredibly difficult. Our group has developed a novel optical technique, partial wave spectroscopy (PWS) nanocytomics, which has allowed us to quantify nanoscale architecture by measuring the spatial fluctuation in the refractive index through a parameter called, disorder strength (Ld) (PNAS 2008, Gastro 2011). We herein hypothesized that changes in high-order chromatin organization, which are beyond the resolution of conventional light microscopy and precede any alteration in transcriptional activity, could be quantified with PWS microscopy, and thus help us in assessing the perturbation of transcriptional activity of cells.

Methods: PWS studies were performed on human colon cancer cell line, HT29, after altering their transcriptional activity by exposing them to different growth conditions (starvation and treatment with Epidermal growth factor, EGF; and Phorbol-ester, PMA). Resulting phenotypes were analyzed with light microscopy and flow-cytometry. Overall transcription was assessed by genome wide mRNA expression profile using Illumina human HG12-T chips. Similar experiments were performed with HT29 cells stably transfected with a specific shRNA against ARID1a, a component of high-order chromatin remodeling complex, Swi/Snf.
Results: Transcriptional modulation of HT29 cells was coupled with change in their behavior (proliferation/apoptosis) and was reflected in significant changes in nuclear Ld (increased with EGF and PMA, and decreased with starvation, Image 1, 2). Additionally, short-duration treatments (<30 mins) led to changes in Ld comparable to long-duration treatment (~5hrs), suggesting that nuclear Ld changes are the result of reorganization of pre-existing nuclear structures rather than addition of new mass/structures. Moreover, ARID1a-deficient HT29 cells (shRNA knock-downs), which showed no change in proliferation/apoptosis upon treatments, also didn't show any change in nuclear Ld, implicating high-order chromatin-remodeling in determination of nuclear Ld. Also, through mRNA expression profiling Illumina human HG12-T chips, we proved that nuclear Ld changes don't reflect heterogeneous genetic/epigenetic changes, but their nanoarchitectural consequences.
Conclusions: We herein demonstrated that nuclear Ld could become a surrogate marker of the transcriptional perturbations in a cell. Because subtle changes in transcriptional activity are inherent features of carcinogenesis and drug-responsiveness, PWS nanocytomics could potentially emerge as a novel non-invasive optical technique for cancer risk-stratification and chemoresponsiveness assessment.

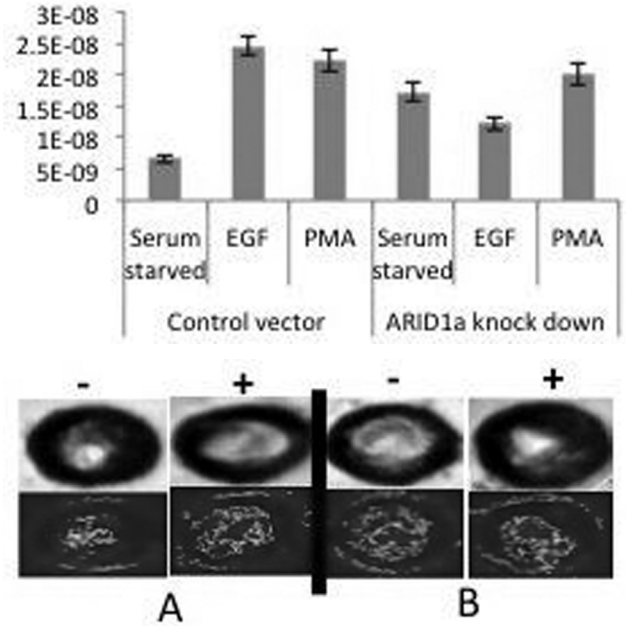

A: HT29; B: ARID1a deficient HT29
Upper panel: high-resolution images
Lower panel: heat map (Ld)
+ means transcriptional stimulation
- means transcriptional silencing

Paper 43: Trans Arterial Hepatic Embolization (TACE) Adopting Polyvinal Alcohol Microspheres Preloaded with Irinotecan (DEBIRI) versus Systemic Therapy (FOLFIRI) for Liver Metastases (LM) from Colorectal Cancer (CRC): A Randomized Study of Efficacy, Toxicity and Quality of Life

G. Fiorentini, C. Aliberti, P. Coschiera, M. Cantore, L. Mulazzani, V. Catalano

Objectives: Surgical resection of LM from CRC continues to remain a potential curative option; however, 70% of patients have unresectable disease at presentation, and the long-term survival rate remains low for these patients. TACE using DEBIRI (D) is a feasible procedure. FOLFIRI (CT) is active for the treatment of CRC. We planned a phase III study to assess survival as primary endpoint to increase median overall survival (MOS) by 40% at 2-y (HR=0.72). QoL, responses, progression free survival (PFS), costs and safety are secondary endpoints.
Methods: Between December 2006 and December 2008, 74 pts were randomized, 38 patients to D (DC Beads loaded with IRI 200 mgr total dose) and 39 to CT. Two D patients had early progression, one refused and four CT patients refused. 70 cycles of D were administered in 35 pts, with a dose intensity (DI) of 99%, and 292 CT cycles were delivered to 35 pts with a DI of 90%.
Results: At a median follow up of 47 months (38-60) we reported (D vs CT): MOS 56% vs 32% at 24 months, 34% vs 9% at 36 months, 15% vs 0% at 50 months; Response Rate 68.6% vs 20%; Acute Toxicity 70% vs 20%; Late Toxicity 20% vs 80%; QoL improvement 65% vs 25%, Costs for each patient 7,000 vs 24,000 Euro.
Conclusions: D increased the 24-36-50 Months MS compared to CT. D improved responses, Performance Status and reduced costs. D reported higher immediate toxicity, mainly fever and abdominal pain than CT. Late toxicity, mainly haematological, diarrhea, asthenia and alopecia, was more common in CT. We conclude that D compared to CT increases survival and palliative results.

Paper 44: Transarterial Chemoembolization for Metastatic Colorectal Liver Metastases Using M1 DC Beads®: Initial Experience

A. Farghal, T. Cabrera, D. Valenti

Objectives: This is a pilot study aiming to evaluate the efficacy, patient tolerance and potential complications of chemoembolization with M1 DC beads® (70-150 μm) versus (100-300 μm) beads loaded with 100 mg Irinotecan for colorectal liver metastases.
Methods: All patients with metastatic colo-rectal liver cancer (mCRC) treated with DC beads from June 2010 to January 2012 were included in this study. Beads were loaded with 100 mg Irinotecan. Efficacy was evaluated by measuring the largest axial diameter of the largest enhancing lesion in the pre- and post-embolization contrast enhanced CT. Patient tolerance to treatment was assessed by counting the days of inpatient admission post-chemoembolization as a result of post procedure pain. Embolization related complications were also assessed.
Results: 15 patients were treated from January 2011 to January 2012, 8 of which treated with M1 DC beads and 7 patients were treated with 100-300 microns DC beads; all were loaded with 100 mg Irinotecan. Target lesions increased in size by a mean of 14% over a mean of 84 days in the M1 group versus 32% increase in the (100-300 μm) group over a mean of 41 days. All patients had rapid onset right upper quadrant pain in the M1 group and 3 Patients required admission for an average of 2.3 days. None of the (100-300 μm) group required admission. One patient of the M1 group had post-procedure abscess.
Conclusions: Our initial experience showed that the M1 DC beads are more effective than the 100-300 μm size beads, however the treatment was more painful and required admission for one-third of the patients.

Paper 45: The Use of Therasphere in Metastatic Liver Tumors: Risk Factors Associated with Poor Prognosis

D. Conners, J. Zechlinski, S.B. White, R.A. Hieb, P.J. Patel, W.S. Rilling

Objectives: Liver-directed therapies and Y-90 radioembolization specifically are being used increasingly to treat primary and secondary liver cancer. While prognostic factors influencing patient selection are fairly well defined for HCC, much less is known for patients with liver metastases. The purpose of this study is to define prognostic factors associated with poor survival following Y-90 radioembolization in patients with liver metastases being treated in the salvage setting.
Methods: The institution review board approved this retrospective study. Retrospective review of patients with hepatic metastases treated with Y-90 radioembolization in a six-year period at our institution was performed. Malignancies included neuroendocrine (N=26), colorectal (N=22), and all other primaries (N=22). Notably, neuroendocrine metastases were treated after failure of sandostatin and/or TACE. Variables assessed included performance status, presence of extrahepatic disease, percent hepatic tumor burden, bilirubin, albumin, prothrombin time, creatinine, and glomerular filtration rate. Pre-treatment angiography was also evaluated for evidence of fibrosis to determine if this would adversely affect survival. Ninety-day survival was calculated from the day of radioembolization treatment.
Results: Seventy patients underwent 94 radioembolization sessions for salvage treatment of metastatic disease. Eighty percent (N=56) were alive at 90 days, with median survival of 228 days (95% CI 157-381). Survival was significantly affected by albumin. Even at normal levels, a decrease in albumin of 0.1 g/dL corresponded to a 25% increase in odds of death at 90 days (p=0.01), by logistic regression analysis. The remaining variables including performance status, presence of extrahepatic disease, percent hepatic tumor burden, bilirubin, prothrombin time, creatinine, and GFR did not significantly affect survival. Angiographic evidence of fibrosis had no significant influence on survival.
Conclusions: Albumin was found to negatively impact survival at 90 days following Y-90 radioembolization for treatment of metastatic hepatic tumors. This finding may have clinical impact, as the treatment cohort has strict pre-procedure selection criteria, including performance status, laboratory analysis, and imaging evaluation. The fact that albumin significantly impacted survival within the treatment cohort suggests that stricter selection criteria for albumin may be necessary. However, further study is warranted to verify these results.

Paper 46: Percutaneous Microwave Ablation with High-Powered, Gas-Cooled Antennas: Short-Term Results in 52 patients

T. Ziemlewicz, J. Hinshaw, M. Lubner, C. Brace, S. Wells, F.T. Lee

Objectives: Microwave (MW) ablation is a promising technology that offers several advantages over radiofrequency (RF) ablation including: faster heating, higher (more lethal) tissue temperatures, improved consistency in different tissue types, and potentially greater ablation zone sizes. The purpose of this study was to retrospectively review the results in the first 52 patients with hepatic tumors treated with a new high-power, gas-cooled MW device at a single center.
Methods: Between December 2010 and January 2011, we treated 89 hepatic lesions (47 HCCs, 33 metastases, 6 adenomas, and 3 hemangiomas) in 52 patients via a percutaneous approach utilizing US and/or CT guidance. All procedures were performed with a high-powered, gas-cooled microwave system (Certus 140, Neuwave Medical, Madison, WI) utilizing 1-3 17-gauge antennas. Antenna power and ablation time was determined by the performing physician based on lesion size, location, and imaging findings. Mean power was 90 W (range 55-140 W) and mean ablation time was 5 minutes (range 1-20 minutes). Follow-up imaging was performed immediately post-ablation and at 3, 6, 9, and 12 months with contrast-enhanced CT or MRI for all patients with malignant lesions.
Results: Tumors ranged in size from 0.5 to 13.9 cm (mean 2.5 cm) and median follow-up was 4 months. Six-month follow-up was available for 34 malignancies (22 HCCs and 12 metastases) in 20 patients. All treatments were considered technically successful with no evidence of residual tumor at immediate post-procedure CECT. No local tumor progression was noted on imaging at any time point; however, two patients with large HCCs (6.0 and 4.5 cm) that underwent liver transplantation were found to have small volumes of residual tumor by H&E staining. One major complication occurred (3.8%): a recurrent right pleural effusion which required two thoracenteses for symptomatic relief. No other complication necessitating intervention occurred.
Conclusions: Early experience treating liver tumors using a high-powered, gas-cooled microwave ablation system demonstrates excellent local control for tumors less than 4.0 cm in size with minimal complications. Further study with longer term follow-up appears warranted.

Paper 47: Phase II Clinical Trail of Yttrium-90 Resin Microspheres for the Treatment of Metastatic Neuroendocrine Tumor

J.H. McElmurray, P.R. Bream, E. Grzeszczak, I.D. Feurer, J.D. Berlin, S.G. Meranze

Objectives: This prospective study evaluated efficacy and toxicity of Yttrium-90 resin microspheres (Y90RM) for the treatment of metastatic neuroendocrine tumor (MNET).
Methods: Adults with MNET were enrolled in a phase II clinical trial with the primary endpoint of tumor response measured on CT using response evaluation criteria in solid tumors (RECIST 1.0). Tumor response is reported in relation to pre-treatment data through 2 years or until transarterial chemoembolization (TACE) or death. Secondary endpoints were survival, toxicity, and patient-reported health-related quality of life (HRQOL). Toxicity was assessed using the Common Toxicity Criteria version 3.0, and HRQOL was measured using the SF-36® Health Survey. Data were analyzed using frequencies, mixed effects models, and Kaplan-Meier survival methods.
Results: Ten adults underwent 11 Y90RM treatments (9 single lobar, 1 planned sequential lobar) between 2/2004 and 10/2005. Stable disease or a partial response was observed within the first 6 months following all treatments (Table). Patient survival averaged 45±9 (SEM) months (range 8-78) and was 100% at 6 months, 80% at 1 year, 70% at 2 years, and 60% at 3 years. While physical and mental HRQOL averaged within general population standards (40-60) before Y90RM, 4 patients (40%) had impaired (<40) physical and 1 patient (10%) had impaired pre-treatment mental HRQOL. After controlling for baseline score category, physical HRQOL did not change significantly after Y90RM treatment (p=0.467) and mental HRQOL improved over time (p=0.044). There was no evidence of hepatic toxicity or acute carcinoid crisis following Y90RM treatment.
Conclusions: In this small prospective phase II study, targeted Yttrium-90 resin microspheres as first-line therapy for mNET resulted in stable disease or partial response in the first 3-12 months, stable or improved HRQOL through 24 months, and minimal toxicity or short-term morbidity or mortality. With extended follow-up, the survival rate is comparable to other locoregional therapies for MNET with potentially fewer total treatments.

TUMOR RESPONSE AND EVENT FREQUENCIES

TUMOR RESPONSE AND EVENT FREQUENCIES (N=11 treatments in 10 patients)					
RECIST assessments and exclusion events	Month 3	Month 6	Month 9-12	Month 15-18	Month 24
Stable Disease	8	7	4	3	2
Partial Response	3	3	3	2	2
Progressive Disease	0	0	0	0	1
TACE treatments (cumulative preceding)	0	1	2	3	3
Deceased (cumulative preceding)	0	0	2	3	3
TOTAL RECIST assessments reported	11	10	7	5	5

Paper 48: Differential Response to Radioembolization for Colorectal Cancer Metastases to the Liver in KRAS Mutant Patients

D. Coldwell, M. Schacht, V. Sharma

Objectives: Use of hepatic intra-arterial brachytherapy by implanted resin microspheres containing Yttrium-90 (radioembolization) has been utilized since approved for use in colorectal liver metastases in 2002. This investigator-initiated study focuses on the time to progression in patients having KRAS wild type gene versus those with the KRAS mutant gene.
Methods: This is a retrospective single institutional study to analyze the outcome of consecutively treated metastatic colorectal cancer patients who were stratified by their KRAS gene type. IRB approval was obtained from the institution. Primary endpoint was the intra- and extra-hepatic time to progression.
Results: 25 patients (14 M, 11 F) received 26 radioembolization treatments. The mean age was 58.7 years with a median number of treatments per patient is 1. All patients, but one, were treated with selective right and left hepatic arterial deposition of the Yttrium-90 beads. This patient received lobar therapy with one month interval between dose administrations. Extrahepatic disease was present at the time of treatment as identified on CT or CT/PET in 11 patients. All but one patient had received FOLFOX chemotherapy and failed. A single patient underwent the first round of FOLFOX concurrent with the radioembolization. 22/25 patients had received multiple lines of chemotherapy before undergoing radioembolization (mean = 3). Mean follow-up was 8 months. There were 6 KRAS mutant types within the cohort. The mean time to progression extra-hepatically was 2.4 months while those who had the KRAS wild type was 6.2 months. The time to intrahepatic progression in the KRAS mutant type was 4.4 months while those with KRAS wild type was 9 months. Of the KRAS mutant type patients, none are alive after 8 months with a mean survival of 7 months. The median survival of the treated patients with KRAS wild type has not been reached. Further data analysis will be performed.
Conclusions: Use of radioembolization in patients with KRAS wild type genetic profile should be followed closely for extra-hepatic disease and concurrent aggressive chemotherapy should be considered. Further research with larger cohorts is necessary to determine the precise role of this mutation on the survival of patients treated with radioembolization for hepatic dominant metastatic colorectal cancer.

Paper 49: Prognostic Factors of Resin-Based Yttrium-90 Radioembolization for Unresectable Metastatic Neuroendocrine Tumors

E.B. McIntosh, H.J. Prajapati, T.O. Lawal, B.F. El-Rayes, J.S. Kauh, H.S. Kim

Objectives: Hepatic metastases are a poor prognostic factor in patients with neuroendocrine tumors (NET). Resin-based Yttrium-90 (Y-90) delivers high doses of radiation to hepatic tumors and is a promising treatment option for metastatic NETs. The aim of this study was to evaluate the success of Y-90 in patients with unresectable metastatic NETs.
Methods: Consecutive patients with unresectable metastatic NETs treated with Y-90 from January 2006 to January 2012 were evaluated retrospectively. Survival was calculated by the Kaplan Meier Method, and potential prognostic variables were identified using the log-rank test. Changes in laboratory values were analyzed using dependent sample T-tests, and multivariable analysis was done using Cox Proportional Model. All analyses were done using SPSS v19.
Results: 44 patients were included in this study (13 Male, 31 Female, mean age 59 +/- 11). Primary NET was located in the pancreas (n=17), bowels (n=7), lung (n=4), urogenital tract (n=3), or unknown (n=13). 21 were classified as carcinoid, 6 as islet cell, 2 as insulinoma, 1 as glucagnoma, 1 as large cell, and 13 as NET unspecified. The mean size of largest hepatic tumor was 6.0 cm +/- 3.5 cm. 37 patients were Child Pugh Class A and 7 were Child Pugh Class B. The mean Y-90 dose infused per patient was 1846.3 MBq +/- 1010.1 MBq. Y-90 was done on a single lobe in 17 patients, both lobes concurrently in 7 patients, and each lobe separately in 20 patients. At diagnosis of primary, 22 patients had hepatic metastases; the mean time to diagnosis of metastases from primary diagnosis in the remaining patients was 3.9 years. The mean time from hepatic metastases to first Y-90 treatment was 1.5 years. Half of patients had extrahepatic metastases at Y-90. Previous or concurrent treatments included sandostatin therapy (56%), primary NET resection (47%), other systemic chemotherapy (43%), other IR procedures such as chemoembolization (23%), or hepatic resection (13%). The median survival from first Y-90 was 2.0 years and the mean survival was 2.9 years. 1 year, 2 year and 3 year cumulative survivals from Y-90 were 68%, 37%, and 18% respectively. On univariate analysis, Child Pugh Class was statistically significant. On multivariate analysis, Child Pugh Class (HR = 13.3 p=.001) and tumor burden (HR = 1.2, p=.046) were statistically significant, while Y-90 dose infused (p=.059), history of systemic chemotherapy (p=.125), age at Y-90 (p=.568), and extrahepatic metastases (p=.680) were non-significant. Laboratory tests of liver function and status were measured before and after first Y-90 treatment, and results are shown in Table 1. Creatinine significantly decreased (Δ= .07 mg/dl, p=.007) after Y-90.

Conclusions: Y-90 is an effective treatment option for patients with unresectable metastatic with median survival 2.0 years and 1 year survival 68%. Liver function labs suggest that Y-90 radioembolization is not liver-toxic for these patients. On multivariable analysis, Child-Pugh Class and tumor burden were significant prognostic factors.
Table 1: Change in liver function tests measured before and after Y-90

Laboratory Test	Δ	P-value
Total Bilirubin (mg/dL)	.07	.146
Albumin (g/dL)	-.20	.069
Creatinine (mg/dL)	-.07	.007
INR	.10	.130
AST (IU/L)	8.00	.236
AST (IU/L)	5.97	.522

AST = Aspartate aminotransferase
ALT = Alanine aminotransferase
Δ = Change in level before and after Y-90

Paper 50: Single Center Experience with GlassBbased Yttrium 90 Embolization in Neuroendocrine Liver Metastases

B. Arslan, A. Sardari, R. Shridhar, J. Sweeney, B. Biebel, J. Choi

Objectives: To evaluate glass-based Yttrium 90 (Y90) radioembolization in management of neuroendocrine tumors (NET), specifically to assess toxicities and short-term imaging response.
Methods: Retrospective review of all patients who had neuroendocrine metastases to the liver that underwent radioembolization with Y-90 was performed. Electronic patient charts were reviewed to analze demographics, radiation dosimetry, clinical findings, laboratory data, and imaging findings. Toxicities and side effects reported during the first 3 months of the procedures were identified from clinical notes. Short-term imaging response was assessed using EASL and modified RECIST criteria by reviewing latest imaging study in comparison to pre-treatment studies.
Results: A total of 48 patients received 88 radioembolizations between December 2009 and May 2011. 34 patients had adequate follow up. Total of 60 lobar and segmental radioembolizations were performed in 34 patients. There were 18 males and 16 females with a median age of 61 y/o (43 to 80 y/o). The radiation dose ranged from 74.9 Gy to 347.1 Gy with an average of 150.9 Gy. 22 patients (65%) complained of fatigue. 15 (44%) right sided abdominal pain and 8 (24%) noted weight loss ranging from 3.5 kg to 11kg. 7 (21%) patients had nausea, but none experienced vomiting. There was no mortality. Response assessment were made per each lobe/segment treated and average duration for follow up was 8 months. There were 82.0 % partial response, 10.3 % stable disease, and 7.7 % progression.
Conclusions: Glass-based Y90 radioembolization has low toxicity and good imaging response in management of NET metastases to liver.

Paper 51: Local Control of Focal Hepatic Malignancies Treated with Microwave Ablation with a High-Power Applicator System in 165 Patients

T. Tondolo, L. Cova, G. Mauri, T. Ierace, S. Goldberg, L. Solbiati

Objectives: To assess the efficacy and safety of microwave ablation for the treatment of hepatic malignancies using a high-power applicator system.
Methods: Over a 23-month period, 287 hepatic malignancies (176 HCC and 111 metastases) in 165 patients were percutaneously treated under US guidance using a high-power (140 Watt, 2.45 GHz) microwave system (AMICA-Probe: Hospital Service, Aprilia, Italy). One (n= 223) or two (n=64) antenna insertions were performed. Power and time of application ranged from 45 to 100 Watt and from 4 to 15 min, respectively. Imaging (either contrast-enhanced MDCT or MRI) at 3-6-9-12 months was used for post-ablation follow-up. Results were assessed after a minimum 6-month follow-up for a total of 118 malignancies (88 HCCs and 30 metastases, size range 0.4-6.6 cm, mean 2.3) in 82 patients.
Results: Immediate complete ablation was achieved in 296/287 malignancies (93.7%); 169/176 (96%) of HCCs and 100/111 metastases (90.1%). At 6-month follow-up, local tumor progression (LTP) occurred in 14/118 malignancies (11.8%): 2/48 (4.2%) with sizes ≤1.9 cm, 5/36 (13.9%) for tumors ranging 2.0-2.9 cm; and 7/34 (20.5%) for tumors > 3 cm. All LTPs was successfully re-treated within 4 months using the same method. Minor complications (pleural effusions, edema of the gallbladder wall and small peri-hepatic effusion) occurred in 27/165 (16.4%) patients. No major complication was noted.
Conclusions: Even lesions bigger than 3 cm were successfully treated with few antenna insertions and in a short time. However, with a longer follow-up time it will be likely possible to achieve more accurate standardization of treatment parameters (power applied and duration of energy application) and more precise correlation between these parameters and the outcome of ablations (volume of necrosis and occurrence of local tumor progression).

Paper 52: Yttrium-90 Radioembolization for Intrahepatic Cholangiocarcinoma

S. Mouli, K. Memon, A. Riaz, R.K. Ryu, R. Salem, R.J. Lewandowski

Objectives: The objective of this prospective study is to present data on the safety and efficacy of radioembolization with Yttrium-90 (Y90) microspheres in patients with intrahepatic cholangiocarcinoma (ICC).
Methods: This was a single institution prospective study over a 7-year period. Forty-six patients with histologically confirmed ICC were treated with radioembolization using Yttirum-90 (Y90) microspheres. Patients were stratified according to Eastern Cooperation Oncology Group (ECOG) performance status, tumor distribution (solitary or multifocal), tumor morphology (infiltrative or peripheral), and the presence or absence of portal vein thrombosis (PVT). Primary endpoints included biochemical and clinical toxicities. Secondary endpoints included imaging response (World Health Organization: WHO; European Association for the Study of Liver Disease: EASL criteria) and overall survival. Uni/multivariate analyses were performed.
Results: Fatigue and transient abdominal pain were reported in 25 patients (55%) and 13 patients (29%), respectively. One patient (2%) developed a treatment-related gastroduodenal ulcer. Imaging followup was available in 45 patients (98%). WHO imaging findings included partial response (n=12; 27%), stable disease (n=32; 71%), and progressive disease (n=1; 2%). EASL imaging findings included partial/complete response (n=33; 73%) and stable disease (n=12; 27%). Median overall survival for the entire cohort (n=46) was 14.9 months; this varied by baseline characteristic [ECOG 0, 1, 2: 31.8, 11.7 and 9.9 months respectively (P=0.4); peripheral versus infiltrative: 31.8 and 6.6 months, respectively (P =0.005)]. Six patients (13%) were downstaged to surgical resection following treatment.
Conclusions: Radioembolization with Y90 is safe and effective in select patients with ICC. Confirmatory trials are underway.

Paper 53: Yttrium-90 Radioembolization for Chemorefractory Unresectable Intrahepatic Cholangiocarcinoma (ICC): Survivals and Prognostic Factors

H.J. Prajapati, T.O. Lawal, E.B. McIntosh, B.F. El-Rayes, J.S. Kauh, H.S. Kim

Objectives: To investigate the safety, efficacy, median overall survival (OS) and factors associated with improved progression free survival (PFS) or OS in patients (pts) with unresectable ICC treated with 90Y radioembolization.
Methods: Under IRB approval, our institute's cancer registry database was researched for pts diagnosed with unresectable ICC starting from first treatment in December 2002 to January 2012. The analysis of the cohort is shown in figure 1. Baseline characteristics and biochemical/clinical toxicities of pts with unresectable ICC and median OS from diagnosis were studied. The prognostic factors of PFS and OS amongst pts treated with Y90 after progression with standard chemotherapy were analyzed. Adverse events were recorded as per the CTCAEv3 criteria. RECIST1.1 criteria were used to assess the treatment response in pts who received 90Y therapy. Kaplan Meier estimator by log rank test and Cox Proportional Hazard model were used for survival analysis. Chi square test and t-test were used to compare categorical and continuous variables accordingly.
Results: Twenty four pts underwent 90Y therapy after progression with chemotherapy (Group A), 31 pts had systemic chemotherapy only (Group B) and 33 pts had no therapy (Group C). The groups A, B and C were similar for age, sex and race (p>0.05). The group A and B were similar in Child Pugh Class (p=0.2) at the time of initial oncology clinic visit. However the group C had more Child Pugh Class C cases (30.3%). The median OS were 22.2, 7.8 and 3 months from the diagnosis in group A, B and C respectively (p=0.001). The median OS from 1st 90Y therapy (OS-90Y) in group A was 11.5 months. The 6 and 12 month survivals from first 90Y therapy were 62.5% and 42.7 % of pts. Mean 90Y dose infused per patient was 1684.6 GBq (SD 854). The median PFS was 9.2 months (95 CI: 3.9, 14.4) after first 90Y therapy. Pts with Child Pugh class A (87.5%) and B (12.5%) had corresponding median PFS of 9.3 and 1.4 months from 90Y therapy (p=0.02). In 23 pts, initial imaging study was available and median OS-90Y in pts with <5 ICC tumors (n=12) was 21.8 months versus 4.8 months in pts with >5 ICC tumors (p=0.02). In 70.8% of pts (n=17), CA 19-9 serum level values were available. The median OS-90Y in pts with CA 19-9 serum level value <100U/ml (n=9) was 28 months versus 7.9 months in pts (n=8) with CA 19-9 serum level value >100U/ml (p=0.009). The common clinical toxicities were fatigue (16.7%), increased abdominal pain (16.7%) and self-limiting grade III bilirubin toxicity (8.3%). The mild GI bleeding with conservative treatment from duodenal ulceration was present in 1 patient.
Conclusions: Radioembolization with resin-based 90Y is an effective and safe therapy for pts with unresectable chemorefractory ICC. The CA 19-9 serum level value <100U/ml and < 5 ICC tumors were predictors of prolonged survival. The Child Pugh Class A was predictor of prolonged PFS.

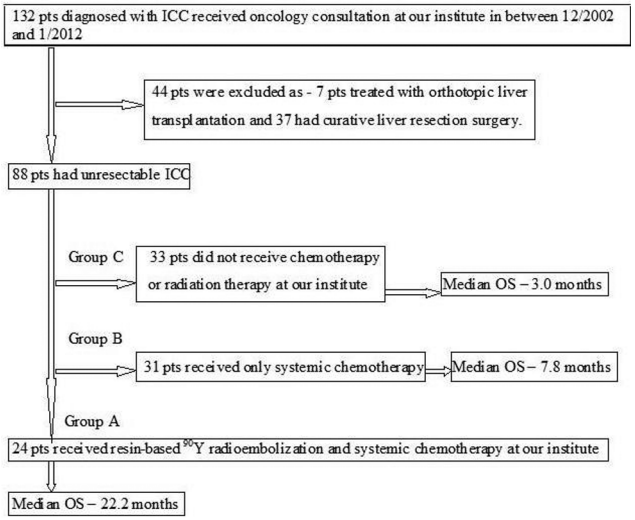

Figure 1 Analysis of Cohort

Paper 54: Long-Term Outcomes of Thermal Ablation for Metastatic Tumors in the Lung

J. Meyer, J.J. Urbanic, B. Steadman, J.A. Requarth, D. Childs, H. Clark

Objectives: Patients having limited metastatic disease (oligometastasis) can be treated using local therapies with the goal of improving progression free survival largely based on surgical data. Limited long-term data has been reported to this point of thermal ablative (TA) techniques. Most report series and studies have follow-up in the 1 to 2 year range. We report our mature experience of metastatic cancer patients treated with TA for control of thoracic oligometastasis.

Methods: All metastatic patients (pts) consecutively treated between 2004 and 2011 with TA at Wake Forest were reviewed. Pts excluded if treated for local failure after radiotherapy. TA technique varied over time by type and manufacturer. IRB approval was obtained. Radiographic and clinical information was reviewed from records available. Patients were scored regarding to local (at the site treated) or distant failure. Local control from date of procedure to last known imaging. Local control defined be modified RECIST and PET as needed taking into account TA effects. Toxicity graded per NCI CTCAE v4.0. Descriptive statistics used to report toxicity. Kaplan Meir estimation of local control (LC) and overall survival (OS). Unpaired t-test used for comparison.

Results: 79 pts were treated during a total of 106 TA procedures to total 117 tumors. 9 pts multiple tumors same day, 5 pts repeat TA for local failure, 8 pts with 3 or more lesions ablated; 22 total pts treated to multiple sites or repeat. Median age 65.5 years (18-86). Thermal ablation was radiofrequency 86, cryoablation 24, microwave 7. Average length of stay 1.7 nights (0-12); 11 pts with > 3 night LOS. Anesthesia was general 57, conscious 49. Metastatic tumor subtype by patient: NSCLC 27, colorectal (CRC) 16, renal 11, head and neck 12, other 13. Median fu 20.5m entire cohort (0.2-82) and 29m (2-82) among living pts. Median OS 40m all pts (range 30 months NSCLC to 48m CRC p 0.05). 1 yr, 3 yr, 5 yr OS: 83.9%, 51.5% (95% CI 38.6 - 64.4m), 24.1%. Median OS 26 months single lesion vs not reached multiple lesions (20 pts) p=0.0003. Median tumor size 14 mm (3-68). Local control: 1 yr 92.6%, 2 yr 83.1%, 3 yr 72.4% (95% CI 61.7-83.1), 5 yr 40.9%. 2 year local control <2cm tumor 89.1%, > 2cm tumor 60.2%. LC not different by TA modality. Of 32 local failures, 9 salvaged with RT, 5 repeat TA, 1 surgery. 1 pt with grade 5 toxicity due to TA; 39 pts Grade 2 pneumothorax (PTX), 17 additional pts PTX iatrogenic for procedure; 4 pts grade 2 hemorrhage, 3 pts grade 2 effusion, 2 pts grade 3 empyema.

Conclusions: For patients with oligometastatic thoracic disease, thermal ablation is safe and provides durable control for tumors < 2.0 cm with long term follow-up. Survival better in patients with multiple tumors likely due to patient selection bias. Additional prospective studies with long term efficacy endpoints needed.

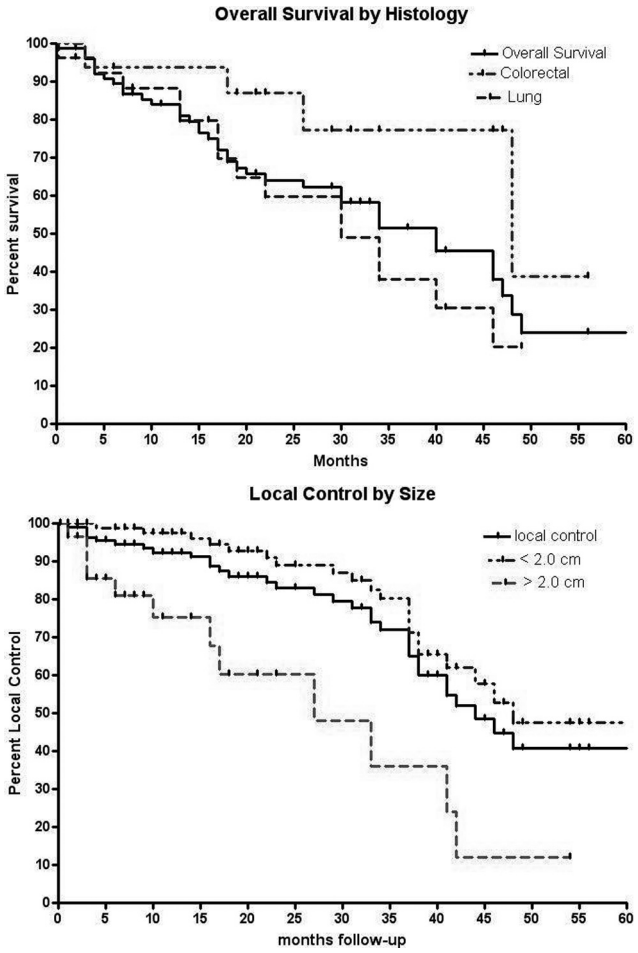

Paper 55: Factors that Influence Pneuthorax and Chest Tube Placement Following Microwave Ablation of Lung Malignancy

S. Kishore, J.P. Erinjeri, E. Petre, C. Sofocleous, M. Maybody, S. Solomon

Objectives: To determine the factors that influence the likelihood of pneumothorax and chest tube placement following microwave ablation of lung malignancy.

Methods: Retrospective review of an IRB-approved, HIPAA-compliant database revealed that between May 2008 and August 2011, 47 patients underwent microwave ablation (MWA) of 75 lung lesions. We assessed demographic (age, sex), clinical (prior chemotherapy, radiation therapy, ipsilateral chest surgery, COPD) and tumor (pathology, size) parameters. We also measured the distance from both the tumor and ablation probe to the visceral pleura and nearest bronchus. Univariate logistic regression (continuous variables) and chi square tests (categorical variables) were used to determine the factors which significantly affected the likelihood of pneumothorax (PTX) and chest tube placement following MWA. Multivariate logistic regression was performed to determine the factors which were independent predictors.

Results: The mean age of patients was 61+/-10 years. There was no correlation between the likelihood of PTX and age ($p<0.63$) or sex ($p<0.13$). The risk of PTX following MWA was not significantly different in patients with COPD ($p<0.16$), prior chemotherapy ($p<0.78$), or prior radiation therapy ($p<0.31$). The risk of PTX was significantly higher in patients without prior chest surgery compared to those with prior chest surgery (57% vs 28%, relative risk 2.0, $p<0.025$). The average tumor size was significantly smaller in patients who experienced PTX compared to those patients without PTX (10.9 vs 17.2mm, $p<0.01$). Patients with tumors <3cm had a significantly higher risk of PTX than those >3cm (53% vs 12%, relative risk 4.3, $p<0.05$). Tumor pathology showed no significant effect ($p<0.51$). The average distance between the pleura and the tumor margin was significantly greater in patients who experienced PTX than those without PTX (14.7 vs 9mm, $p<0.01$). No significant difference in PTX rate was seen when examining the probe-pleura distance ($p<0.09$), airway-tumor distance ($p<0.41$), and airway-probe distance ($p<0.10$). The average tumor size was significantly smaller in patients who required chest tube placement compared to those patients who did not require chest tube placement (11.3 vs 16.5mm, $p<0.03$). The average distance between the pleura and the tumor margin was significantly greater in patients who required chest tube placement than those who did not require chest tube

placement (14.5 vs 9.4mm, p<0.025). Under multivariate analysis, prior chest surgery and tumor size remained independent negative predictors of PTX after MWA (p<0.002 and p<0.02, respectively), while tumor-pleura distance was an independent positive predictor (p<0.04). Prior ipsilateral chest surgery was the only independent negative predictor of chest tube placement (p<0.05), and tumor-pleura distance approached significance (p<0.065).
Conclusions: Decreased distance between the target tumor and the pleura, increased tumor size, and prior ipsilateral chest surgery convey a lower risk of pneumothorax and chest tube placement following microwave ablation of the lung.

Paper 56: Irreversible Electroporation of Lung Metastases: Initial Experience

T. de Baere, J. Joskin, F. Deschamps, G. Farouil

Objectives: To reported our initial experience with Eletroporation (IRE) for treatment of lung metastases in contact with large vessels.
Methods: 7 male patients aged 37 to 74 years were treated for a single lung metastasis in contact with vessels 4 mm or larger. The metastases measured 15.1±3.7 mm [9-21] abutting a pulmonary vessel 4 to 9 mm in diameter or the aorta (n=1). Priaty tumors were colorectal (n=4), renal (n=2), or pancreatic. Two electrodes were inserted in 5 patient and 3 electrodes in 2 patients. Under general anesthesia and short pulses of current 1900 to 3000 volts/cm were delivered using a dedicated generator (Nanoknife®, Angiodynamics, Latham, NY).
Results: Treatment was well tolerated in all patients. We drained 3 pneumothoraces. Immediate post-ablation imaging showed a zone of alveolar condensation around the treated tumor. CT obtained at day 1 or two demonstrated an opacity with a maximum diameter 60% larger than the tumor. CT performed at 3 months demonstrated a decrease by 57% of the diameter of the ablation zone when compared to initial tumor size. This decrease was 25% at 1 month. After a median follow-up of 77 days, no tumor demonstrated local recurrence at CT (n=7) or at PET-CT (n=4). One tumor shows a major decrease in size and remains PET doubtful and is under follow-up.
Conclusions: IRE is well tolerated and induces a rapid decrease in size of the treated tumor when compared to thermal ablative therapies. Encouraging initial results warrant further investigations.

Paper 57: Percutaneous Irreversible Electroporation of Renal Lesions in 10 Patients

S. Barry, C. Shaw, J.D. Meler

Objectives: To retrospectively evaluate 10 renal irreversible electroporation (IRE) ablation cases for technical feasibility, clinical safety, effectiveness and durability of treatment.
Methods: This is a retrospective evaluation of 10 renal IRE ablation cases performed between September 2010 and late October 2011. All cases were performed percutaneously utilizing CT guidance under general anesthesia with cardiac synchronization. Age, gender, lesion location, lesion size as well as serum creatinine (Cr) pre- and post-ablation, complete evidence of ablation, number of probes used per case, procedure time, length of stay and complications were analyzed.
Results: All 10 lesions treated with IRE between September 2010 and October 2011 were successfully ablated and remain without evidence of recurrence. Seven patients were male and 3 were female. Mean age was 64.2 years (46-78). Seven of the ten lesions were located centrally near the collecting system, one was hilar and two were felt to be too close to adjacent organs to be ablated with RFA. Nine of the ten lesions were renal cell carcinoma and one was ultimately determined to be an oncocytoma. Average pre-treatment lesion size was 2.29 cm (1.4-3.3 cm). Average pre-procedure serum Cr was 1.46 mg/dl (1-3.1 mg/dl), the average serum Cr 24 hours post procedure was 1.33 mg/dl (0.8-3.1 mg/dl). The median number of probes placed was 3 (2-4) per lesion. The average procedure time was 2.22 hours (1.25-4). All patients were discharged within 24 hours. The only known complication was a cutaneous nerve injury that resolved spontaneously at 4 weeks.
Conclusions: IRE of renal lesions is technically feasible and appears to be effective, safe and durable in the studied patients. With follow up ranging from 3 months to 18 months there have been zero recurrences to date. Procedural times were initially 4 hours, but later decreased to less than 2 hours irrespective of the number of probes placed. This suggests the need for further publication on the technical aspects of IRE and proper lesion selection. Additionally, longitudinal studies are needed to confirm our findings of a consistent reduction in tumor size, stable creatinine levels, and durable treatment effect beyond 18 months.

Paper 58: Histological Determination of Non-Lethal Margins during Renal Cryoablation

C. Georgiades, R. Rodriguez, E.M. Azene, C.R. Weiss, A. Chaux, G. Netto

Objectives: During percutaneous, image-guided renal cryoablation, the operator visualizes the "ice-ball" but not the lethal -25°C isotherm, Fig. 1. Our objective was to determine the width of the non-lethal ablation zone (termed "intermediate zone") between the visible "ice-ball" margin and the lethal -25°C isotherm.
Methods: The Institutional Animal Care and Use Committee approved the study. 9 adult female swine were anesthetized and the left renal artery was catheterized under angiographic guidance. Under MRI guidance a cryoprobe was placed in the left kidney. At the end of the 10 minute freeze — 8 minute thaw — 10 minute refreeze cycle, tissue dye was infused via catheter. The animal was sacrificed prior to final thawing. Histological examination was performed to determine the width of the frozen but viable intermediate zone (no necrosis, no dye in vessels or glomeruli). The intermediate zone width was defined as the mean distance between the lethal zone (100% necrosis, no dye in vessels or glomeruli) and the non-frozen zone (no necrosis, dye present in vessels and glomeruli). 5 animals were first used to determine the optimum of three available dyes (methylene blue, black tissue stain and black India ink). Another 6 animals were used to determine the width of the frozen but viable intermediate zone.
Results: Black India ink showed the best staining characteristics and was used exclusively for the 5 test animals. 29 slides were prepared from the 5 ablated kidneys. 136 measurements were made of the intermediate zone. The mean width of this band of frozen but viable tissue had a maximum of 1.15 ± 0.51 mm and a minimum of 0.75 ± 0.44 mm. The width was increased adjacent to large blood vessels due to a "heat source" effect that prevented necrosis at the perimeter of the lethal zone. However, no heat source effect was noted within the lethal zone.
Conclusions: The minimum width of the frozen but viable band of tissue ("intermediate zone") surrounding the lethally ablated core during cryoablation of normal porcine kidney is 0.75 ± 0.44 mm. This intermediate zone can reach a maximum of 1.15 ± 0.51 mm due to the "heat source" effect. No heat source effect was noted within the lethally ablated region.

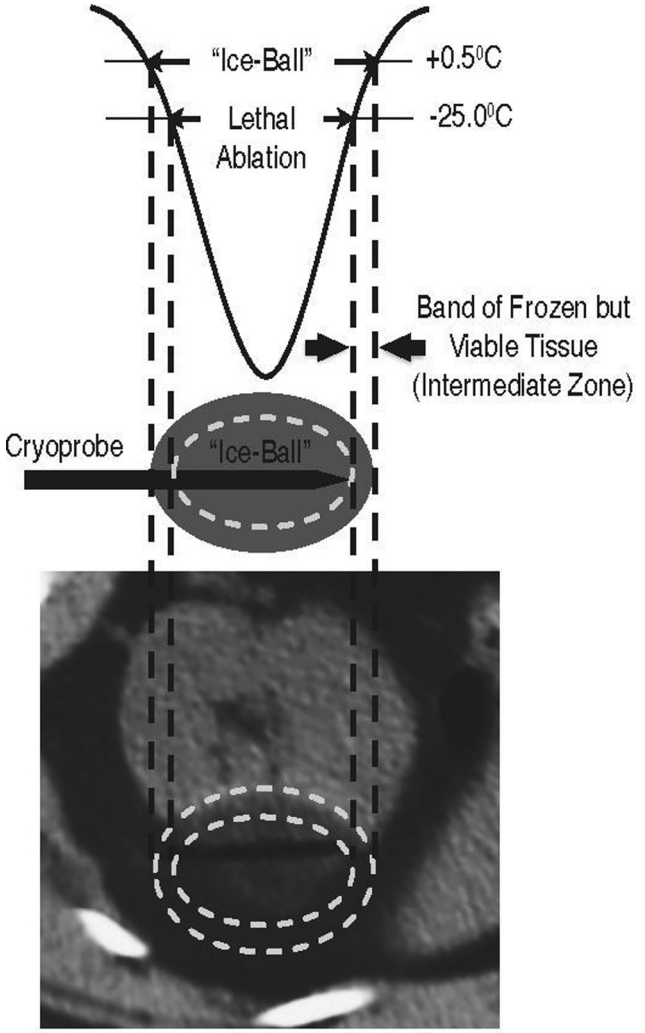

Figure 1

Paper 59: Ultrasound-Guided Percutaneous Microwave Ablation of Renal Cell Carcinoma: Intermediate-Term Results

P. Liang

Objectives: To retrospectively review intermediate-term clinical outcomes (median 20.1 months) after microwave ablation (MWA) of renal cell carcinoma (RCC).
Methods: This retrospective study was approved by our Institutional Review Board. We reviewed the results of 46 patients with 49 RCC nodules (diameters from 0.6–7.7 cm; mean 3.0±1.5 cm) treated using ultrasound-guided percutaneous MWA with cooled-shaft needle antenna from April 2006 to December 2010. One antenna was used for tumors < 2 cm, two for tumors ≥ 2 cm. The patients were followed with contrast enhanced imaging (ultrasound, computed tomography and/or magnetic resonance imaging) at 1, 3 and 6 months, and every 6 months thereafter. The effect of changes in key parameters (including overall survival, disease-free survival and local tumor progression rate) was statistically analyzed by using the log–rank test.
Results: Technical effectiveness (complete ablation on a follow-up enhanced imaging performed one month after MWA) was achieved in 48 of 49 (98.0%, 48/49) tumors and metastasis-free rate were 100% (46/46). The 1-, 2-, and 3-year local tumor progression rates were 4.6%, 7.7%, and 7.7%, respectively. The cancer-specific survival was 100% (46/46) and 1-, 2-, and 3-year overall survival rates were 100%, 100%, and 97.8%, respectively. The 1-, 2-, and 3-year disease-free survival rates were 95.4%, 92.3%, and 92.3%, respectively. No major complications occurred. Multivariate analysis showed that tumor number (P=0.046), growth patterns of tumours (P=0.003) and ablation time (P=0.04) were independent unfavorable prognostic factors.
Conclusions: In the intermediate term, ultrasound-guided percutaneous MWA appears to be a safe and effective technique for the management of RCC especially small RCC in selected patients.

Paper 60: Percutaneous Cryoablation as a Follow-Up Modality for Locally Progressive RCC after Laparoscopic Partial Nephrectomy

M. Morgan, E.J. Trabulsi, C.D. Lallas, L. Pino, D.B. Brown

Objectives: Laparoscopic partial nephrectomy has a 3-4% incidence of local treatment failure. The purpose of this presentation is to determine efficacy of percutaneous cryoablation for locally progressive renal cell carcinoma after laparoscopic partial nephrectomy.
Methods: Five consecutive patients were referred to our quarternary center's small renal mass clinic for assessment after failure of laprascopic partial nephrectomy. Tumor size and location (exophytic, parenchymal, or central) was noted. Details are in the Table. Cryoablation was performed under CT and CT fluoroscopic guidance using an argon/helium-based system (Healthtronics, Austin, TX). Patients were observed overnight and discharged. Follow-up imaging and patient status was tracked at small renal mass clinic to document treatment success.
Results: Of the 5 tumors, 4 were parenchymal and 1 was exophytic. Sizes ranged from 1.8-4.0 cm (median 2.2 cm). Two or three needles were used for the ablations based on tumor size and position within the kidney. Patients were followed for 12.6-30.6 months (median 21.7 months). The patient with a 4.0 cm parenchymal tumor developed a 2.9 cm exophytic area of local progression 13.3 months following ablation. The tumor was successfully retreated and no active disease is present at an additional 15.5 months of follow-up. Two patients developed self-limited hematuria which was managed conservatively and had stopped by discharge the day after treatment. No other complications occurred. No patients developed progressive renal insufficiency and the average change in creatinine at the last recorded follow-up was 0.1 mg/dL (range: -0.1 to +0.3). All patients remained at their baseline for activities of daily life.
Conclusions: Percutaneous cryoablation appears to be a safe and effective nephron-sparing modality for continued control of locally progressive disease following laparoscopic partial nephrectomy and avoid the disadvantages of a second laparoscopic procedure. Most recurrent tumors are parenchymal.
Patient Characteristics

Patient Number	Laterality	Location	Diameter
1	Right	Parenchymal	2.2 cm
2	Right	Parenchymal	4.0 cm
3	Left	Exophytic	1.8 cm
4	Left	Parenchymal	2.2 cm
5	Right	Parenchymal	2.3 cm

Paper 61: Preliminary Clinical Experience with the Use of the ExAblate® Magnetic Resonance Guided Focused Ultrasound Surgery (MRgFUS) System for Focal Treatment of Organ-Confined Low-Risk Prostate Cancer

V.G. Turkevich, A.K. Nosov, A.V. Mishchenko, S.A. Rozengard, S.V. Kanaev, M.S. Molchanov

Objectives: The ExAblate® system (InSightec, Haifa, Israel) is a technological platform with specific adjustments for various indications. Indications include uterine fibroids and bone tumors which are commercial in many countries, as well as investigational indications such as, neurological brain disorders, breast cancer, prostate cancer, and facet joint syndrome. In Petrov Research Institute Oncology, (St. Petersburg, Russia), we were the first to use the ExAblate® system with a 1.5 T GE MRI, for treating patients with locally-confined low-risk prostate cancer. The current abstract presents preliminary results of the first eight that we patients treated with this device.
Methods: Patients were recruited, treated and followed under an IRB-approved single arm, prospective, feasibility study protocol. Patients with elevated PSA <10ng/ml; with previously confirmed or suspected prostate cancer where offered to participate in the study. In the presence of one or two positive low-grade prostate cancer foci i.e., Gleason score <6 (=3+3; no 4 or 5 grades), and in the absence of calcifications near the rectal wall or any evidence for extracapsular cancer extension – patients meeting all other eligibility criteria, were focally treated by the ExAblate® MRgFUS system.Treatment was performed in the MRI suite, under epidural anesthesia with conscious sedation, and with continuous draining the urinary bladder by a Foley catheter. Patients were followed for 6 months and periodically evaluated for the occurrence and severity of adverse events; validated self-reported quality of life questionnaires were used to assess post-treatment quality of life, including, urinary symptoms, incontinence and sexual function. Preliminary efficacy was evaluated by repeated mapping biopsy at 6-month follow-up. In addition PSA levels were taken at baseline, and at 1, 3 and 6 months post-treatment.
Results: From Feb 2010 to Dec 2011, seven eligible patients underwent eight MRgFUS treatments. One patient underwent a second treatment due to a newly detected cancerous focus at 6-month follow-up mapping biopsy. All patients were stage 1C clinically. In seven cases a single tumor focus was detected; one treatment was done for two biopsy proven tumor foci, both foci were separately targeted. Seven tumor foci detected were of Gleason score 6 (3+3), three were of lower Gleason scores (i.e., 3+0, 3+1 and 3+2). Pre-procedure multifunctional MRI with DCE-MRI and MRI Spectroscopy detected tumor foci that correlated with biopsy findings only in two patients. Immediate post-treatment contrast-enhanced MRI demonstrated the desired non-perfused volumes (NPVs) corresponding to the treatment plan. No patient reported hematuria, perineal pain, post-treatment urinary incontinence, or bowel-related symptoms. Six patients were potent at before treatment, four of them returned to baseline sexual and erectile function within 3 months from treatment. PSA levels were reduced only after four treatments. In fact, PSA was lower in the patient who had a positive follow-up biopsy than in other patients with negative biopsies.
Conclusions: So far the safety of the ExAblate treatment for locally confined prostate cancer was demonstrated in our Institute with 8 treatments involving minimal morbidity. According to these preliminary findings, ExAblate has the potential of being a very attractive management option for patients with early low risk prostate cancer, encountering the dilemma of choosing between active surveillance and some definitive mutilating treatment.

Paper 62: Percutaneous US-Guided Interstitial Laser Ablation of Metastatic Lymph Nodes in the Neck from Papillary Thyroid Carcinoma following Thyroidectomy and Lymphadenectomy

G. Mauri, L. Cova, T. Ierace, T. Tondolo, L. Solbiati

Objectives: We report our experience with percutaneous US-guided interstitial laser ablation for metachronous cervical nodal metastases from papillary thyroid carcinoma following total thyroidectomy and central + laterocervical lymph node.
Methods: Twenty-three metachronous metastatic nodes (mean size 1.2 cm; range 0.6-2.6 cm) in 19 patients were treated. A 1,064 nm Nd:YAG laser (EchoLaser X4, Esaote, Genoa, Italy) was used. All cases were negative at 131I whole body scan, but had positive 18F-FDG PET and elevated serum levels of thyroglobulin. Under local anaesthesia, a 300 mm quartz fiberoptic guide was placed into the node through a 21G needle. Nodes were treated with one (17 cases) or two (6) fibre insertions, each one with 3 W power for 400-600 sec (total energy 1,200-1,800 joules). All cases were followed at 3 and 6 months with B-mode US, CEUS, 18F-FDG PET and assessment of serum levels of Tg.
Results: Laser ablation was technically feasible and well tolerated in all patients, with no either immediate or late complications. In 21/23 (91.3%) nodes complete ablation (lack of enhancement at CEUS, negative 18F-FDG PET with normalisation of SUV and >90% decrease of Tg serum levels) was achieved. In 2 cases, residual uptake at 18F-FDG PET with abnormal SUV was found and laser ablation was repeated.
Conclusions: Percutaneous US-guided interstitial laser ablation seems to be an effective, low cost and safe therapeutic tool for the treatment of metachronous nodal metastases from papillary thyroid carcinoma in the neck which would otherwise require often challenging further resections.

Poster 1: Microvascular Perfusion Changes in Rabbit VX2 Liver Tumors Following Embolization

C. Gacchina, K. Sharma, E. Levy, A. Lewis, B. Wood, M. Dreher

Objectives: Transarterial chemoembolization (TACE) is used to treat patients with HCC. Angiography is used to monitor tumor perfusion as atreatment endpoint during

TACE, yet it only resolves large blood vessels (>1mm). The objective of this study was to quantify changes in tumor microvascular (<1mm) perfusion changes as a function of angiographic endpoint.

Methods: Rabbit hepatic Vx2 liver tumors were embolized from the common/proper hepatic artery with 100-300μm LC Beads (Biocompatibles; 1:20 dilution) to sub-stasis (1cc) or complete stasis (3-6cc packed bead volume). Degree of stasis was assessed by angiography. Microvascular perfusion was evaluated by administration of 2 different fluorophore-conjugated perfusion markers (lectins) via the catheter before embolization (native tumor perfusion) and 5 minutes after reaching the desired endpoint (embolization affect). Tumor microvasculature was labeled with a CD31 antibody and analyzed with fluorescence microscopy for perfusion marker overlap/mismatch. Values (mean±SEM) were analyzed with an ANOVA and post-hoc test (n=3-5).

Results: Within viable Vx2 tumor regions, microvascular density was 168±118 vessels/mm2 and 82±20% of blood vessels were perfused. Considering only the perfused vessels, both coadministration and sequential administration of perfusion markers (17-minute wait to simulate an embolization procedure) had good overlap with 76±6% and 75±7% overlap, respectively (P>0.05). Embolization to stasis stopped perfusion in 61±8% of blood vessels, but 39±8% remained patent (P<0.05 vs. co-administration). Embolization to sub-stasis stopped perfusion in only 9±6% (P>0.05 vs. co-administration) of blood vessels and importantly resulted in a significant increase in patent blood vessels following embolization, i.e., new functional blood vessels (23±2% vs. 13±1% for wait and 0±0% for stasis, p<0.05).

Conclusions: In the rabbit hepatic VX2 tumor model, a significant proportion (~40%) of tumor microvasculature remained patent despite embolization to complete angiographic stasis. Embolization to substasis resulted in a significant increase in newly perfused microvessels, i.e. flow redistribution on a microscopic level which preserved tumor microvascularity in the immediate post-embolization period. This preservation of tumor microvasculature may have implications in tumor response to embolotherapy. Certainly, a better understanding of microvascular perfusion's influence on overall treatment efficacy is needed.

Poster 2: Dose Escalation Study of US-generated Doxorubicin Nanoshards in a Rat HCC Model: Preliminary Results

M. Cochran, S. Hunt, M.C. Soulen, M.A. Wheatley

Objectives: Doxorubicin-loaded US contrast microbubbles can be shattered into nanoshards within tumor vasculature to provide non-invasive selective delivery of drug to HCC. Previous experiments demonstrated tumoricidal tissue dox concentrations sustained at 14 days with sparing of normal liver at a dose of 0.8mg dox/kg. In this study escalating doses of dox microbubbles were administered for two 3-week cycles.

Methods: Morris 3924a hepatomas were implanted in the left lobe of ACI rats and allowed to grow for 3 weeks. Dox-loaded microbubbles were injected IV at dox levels of 0.8 mg/kg, 1.6 mg/kg, and 4 mg/kg and the tumors insonated for 20 minutes at an MI of 0.42. Serum drug concentration was measured 5 after injection. Tumor size and CBC were measured at baseline, 12+/-1 day, and Day 21, at which time a second cycle of therapy was administered at the same dose. Rats were sacrificed on Day 42 and tissues analyzed for dox concentration and histologic response.

Results: Rats tolerated the first cycle at all dose levels with no procedure-related deaths. Serum dox levels at the three dose levels were 0.4 +/- 0.3 mcg/ml, 0.8 +/-0.7 mcg/ml, and 3.2 +/- 1.7 mcg/ml. There was no significant change in hemoglobin or platelet counts at all three dose levels. Almost all rats developed a leukocytosis at 12 days which persisted at 21 days. Tumor size after the first cycle of therapy are in the Table.

Conclusions: Dox-loaded US contrast at doses up to 4 mg dox/kg were tolerated without significant hematologic toxicity. Growth inhibition was not seen after one cycle; results following the second cycle and necropsy will be reported.

Tumor Diameter (cm +/- SD)

Dose Level	Day 0	Day 12	Day 21
0.8mg/kg n=6	0.9 +/- 0.1	1.5 +/- 0.1	2.0 +/- 0.4
1.6 mg/kg n=5	1.0 +/- 0.4	1.6 +/- 0.4	2.4 +/- 0.1
4.0 mg/kg n=6	1.1 +/- 0.1	1.7 +/- 0.1	2.5 +/- 0.1

Poster 3: Isoliquiritigenin Inhibited Malignant Phenotype of Oral Squamous Cell Carcinoma

T. Shieh, S. Hsia, Y. Shih, Y. Huang

Objectives: Oral cancer is the sixth in numbers of deaths and crude death rates from leading cancer. There is almost 90% oral squamous cell carcinoma (OSCC) in oral cancer population. It is helpful to realize the tumorigenesis mechanism of OSCC and to exploit new anti-cancer drugs, which decrease the death rate of oral cancer. Isoliquiritigenin (ISL) was found in licorice. It has various biological actions, including anti-virus, anti-oxidation, anti-inflammation and anti-ulcer activity. It is also utilized in cancer research, such as prostate and breast cancer. However there are a few research papers about oral cancer.

Methods: We set up normal human oral keratinocyte (OK), oral fibroblast (OF) and 5 OSCC cell lines (Ca9-22, HSC3, OECM-1, SAS and SCC4) culture for anti-oral cancer drugs screening platform. Cell viability is detected by MTT assay after variant ISL dosage treatment. Cell cycle and apoptosis was analyzed by flow cytometry. Messenger RNA and protein expression were detected by RT-PCR and western blotting, respectively. The malignant phenotypes including cell colony formation, migration, invasion, were using transwell, and anchorage independent ability was using soft agar assay.

Results: The IC50 of ISL in OK, OF and 5 OSCC cell lines were list in table 1. OK, HSC3, and SCC4 were sensitive to ISL, but OF, Ca9-22, OECM-1, and SAS were not. Treat OK, OF, HSC3, OECM-1, and SAS with 25 μM and 50 μM ISL, induce cell cycle G2/M arrest and HSC3 apoptosis. ISL induced cell cycle arrest and apoptosis might by ataxia-telangiectasia mutated (ATM) pathway. Furthermore, we verified the malignancy phenotypes of OSCC cells. HSC3 and OECM-1 migration, HSC3, OECM-1 and SAS colony formation, OECM-1 and SAS anchorage independent growth, SAS invasion abilities were inhibited after low dosage ISL 3.125 μM and 6.25 μM treated.

Conclusions: The cell cycle arrested at G2/M phase even the cell lines sensitive or insensitive to ISL. The apoptotic cells were dose dependent increased. All cell lines express upper than 95% viability after 3.125 μM and 6.25 μM ISL treated, but the cell malignant phenotypes, such as migration, colony formation, anchorage independent growth, and invasion, were significant inhibited. These results indicate ISL is a high potential new anti-cancer drug.

Cytotoxic activity of ILG (IC50)

Cell lines	IC50 (μM)
OK	56
OF	>400
Ca9-22	135
HSC3	47
OECM-1	105
SAS	103
SCC4	47

Cytotoxic activity was determined by MTT assay.

Poster 4: Synergistic Anti-Tumor and Anti-Migration Activity of Adlay (Coix *lachryma-jobi* L. var. *ma-yuen* Stapf) Extract and Paclitaxel on Human Endometrial Cancer Cells

S. Hsia, T. Shieh, Y. Shih

Objectives: Adlay has long been used in traditional Chinese medicine and as a nourishing food. Adlay extract has been shown to exert antiproliferative effects on breast cancer cancer cells in vitro. Drug resistance frequently develops in tumors during chemotherapy. Therefore, to improve the clinical outcome, more effective and tolerable combination treatment strategies are needed. In this study, we investigated the effect of adlay extract on synergistic anti-tumor activity with paclitaxel and anti-metastatic potency of adlay extract via modulation of the expression of VEGF and MMP in the highly metastatic human endometrial cancer cell line.

Methods: CalcuSyn software was used to evaluate the synergistic interaction of adlay extract and paclitaxel on human endometrial cancer cells. Cell viability is detected by MTT and BrDU assay after variant adlay extract dosage treatment. Adhesion, wound-healing, and transwell migration assays were performed in endometrial cancer cells (RL95-2 and HEC-1A). Expression of matrix metalloproteinase (MMP)-2, MMP-9, and VEGF were measured by Western blot analysis.

Results: Here, we show that adlay extract (100 and 200μg/ml) enhanced paclitaxel-induced apoptotic death in human endometrial cells (RL95-2, HEC-1A). Wound-healing and transwell migration assays revealed that adlay extract (50μg/ml) inhibited migration in HEC-1A cells. According to chamber migration assay and wound migration assay,adlay extract significantly suppressed the migration of MDA-MB-231 cells at 24 h and 48 h. It was further demonstrated that treatment with adlay extract (100 and 200 μg/ml) significantly decreased the levels of MMP-2, MMP-9.

Conclusions: Our results reveal that adlay extract enhanced the therapeutic efficacy of paclitaxel in human endometrial cancer cells, and indicate that adlay extract is a potential anti-tumer agent to inhibit the migration of endometrial cancer cells through the suppression of various related molecules. This is the first study to demonstrate that adlay extract might be a novel anticancer agent for the treatment of endometrial carcinoma though inhibiting migration.

Adlay (Coix *lachryma-jobi* L. var. *ma-yuen* Stapf)

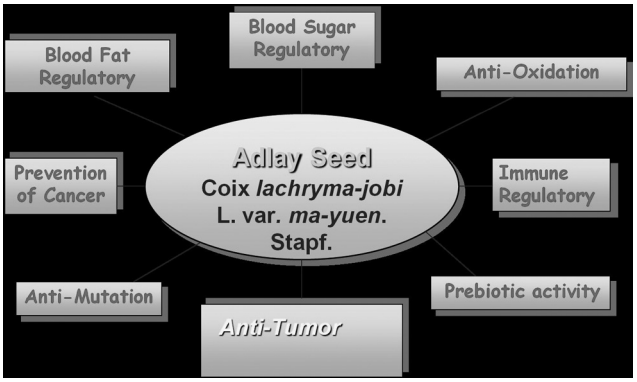

Physiological functions of adlay

Poster 5: Added Criteria Improve Diagnosis in Bosniak IIF and IIIA Group

K.K. Zhang, E. Lang

Objectives: To assess the value of added criteria in further defining and affirming diagnosis of IIF and IIIA Bosniak cystic renal masses.

Methods: Three-hundred-and-eleven Bosniak IIF and IIIA renal cystic masses, classified by 2 phase, 3 phase and 4 phase CT were identified in the files of TMC, New Orleans, SUNY Downstate Medical Center, and Johns Hopkins Bayview Medical Center in the period 1998-2009. 132 patients had a follow-up of at least 12 months or surgical proof of the lesion and were reclassified by 4 phase CT based on added criteria. Criteria added were: (1) increase of HU in arterial phase of 50 HU or greater, (2) in cortico-medullary phase of 50HU or greater, (3) in parenchymal phase of 30HU or greater, (4) washout in parenchynmal or later phase, (5) coarse granular dystrophic calcification, (6) calcifications of variable thickness inside, outisde or within wall of lesion, and (7) soft tissue elements 1mm inside or outside cyst-wall.

Results: Ninety-five lesions were originally classified as IIF lesions, 37 as IIIA lesions. Using the added criteria, 4 phase CTs correctly classified 43 lesions as RCC, 4 as abscess, 1 as AML, 1 as fiborma, 1 as calyceal diverticulum and 79 as multilocular cysts. Three lesions were misdiagnosed, 2 multiloccular cysts (because of step up of HU in cortico-medullary phase and dystrophic calcifications) and one calyceal diverticulum (because of dystrophic calcifications), though overridden by other criteria. One abscess showed dystrpohic calcifications in its wall. The diagnoses were confirmed by surgical specimen in 52 patients and by follow-up CTs in 80. The added criteria improved the diagnosis of RCC to all 43 lesions versus only 29 of the 37 initially staged as Bosniak IIIA lesions.

Conclusions: Added criteria significantly improved accuracy, diagnosing all RCCs, abscesses and benign solid mass lesions.

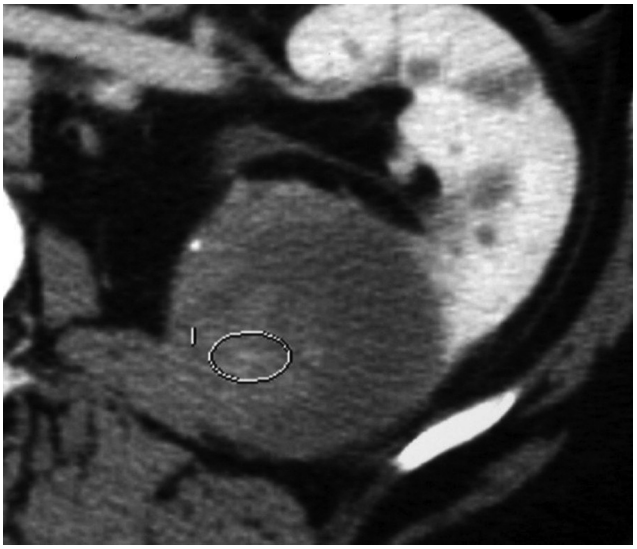

Criteria	True positive	False Positive	False Negative	True Negative	Sensitivity	Specificity
HU +50, early, rim	31	0	12	89	0.721	1
HU +50, corticomed	22	5	21	84	0.512	0.944
HU+30 parenchymal	17	17	26	72	0.395	0.809
30 washout	14	5	29	84	0.326	0.944
Gran calcification	11	2	32	87	0.256	0.978
>1mm calc inside wall	3	1	40	88	0.069	0.989
>1mm calc outside wall	7	5	36	84	0.163	0.944
shell calcification	8	25	35	64	0.186	0.719
>1mm soft tissue inside wall	8	0	35	89	0.186	1
>1mm soft tissue outside wall	8	0	35	84	0.395	0.944

Poster 6: Safety and Efficacy of Cryoablation of Renal Tumors in a High-Risk Patient Population at a Community Hospital

M. Oselkin, J. Kashanian, Y. Eldouaihy, S. Honig, D. Silver, S. Sobolevsky

Objectives: This report represents our experience with image guided percutaneous cryoablation of renal tumors in 66 patients treated at a community hospital. The goal of this study was to show safety and efficacy of cryoablation as a means of treating renal tumors in high surgical risk patients who require maximal preservation of renal function. We also aimed to identify variables which correlated with the incidence of postoperative complications.

Methods: A retrospective chart review of patients with renal masses treated with image guided percutaneous cryoablation between 2007 and 2011 was performed. Indications for cryoablation of renal tumors included multiple medical co-morbidities, solitary kidney, synchronous bilateral renal masses, horseshoe kidney, Von-Hippel-Lindau syndrome, or renal insufficiency. US and CT guidance was used to guide cryoprobe insertion. A procedure was considered technically successful when an ice ball margin was at least 5 mm. Percutaneous needle biopsy was performed at the time of cryoablation in most cases unless a previous biopsy demonstrated renal cell carcinoma (RCC). Post-treatment imaging was used to assess efficacy of treatment and was obtained at three, six, and 12 months post treatment and annually thereafter.

Results: From 2007 to 2011 a total of 70 tumors were ablated in 66 patients. The mean patient age was 70 years-old. Six patients had a solitary kidney, five patients had previous partial nephrectomy, and one patient had a horseshoe kidney. Co-morbidities included morbid obesity, severe hypertension, poorly controlled diabetes mellitus, moderate to severe coronary artery disease, severe pulmonary disease, and renal insufficiency. Mean tumor size treated was 3.0 cm in largest diameter, ranging from 1.4 to 6.5 cm. One patient had simultaneous bilateral cryoablation and one patient with a solitary kidney had three separate tumors ablated. Fifty-six patients were discharged within 24 hrs. There were no deaths. One case was technically unsuccessful due to equipment failure. One patient had re-ablation at three months due to perceived residual tumor in the zone of ablation. Complications were observed in nine cases, all associated with postoperative hemorrhage in the zone of ablation or significant hematuria. Four of these patients required only pRBC transfusions prior to discharge with no sequelae. Among the other five patients: one patient developed bilateral hydronephrosis due to hematuria, which resolved spontaneously; one patient was re-admitted for small bowel ileus, which resolved spontaneously; one patient developed bowel ischemia leading to hemi-colectomy and progressed to ESRD; and one patient had a NSTEMI requiring no intervention prior to discharge. In eight patients with major bleeding complications requiring transfusions, average pre-operative hemoglobin was 11 mg/dl. Incidence of

complications did not correlate with tumor location within the kidney or proximity to vital structures. The incidence of post-operative hemorrhage was significantly higher in patients who had five or more probes inserted and in patients with single tumor size greater than 4 cm in largest diameter.
Conclusions: Image-guided percutaneous cryoablation of the renal tumors is safe in patients with renal cancer who are poor surgical candidates. Results of our study underscore the need for pre-operative optimization of hemoglobin in order to decrease the incidence of postoperative complications. In addition, patients who had greater than four probes per tumor inserted should be carefully monitored for postoperative hemorrhage.

Poster 7: Percutaneous Radiofrequency Ablation of Renal Cell Carcinoma

T.D. McClure, N. Tan, S. Raman

Objectives: To determine the oncologic efficacy of radiofrequency ablation renal cell carcinoma and determine predictors of successful radiofrequency ablation.
Methods: After IRB approval, the records of patients who underwent percutaneous RF ablation for the treatment of proven renal cell carcinoma between 2002 and 2011 were reviewed. Primary, secondary, technical success and technique effectiveness was defined per the International Working Group on Image-Guided Tumor Ablation. The clinical, pathological, technical and clinical outcomes were collected. Multivariate logistic regression analysis was performed to determine predictors of primary technique effectiveness and technique failure. All analyses were done using the statistical software STATA/SE® 11.2. Alpha of 0.05 was considered significant.
Results: 101 patients underwent 135 radiofrequency ablations to treat 116 renal cell carcinomas with a mean follow-up of 19.7 months (range 0-92). The mean age was 72.2 years (range 35-93). The mean tumor size was 2.6 cm (range 0.9-8.1). 16/101 (16.2%) patients had a solitary kidney. Primary technique effectiveness was 100/116 (86.2%) and secondary technique effectiveness was 10/116 (8.6%). Total technique effectiveness rate was 110/116 (94.8%). Local tumor progression occurred in 16/116 (13.8%) tumors. Of these tumors, 10/16 (62.5%) underwent successful re-ablation. 6/116 (5.2%) were considered technique failures. Technical success was achieved in 134/135 (99.3%) of RFA sessions. Complications occurred in 14/135 (10.4%) tumors, of these 5/14 (35.7%) were major complications. No deaths occurred. Using univariate analysis, the primary technique effectiveness cohort had larger tumor size (2.4 cm vs 3.9 cm, $p<0.001$), greater interventionalist experience (67.0 mo vs 51.3 mo, $p=0.055$) and non centrally located tumors (44.7% versus 90%, $p<0.01$) were associated with primary efficacy as opposed to secondary technique effectiveness, respectively. Using multivariate logistic regression analysis to predict overall technique effectiveness versus failure demonstrated that larger size (OR 0.34, 95% CI 0.15-0.79) and presence of solitary kidney (OR 0.06, 95% CI 0.004-0.88) were significant negative predictors of success. The 22.6 months actuarial disease specific, metastasis-free, local tumor progression-free and overall survival rates were 98.8%, 100%, 92.8% and 95.2%, respectively.
Conclusions: Percutaneous radiofrequency ablation of biopsy proven renal cell carcinoma is successful with a mean follow up of 19.7 months. Experience and non centrally located tumors are predictors of primary efficacy. Tumor size and solitary kidney are negative predictors of technique success.

Poster 8: Efficacy of Percutaneous Image-Guided Radiofrequency Ablation for Treatment of Cystic Renal Lesions

S. Lee-Felker, E. Felker, L. Alpern, D. Lu, S. Raman

Objectives: The purpose of this study is to determine the efficacy of percutaneous image-guided radiofrequency (RF) ablation for treatment of malignant or potentially malignant complex cystic renal masses.
Methods: After institutional review board approval, our database was searched to assemble a study cohort of all cases of complex cystic renal lesions that were treated with image-guided RF ablation from 2003 to 2012. The clinical history, imaging features, procedural complications, pathology results, imaging follow-up, and clinical outcomes of each case were reviewed.
Results: A total of 18 patients and 45 lesions were identified; 1 patient with Von-Hippel Lindau (vHL) disease had 26 lesions, another patient with vHL had 2 lesions, and 1 other patient had 2 lesions. The other 15 patients each had a single lesion. Diagnostic tissue was obtained in all cases, with the exception of 1 case in which the pathology was suspicious for malignancy but not proven, and another case in which the pathology was non-diagnostic. No significant complications (bleeding, urine leak, tumor seeding) occurred. Clinical follow-up ranged from 0 to 61 months (average 14 months); primary and secondary treatment efficacy were 96% (43/45) and 100% (2/2), respectively. Lesions that required more than 1 session tended to be larger and more central in location. There were no treatment failures.
Conclusions: Percutaneous image-guided RF ablation is safe and effective in the treatment of complex cystic renal masses.

Poster 9: Thermal vs Impedence-based Ablation of Renal Tumours: Does it Matter? Review of Literature

M. Modabber, S. Athreya

Objectives: The increased use of advanced imaging techniques has increased incidental detection of smaller, asymptomatic renal tumours (diameter < 3.5 cm). Earlier treatment of these small renal tumours has shown better survival outcomes than when symptomatic. Over the last decade, Radiofrequency Ablation (RFA) for SRM has been adopted as an alternative to nephron-sparing surgery (NSS) approach, with comparable efficacy and favourable complication rates and renal functional preservation. The use of radiofrequency technology in the treatment of small renal tumours has been well established and its efficacy and safety documented in the literature. Yet given the relative novelty of the RFA technique for the treatment of renal tumours, several uncertainties in its procedural approach remain. Specifically, the efficacy of thermal-based (RITA Medical Systems) vs impedance-based (Tyco-Valleylab & Boston Scientific) generators in ablating renal tumours has been controversial. The literature to date to directly compare the two approaches has been minimal, based on animal-models, and with variable results. This has led to a variety of treatment algorithms based on user preference rather than an evidence-based treatment approach. Therefore, through a comprehensive review of the literature, we seek to assess the relative safety and efficacy of thermal and impedance-based approaches in the context of renal tumour ablation.
Methods: A comprehensive literature review of Pubmed and Medline was performed to study the prevalence, safety and efficacy of thermal-based and impedance-based approaches to RFA. The outcome measures considered were size of ablation zone, minimization of tissue charring, need for repeat ablation, disease-free survival and rate of tumour recurrence, as well as the rate of complications.
Results: A total of 45 original papers were collected and analyzed. The majority were small retrospective studies, with short-term follow-up, mostly accounted for by the novelty of the procedure. In those studies, more patients were treated using the thermal-based approach than the impedance-based model ($P < 0.05$). Less charring, larger ablation zones and reduced need for reablation were found using the thermal based-model. Complication rates were similar. However, given that both approaches utilize an indirect measure of tissue ablation—thermal based using temperature at the probe, and impedance based relying on impedance as a reflection of tissue ablation—both approaches critically lack real-time monitoring of the temperature and tissue ablation at the renal tissue level itself.
Conclusions: To our knowledge, this is the first attempt to directly and quantifiably compare the relative safety and efficacy of the two approaches in RFA for renal tumours in human subjects. Based on the results of the literature review, thermal-based models do possess certain advantages as compared to impedance-based models in the application of RFA for renal tumours. However, further prospective studies, using larger sample sizes and longer follow-ups are warranted.

Poster 10: Percutaneous Thermoblation of Small (< 5 cm) Kidney Cancer

M. Mazzucco, A. Vario, B. Perin, A. Calabrò

Objectives: Background: There is a lack of data on the use and efficacy of percutaneous treatment of small kidney cancers. Aim: To evaluate the efficacy of microwaves (MWTA) or radiofrequency (RFTA) on the percutaneous treatment of kidney cancer.
Methods: Fifty-four patients (41 males, 13 females; age 67,8±11,2, 35 to 85 years) with kidney neoplasm were treated by using the locoregional ablation in our Unit at Este Hospital, Italy, from April 2008 to December 2011. Inclusion criteria were: peripheral solid cancer <5 cm, comorbidities, high-risk for surgery/anesthesia, renal failure, solitary kidney, PT >50%, platelets >50.000 mm3, surgery refusal and technical feasibility of radical ablation. All patients underwent a biopsy and a TC or MRI for the staging of kidney disease. Percutaneous treatments were performed by using AMICA GEN double system RF/MW (RFTA cool tip 17G needles; MWTA 14G antennas) on patients deep sedated with propofol and spontaneously breathing in oxygen mask. Placement of RF needle or MW antennas were US-guided (Hitachi Preirus) and, in some cases, simultaneously monitored by TC or using TC imaging fusion technique.
Results: Imaging and histological analysis revealed presence of 43 clear-cell carcinoma, 2 oncocytomas, 1 sarcoma and 8 undefined tumors. For the known intrinsic characteristics of the two methods, we have treated the tumors bigger than 2 cm with MWTA, e the smaller ones with RFTA (and even all the patients we treated before September 2009 for the unavailability of the MWTA equipment). 59 treatment sessions were performed: 35 RFTA (1 or 2 needles/session; treatment time 12,1±5,5 min) and 24 MWTA (1 antenna/session: treatment time 10,0±3,1min). A total of 56 tumors were treated with a diameter of 26,6±10,7 mm (10-53 mm; MW treatment 33,3±12,2 mm; RF 21,2±9,6 mm). After treatment, monitoring was conducted at month 1 and then every 6 months (mean follow-up: 18,1±11,9 months, 3-44 months). Complete response, defined as both absence of enhancement in the nodule and presence of avascular necrotic area larger than original lesion one month after treatment, was obtained in 50 patients (92,5%). In the other 4 patients, one had a local recurrence nodule of 37 mm after 6 months (treated with nephrectomy), and 3 had residual disease: 2 nodule

of clear-cell carcinoma (25, 53 mm each before treatment) and 1 nodule of sarcoma (35 mm); all of the last successfully underwent a second ablation session. Adverse events occurred in 3 cases: 2 spontaneously resolving subcapsular renal hematomas and 1 loss of MW antenna tip in the abdominal wall. No change in serum creatinine levels was observed during the entire follow-up.
Conclusions: MWTA and RFTA thermoablation is a safe and successful technique for the treatment of small peripheral kidney cancers and might be an option to surgery in selected patients, leaving surgery as rescue therapy. Microwaves treatment, compared to RFTA, is characterized by a higher power, as it gets larger areas of necrosis, shorter duration and fewer insertions, and consequently by a lower technical difficulty.

Poster 11: Optimal Timing of Follow up Imaging After Renal Tumor Ablation

R. Srinivasa, M.C. Soulen, S. Stavropoulos

Objectives: Follow-up imaging after percutaneous cryoablation and radiofrequency ablation (RFA) of renal tumors with MRI and CT is used to assess for residual or recurrent disease. This study was done to evaluate the utility and timing of MRI and CT scans after cryoablation and RFA renal tumors.
Methods: An IRB-approved review of patients who underwent percutaneous CT guided renal mass ablation performed between 2002 and 2011 was performed. A cohort of 80 (37 cryoablation, 43 RF ablation, average age: 73±11.7, age range: 32-92, 59 males and 21 females) patients who had at least 6 months follow up with contrast enhanced MRI or CT after ablation were included in this study (mean follow-up 28.2 months, range: 9-48 months). Mean tumor size was 3.1 cm (range: 0.9-7.6 cm). At our institution, imaging with MRI or CT is performed 1 month after the procedure and then at 3 month intervals for the first year, 6 month intervals for the second year and then at yearly intervals. Residual or recurrent disease was defined as post-contrast tumor enhancement on follow up MRI or CT.
Results: 66 patients had 100% necrotic, nonviable tumors after initial treatment (primary clinical success rate: 82.5%), on 1 month follow-up imaging. 14 patients (17.5%) had residual viable tumor on CT or MRI 1 month after ablation. 4 of these patients were re-ablated immediately. 10/14 patients elected to follow their residual disease with 4 patients being ultimately being re-ablated due to continued growth of residual disease while 6 patients have not been re-ablated as there has been no progression of their residual disease. 5 of 66 patients (7.6%) with no residual tumor on 1 month scan developed recurrent tumor on follow up imaging. 3 were detected on 3 month scan, 0 on 6 month scan, 1 on 9 month scan, 0 on 12 month scan and 1 at 36 months. Mean initial size of tumors that were 100% necrotic after initial treatment was 2.8 cm (range: 0.9-6.5) and mean initial size of tumors that had residual tumor at 1 month scan was 3.7 cm (range: 2-7.6 cm) which was statistically significant (p = 0.009).
Conclusions: The MRI or CT performed 1 month and 3 months after renal tumor ablation helps direct therapy, but additional scans in the first year appear to be of limited value. Patients do require long-term follow up with surveillance imaging.

Poster 12: Utilization of "Nephrometry Score" to Assess Outcomes of Percutaneous Cryoablation versus Partial Nephrectomy in Management of Renal Cancers

J. Sweeney, M. McCain, P. Spiess, B. Biebel, J. Choi, B. Arslan

Objectives: To evaluate outcomes percutaneous cryoablation and surgical partial nephrectomy utilizing predictive value of Nephrometry Score. Nephrometry score is a commonly used tool by urological practices to predict surgical outcomes.
Methods: All patients who underwent percutaneous cryoablation and partial nephrectomy during the past 2 years in our institution were reviewed. Their nephrometry scores were identified by measuring lesion diameter, distance from hilum, anatomical position, as well as presence or absence of exophytic component. All pre-procedure and post-procedure images were reviewed for scoring. Complication rates, hospital stay, procedure cost and recurrence rates were assessed.
Results: 27 patients underwent cryoablation and 127 patients underwent partial nephrectomy. Median follow up for partial nephrectomy group was 4.5 months and cryoablation was 13.3 months. There were no recurrences in the cryoablation group and 6 recurrences in the partial nephrectomy group. This was not statistically significant with a P value of 0.2. There was one major complication in the partial nephrectomy group that required primary ureteral repair and one complication in the cryoablation group that required embolization after treatment of an 8 cm lesion with a nephrometry score of 10X. Overall there were no difference in the nephrometry scores of each group and patient selection was primarily due to urologists' choice.
Conclusions: Using nephrometry score assessment we could not find a significant difference in outcomes of patients undergone partial nephrectomy versus cryoablation within similar nepohrometry score group patients.

Poster 13: Effect of Experimental Consolidatory Chemoterapy Administration on the Numbers of Regulatory T Cells in Peripheral Blood in Patients with Ovarian Carcinoma

T. Brtnicky

Objectives: It was observed that patients with different types of oncological diseases have increased numbers of CD4+CD25+ regulatory T cells (Treg) in the peripheral blood. Treg participate in the control of anti-tumor immunity. Higher levels are an unfavourable factor. The purpose of experimental consolidatory therapy is to strongly decrease the numbers of circulating regulatory T cells and thus theoretically intensify natural anti-tumor immunity against persisting chemoresistant cells. Aims of study: To compare the effect of particular chemotherapeutics in metronomic doses on the number of Treg. To confirm if the percentage of Treg correlates with the prognosis of patients with ovarian carcinoma.
Methods: We follow up 3 groups of patients. Group A: receive low doses of cyclophosphamide (twice a day 50mg orally, 14 days on and 10 days off for 12-24 weeks). Group B: receive low dosis of etoposid (once a day 50mg orally, 14 days on and 10 days off for 12-24 weeks). Group C: without consolidatory therapy. Protocol of the study: (1) radical surgery, (2) 6 - 8 series of combined chemotherapy, (3) experimental consolidatory chemotherapy. The detection of Treg was provided by FACS Aria (Becton Dickinson) flow cytometry. Expression of intracellular FoxP3 antigen was meassured by e-Biosence detection set and antibodies marked by fluorochromium against FoxP3, CD25, CD4 a CD3.
Results: 32 patients is included in the study, median follow up time is six months. 4 patients suffer from early relapse of the disease. We have found normal levels of Treg in patients with consolidatory chemotherapy in contrast to patients without consolidatory chemotherapy. Before 1 relapse of the disease significant elevation of Treg was found. There was no significant difference between relaps free survival curves in patients use cyclophosphamide and etoposide.
Conclusions: Monitoring the numbers of Treg is a hopeful prognostic marker of disease development and may provide insight to both effect of primary treatment and new experimental treatment procedures.

Poster 14: Ultrasound Volume Navigation/Fusion for Image Guided Biopsies: Effect of Radiation Dose, Procedure Time and Clinical Outcome

A.S. Amorosso, J. Erinjeri, M. Maybody, W. Alago, A. Porreca, S. Solomon

Objectives: To prospectively evaluate the efficacy of ultrasound volume navigation/fusion on total intra-procedural radiation dose, procedure time and clinical outcomes of biopsies.
Methods: Ultrasound volume navigation/fusion (v-nav) guidance was utilized on 30 prospectively selected biopsies. All biopsies in this study were performed by the same group of interventional radiologists. A GE E9 ultrasound machine was used to fuse real-time ultrasound images to another cross-sectional imaging study (MRI=14, PET/CT=5, CT without contrast=3 and CT with contrast=8). We measured the total dose length product (DLP) of v-nav guided biopsies (n=30): v-nav only guided biopsies (n=24) and v-nav/CT guided biopsies (n=6). As a control group, we retrospectively measured the total radiation doses of the last consecutive CT guided biopsies (n=60). Clinical outcome was defined as the adequacy of samples for cytological interpretation. We measured the rate of adequacy from the v-nav cases and compared it to the control group of CT guided biopsies for comparison. We defined procedure time as the interval between the time the patient was prepped and the time of bandage or dressing placement. We recorded the procedure time for the v-nav only guided biopsies (n=24) and compared it to a subset of the control group of CT only guided biopsies (n=34) where procedure times were available.
Results: Of the 30 prospectively selected biopsies, 80% (24/30) of cases performed achieved the desired plan with no total intraprocedural radiation dose (0.0 Gy-cm). 20% (6/30) of cases performed required one low dose CT scan (DLP=104.02 +/-81.28 Gy-cm) intraprocedurally. The average radiation dose for the v-nav guided biopsies was significantly smaller than the average radiation dose of the control CT cases (DLP= 20.8 vs. 392.8 Gy-cm, p<.00001). Even after excluding V-nav only cases with no dose, the average dose per case remained significantly smaller (DLP=104.0 vs 392.8 Gy-cm, p<.00001). There was no significant difference in clinical outcomes of the v-nav guided biopsies when compared to the control CT guided biopsies (93% vs 95% adequacy, p<.744). There was no significant difference in the procedure time in the v-nav only guided biopsies when compared to the subset of control CT guided biopsies where procedure times were available (30.95 +/- 9.46 minutes vs. 29.71 +/- 15.75 minutes, p<.715).
Conclusions: Ultrasound volume navigation-fusion guidance for biopsies can minimize total intraprocedural radiation dose without compromising clinical outcome or increasing procedure time. As radiation dose during image guided procedures becomes an increasingly important quality assurance and safety metric, ultrasound fusion may prove useful in reducing radiation exposure while maintaining clinical standards and room efficiency.

Utilizing an accurate registration with ultrasound fusion can help to accurately plan a trajectory to biopsy or treat a difficult target.

Poster 15: Utilizationation of IG4 Treatment Planning Software in Bone Ablation and Verification with Contrast Enhanced MRI

M. Maybody, C. Stevenson, A.S. Amorosso, S. Solomon

Objectives: Ablation of bony targets is challenging as the ablation zone is not visible with any of the thermal ablation modalities (hot or cold). Additionally, except when MRI is used for imaging guidance, the ablation zone cannot be verified with immediate post ablation contrast-enhanced imaging. MRI is not the main imaging guidance modality for the majority of bone ablations. Having a better understanding of the geometry of the ablation zone during any ablation directly impacts outcome, as suboptimal coverage of a target results in residual tumor or early recurrence. We applied the Veran Ig4 treatment planning software during CT guided radiofrequency ablation (RFA) of bony lesions in five patients and verified its treatment plan with contrast enhanced MRI obtained 6-8 weeks post ablation.

Methods: Between November 2011 to January 2012, five patients (age 9-43, male n=3, female n=2) underwent CT guided RFA of bony lesions (osteoid osteoma n=3, breast metastasis n=1, sarcoma metastasis n=1)(acetabulum n=2, ilium n=1, femur n=1, tibia n=1). Non-tined Covidien Cool-Tip probes were used for all cases (one probe n=4, two probes n=1). The ablations were performed using cautery mode without chilled saline for osteoid osteomas and RFA using chilled saline for metastatic cases. A hub mounted tracking assembly was used on each ablation probe. Veran Ig4 treatment planning software was applied to each case. Probe position was adjusted based on visual feedback from the software prior to initiation of each ablation. The actual ablation zones on contrast enhanced MRI obtained 6-8 weeks post ablation were retrospectively matched against the treatment plan provided by the software during ablation (figure 1).

Results: The average total time added to each ablation case for using Ig4 software was 5.97 minutes. The size of the actual ablation zone is 1- 4 mm larger in maximum dimension. The shape of ablation zone closely matches the shape on treatment planning with slight extension into the bone. This may be due to the oven effect of bone in comparison to adjacent soft tissue or an inherent inaccuracy caused by the hub mounted tracking assembly on a relatively flexible RFA probe. The visual feedback of the ablation zone and its relationship to the target tumor was found important by the operating physician in each case (figure 2).

Conclusions: Ig4 treatment planning software is helpful to finely adjust the position of ablation probes during thermal ablation of bony lesions.

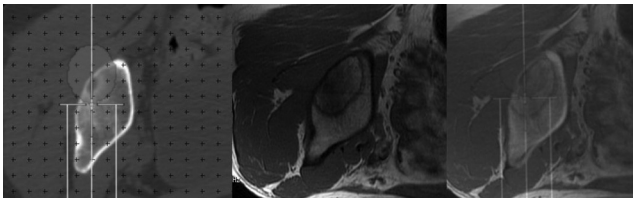

Figure 1- Left: Proposed ablation zone for a right supra acetabular lesion. Middle: Corresponding actual ablation zone on MRI 6 weeks post ablation. Right: Retrospective matching of the two ablation zones.

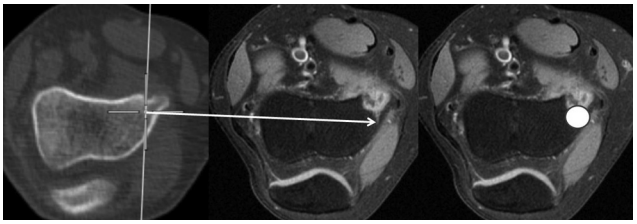

Figure 2- Left:Tracking of the RFA probe tip (green cross) predicts the ablation zone to fall beyond the cortical target (osteoid osteoma). The RFA probe was repositioned into the lesion using the visual feedback from Ig4 treatment planning software. Middle: contrast enhanced MRI 6 weeks after ablation shows appropriate coverage of target by ablation zone. The original position of RFA probe tip beyond the target is visible (white arrow). Right: The presumed location of ablation zone (white circle) had the ablation been performed in the original probe position.

Poster 16: Fiducial Marker Placement in the Spine for Image-Guided Radiation Therapy: Tips and Tricks

T.H. Nguyen, J. Kuo

Objectives: Correct placement of fiducial markers is very important for accurate and safe delivery of radiation dose during Image-guided Radiotherapy (IGRT) or Intensity Modulated Radiotherapy (IMRT). We present the basic principles, with tips and tricks to achieve the best outcome.

Methods: Fiducial markers were placed under fluoroscopic guidance in 11 patients with vertebral metastases (total of 22 levels). Vertebroplasty was also performed at the same time for early pain relief and spinal stability. These patients subsequently underwent IGRT/IMRT to the involved spine, receiving maximum dose to the area of tumor, and minimal dose to the adjacent critical neural structures (i.e. spinal cord, nerve roots). Type, size, number, location, distribution, geometry, and artifacts related to the implanted markers were analyzed for best outcome.

Results: A minimum number of markers (two) should be placed within the vertebra to be treated though three are best in order to provide redundancy in the event of marker seed loss and to provide an additional check for analyzing translation and rotational shifts. These should be separated by at least 10 mm and placed in different planes to avoid overlapping or artifacts when viewed from either orthogonal orientation. Markers should be small (5 mm), but radiopaque enough to be visible on orthogonal treatment planning radiographs and IGRT imagers. Newer models feature textured surfaces to maximize tissue "grip" and minimize post-implantation shift. These textured markers are particularly useful for implantation into softer tissues such as near mucosal surfaces. The carbon-based markers are best for CT planning due to lack of or very minimal artifacts generated and are often preferred by those concerned about imaging artifact in post-treatment follow up scans. If particularly critical structures, such as the spinal cord, are in close proximity to the target lesion then placement of one or two marker seeds in the aspect of the target lesion closest to the critical structure can maximize positional accuracy in that direction.

Conclusions: Placement of fiducial markers within the metastatic spine is crucial for motion correction to achieve successful treatment with IGRT or IMRT. The minimum number, distribution, and type of markers to be placed were found to be very useful and important.

Poster 17: Radiofrequency Ablation of Hepatic Tumors Located in Dangerous Areas: Comprehensive Review

J. Choi, J. Lee, Y. Park, C. Lee, K. Kim, C. Park

Objectives: Radiofrequency ablation (RFA) is widely used to treat hepatic tumors including hepatocellular carcinoma and metastasis. However, the application of RFA can be limited when a target tumor is located near the vital vascular structures or adjacent organs such as bowels, gallbladder, heart, or diaphragm where it could lead to collateral thermal injury. 1) To review dangerous areas for RFA where hepatic tumors are located adjacent to vital structures or organs. 2) To understand the potential complication when performing RFA on hepatic tumors situated in dangerous areas. 3) To learn RFA techniques to maximize treatment outcome and to minimize complication in treating tumors in dangerous areas.

Methods: We retrospectively reviewed our 10 year experience of RFA on hepatic tumors. Among these cases, we selected cases where hepatic tumors were located in dangerous areas. Dangerous areas is defined as hepatic tumors located adjacent to the intrahepatic structures such as portal vein, bile duct, or hepatic veins; or tumors adjacent to the gallbladder, bowel, kidney, heart, or diaphragm. In this exhibit, we demonstrate outcome and possible complications of RFA treating hepatic tumors in dangerous areas, and how to prevent the possible complications, such as RFA planning route and artificial ascites injection.

Results: RFA appears to be an effective and safe treatment modality for hepatic tumors located in dangerous areas when applied with appropriate techniques to prevent

the possible complications. Awareness of proper RFA approaches and techniques helps treat hepatic tumors in dangerous areas without complications.

Conclusions: RFA appears to be an effective and safe treatment modality for hepatic tumors located in dangerous areas when applied with appropriate techniques to prevent the possible complications. Awareness of proper RFA approaches and techniques helps treat hepatic tumors in dangerous areas without complications.

Poster 18: The Efficacy, Safety, and Tolerability of Radioembolization in Unresectable Hepatocellular Carcinoma with Whole-Liver, Lobar, or Segmental Treatment

F. Fiore, J.I. Bilbao, L. Carpanese, R. Cianni, R. Golfieri, D. Gasparini

Objectives: To evaluate whether treatment of either whole liver or part of the liver impacts on the safety, tolerability and overall survival following radioembolization with ^{90}Y resin microspheres in patients with predominantly intermediate- or advanced-stage hepatocellular carcinoma (HCC).

Methods: This was a multicenter retrospective study conducted in 325 consecutive patients with unresectable HCC who received ^{90}Y-resin microspheres (SIR-Spheres; Sirtex Medical) between 09/2003 and 12/2009. Candidates for radioembolization had typically good liver function (Child-Pugh class A: 82.5%), and a good Eastern Cooperative Oncology Group (ECOG) performance status (PS) (ECOG 0–1: 87.7%) and 41.5% had had a prior procedure. Most (78.5%) had underlying cirrhosis with an aetiology identified as hepatitis B or C in 13.0% and 44.3% of cases, respectively. The HCC was characterized as predominantly multinodular (75.9%), invading both lobes (53.1%) including some with high alpha-fetoprotein levels (>400 ng/mL; 34.9%), portal vein occlusion (23.3%) and extrahepatic disease (9.2%).

Results: Most patients received whole-liver (155; 47.7%, including 5 with prior left lobectomy and subsequent right lobar radioembolization, and 3 receiving sequential lobar radioembolization) or right-lobe administration (118; 36.3%) and a few left-lobe (28; 8.6%) or selective segmental treatment (24; 7.4%), as a single session (>90% of cases). Compared with lobar or segmental approaches, whole-liver treatment was associated with a higher target liver volume (median whole-liver: 1757; right-lobe: 1197; left-lobe: 584; segmental: 400 mL; p<0.001) and occlusion of non-target arteries was more common (whole-liver: 84.5%; right-lobe: 40.7%; left-lobe:46.4%; segmental: 25.0%; p<0.001), with a non-significant difference in delivered activity (median whole-liver: 1.7; right-lobe: 1.4; left-lobe: 1.4; segmental: 1.2 GBq; p=0.153). Treatment approach differed significantly according to the number of nodules, distribution (uni- vs. bi-lobar), PS and Barcelona Clinic Liver Cancer (BCLC) stage (p<0.001). Patients with early (stage A) vs. advanced (stage C) HCC were more likely to receive segmental treatment (45.8% vs. 33.3%) than left-lobe (32.1% vs. 42.9%), right-lobe (14.4% vs. 50.8%) or whole-liver (9.7% vs. 66.5%) treatment. Median survivals [95%CI] for patients treated with segmental, left-lobe, right-lobe and whole-liver approaches were 23.7 [9.0–not reached], 13.8 [8.7–27.4], 13.1 [10.2–18.4] and 12.4 [10.4–15.4] months, respectively (p=0.176). No treatment approach further compromised liver function (bilirubin, albumin, ALT, INR or platelets) as measured by an increase in CTCAE grade >3 from baseline to 3 months (p>0.05) (Table 1). Transient fatigue was common (54.5%) and more frequent with whole-liver than lobar/segmental treatment (p<0.001). The incidence of GI ulcers was 3.7% (overall) and 5.8% (with whole-liver treatment; p=0.102).

Conclusions: Radioembolization using ^{90}Y-resin microspheres tended to be tailored to the burden of HCC and the liver was not further compromised irrespective of the extent of hepatic volume treated. Disease stage, rather than treatment approach, was the main driver of survival.

Table 1. Main Laboratory Adverse Events to Month 3

CTCAE v3	Cohort	N	Pre-Treatment		Month 3		p-value†
			All Grades	Grade ≥3	All Grades	Grade ≥3	
Total Bilirubin	Whole Liver	145	18.6%‡	0	49.7%‡	6.2%	p=0.604
	Right Lobe	104	26.0%‡	0	49.0%‡	5.8%	
	Left Lobe	21	38.1%‡	0	42.9%‡	4.8%	
	Segmental	22	18.2%‡	0	45.5%‡	4.5%	
Albumin	Whole Liver	115	42.6%	0	37.4%	0	p=0.153
	Right Lobe	85	37.6%	0	42.4%	2.4%	
	Left Lobe	18	33.3%	0	55.6%	0	
	Segmental	19	15.8%	0	26.3%	0	
ALT	Whole Liver	143	71.3%	2.1%	67.8%	3.5%	p=0.606
	Right Lobe	98	47.2%	1.1%	49.4%	3.4%	
	Left Lobe	19	47.4%	5.3%	47.4%	5.3%	
	Segmental	21	42.9%	0	28.6%	0	
INR	Whole Liver	138	26.1%	0	37.0%	3.6%	p=0.140
	Right Lobe	98	19.4%	0	29.6%	0	
	Left Lobe	20	10.0%	0	20.0%	0	
	Segmental	21	23.8%	0	14.3%	0	

† significance across sub-groups by the Kruskal-Wallis test; ‡ significance p<0.001 for entire cohort by exact McNemar test

Poster 19: Impact of Prior Procedures on Safety, Tolerability and Overall Survival Following Radioembolization in Patients with Unresectable Hepatocellular Carcinoma

F. Fiore, J.I. Bilbao, L. Carpanese, R. Cianni, R. Golfieri, D. Gasparini

Objectives: Radioembolization, which enables the delivery of high-dose radiation preferentially to liver tumours, is used in some specialist centers as part of the multimodal treatment of unresectable hepatocellular carcinoma (HCC) with intermediate and advanced-stage disease. This retrospective analysis by the 8 centers comprising the European Network on Radioembolization with ^{90}Y microspheres (ENRY) evaluated the impact of prior hepatic-directed procedures on the outcomes following radioembolization.

Methods: Patients were considered eligible for radioembolization with ^{90}Y resin microspheres (SIR-Spheres; Sirtex Medical) if they were not suitable for surgery (resection, liver transplantation) or ablation (percutaneous ethanol injection [PEI], radiofrequency ablation [RFA], cryoablation), or had progressed on prior surgery, ablation or vascular therapy (transarterial [chemo]embolization [TACE/TAE]). Consecutive candidates (n=325) for radioembolization who were evaluated between 09/2003 and 12/2009 were mostly Child-Pugh class A (82.5%), with cirrhosis (78.5%) and good performance status (ECOG 0–1: 87.7%) but many had multinodular (75.9%), bilobar (53.1%), advanced (BCLC) stage C HCC (56.3%) and/or portal vein occlusion (23.3%). Patients were evaluated from baseline to month 3 post-radioembolization for adverse events; differences between cohorts in CTCAE grade from baseline to month 3 were assessed by the Wilcoxon rank sum test. Kaplan-Meier analysis with stratification by prior treatment was used to estimate overall survival. All statistical algorithms were conducted using SAS (Cary, North Carolina) analytical software.

Results: 135 patients (41.5%) had had a prior procedure including: prior hepatic surgery (n=59; 18.2%), ablation (n=30; 9.2%) and/or vascular procedures (n=89; 27.4%). The analysis found few differences in baseline characteristics between prior procedure groups, except for a higher baseline total bilirubin in treatment-naïve patients (mean 1.2 vs. 1.0 mg/dL; p=0.001). A slightly higher activity was administered to treatment-naïve patients (median 1.7 vs. 1.5 GBq; p=0.002) reflecting the higher target tumour volume (median 250.0 vs. 180.0 mL). No significant differences were observed in overall survival between the prior procedure and treatment-naïve groups (median [95% CI]: 12.8 [10.8–18.8] vs. 12.5 [10.4–16.6] months; p=0.533). Overall survivals did not differ significantly when patients were stratified by type of prior procedure (surgical, vascular or ablative), or by BCLC stage. The pattern and severity of clinical and laboratory adverse events varied little between patients stratified by any or no prior procedure. A greater proportion of patients who had had any prior treatment experienced transient Grade 1/2 fatigue (p=0.026) and Grade 1/2 abdominal pain (p=0.034) post-radioembolization. The incidence of Grade ≥3 thrombocytopenia was low, but more prevalent at 3 months post-radioembolization in those patients who had no prior procedure; these changes were unlikely to be clinically relevant.

Conclusions: Patients who have failed prior procedures can be effectively and safely treated with radioembolization and had outcomes similar to those who were treatment naïve. Radioembolization could be considered as a valuable treatment option for patients who relapse following surgical, ablative or vascular procedures and who remain suitable candidates for treatment.

Poster 20: Assessment of Chemoembolization Combined with preTACE Gelfoam to Treat Unresectable Hepatocellular Carcinoma and Arteriovenous Shunting

D.R. Marker, K. Hong, C. Georgiades, N. Bhagat, A. Jain, J.H. Geschwind

Objectives: Chemoembolization for the treatment of hepatocellular carcinoma (HCC) is reliant on the synergistic effect of locoregional chemotherapy and embolization. HCC arteriovenous shunting is considered a relative contraindication for TACE by compromising this synergy, potentially with systemic escape or damage to healthy liver. PreTACE Gelfoam embolization has been suggested as a potential intervention. The purpose of the present study was to assess the safety and efficacy of Gelfoam prior to TACE for the treatment of patients who have unresectable HCC and arteriovenous shunting.

Methods: Between August 2001 and September 2011, a total of 16 patients (12 males and 4 females) with a mean age of 63 years (range 41 to 88 years) had imaging evidence of arteriovenous shunting (14 arterioportal and 2 arteriohepatic) and were treated with Gelfoam occlusion. There were 9 patients treated with CAM conventional TACE and 7 with DEB-TACE. Mean follow-up to the time of death or end of study was 17 months (range, 4 to 54 months). All complications were noted and liver enzymes were assessed following treatment. Efficacy of the procedure was compared to historical controls without shunting.

Results: Follow-up CT scans demonstrated good tumoral distribution of the chemotherapy mix. 19% (3 of 16) of the patients required repeat Gelfoam during subsequent chemoembolization treatments due to residual arteriovenous shunting. All patients experienced pain, nausea, vomiting, and/or generalized weakness, and one patient refused additional treatments due to these effects. However, there were no asso-

ciated acute complications, such as hepatic infarction or acute liver failure. Mortality was 0% at 30 days post-procedure. Survival rates were 88% at 6 months, 71% at 1 year, and 33% at 2 years.

Conclusions: There are limited studies that have reported the outcomes for TACE in patients who have HCC with arteriovenous shunting. Some of the treatment approaches reported for these cases include preTACE ethanol, histoacryl, coils, and polyvinyl alcohol particles. The results of the present study suggest that preTACE Gelfoam is a safe and effective option. The survival rates of the present cohort are similar to recently reported outcomes in studies that have assessed chemoembolization in patients who did not have shunting.

Poster 21: Comparison of Various Criteria to Evaluate Response and Efficacy in Treatment of HCC by Lobar Therasphere Y90 Radioembolization: A Single Institute Experience

B. Kolar, A. Sharma, J. Xue, D. Lee, A. Katz, D. Waldman

Objectives: To evaluate efficacy and radiological response to lobar radioembolization of hepatocellular carcinomas (HCC) based on various evaluation criteria such as RECIST, mRECIST, WHO and EASL. To evaluate efficacy and response to lobar radioembolization of recurrent/residual hepatocellular carcinoma (HCC) treated previously.

Methods: This prospective study included 26 patients with HCC having 79 tumors. 19 patients were treatment naïve (Group 1) before radioembolization whereas 7 patients (Group 2) had received prior treatment [transarterial chemoembolization (4), Cryoablation (1), RFA (1) and combined TACE and Cryoablation (1)]. There were 48 hepatocellular carcinomas in Group 1 (19 treatment naïve patients) and 31 tumors in Group 2 (7 previously treated) patients. Group 1 (19 treatment naïve) patients underwent 22 lobar injections and Group 2 patients (7 who had previous treatment) underwent 8 lobar injections. Response of the tumors was evaluated with various evaluation criteria such as RECIST, mRECIST, WHO and EASL using pre- and post-treatment MRI. The follow up MRI was done at 3 and 6 months. As per mRECIST, the reduction rate of tumor was calculated by measuring the amount of enhancement in the treated tumor and comparing it to pretreatment enhancement. In RECIST and WHO criteria, reduction rate was calculated by comparing pre and post treatment size of tumor. Lobar response was calculated by comparing the number of lobes that were treated which showed complete or partial response by the various criteria.

Results: The mean reduction rate of treated tumor by mRECIST criteria in Group 1 (treatment naïve) hepatocellular carcinomas was 71.95% at 3 months and 89% at 6 months and in Group 2 (previously treated) patients was 64% at 3 months and 89.33% at 6 months. Mean lobar tumor response including both groups of patients at 6 months according to mRECIST was 90% (27/30) with progression of disease in the other three lobes of different patients. EASL correlated well with mRECIST criteria showing complete response in 11, partial response in 15 lobes, stable disease in 1 and progression of disease in the other three lobes with mean response rate of 86.67% (26/30). Both the evaluation criteria depending on size (RECIST and WHO) had response rates of 26.67% (8/30) with stable disease in 19 and progression in 3 lobes.

Conclusions: 1. There is a significant and effective response of hepatocellular carcinomas to lobar radioembolization with therasphere Y-90 radioembolization. 2. Patients treated previously by other modalities such as TACE and cryoablation with persistent or recurrent lesions also had a significant response rate when treated with radioembolization. 3. Among the different criteria, mRECIST and EASL are better indicators of the response to radioembolization.

Poster 22: Efficacy and Safety of Arterial Closure in Thrombocytopenic Patients with Hepatocellular Carcinoma

S.J. Sequeira, A.P. Gould, A.J. Frangos, J.W. McCann, D.B. Brown

Objectives: Many patients with hepatocellular carcinoma (HCC) presenting for intra-arterial therapy are thrombocytopenic. We routinely use an arterial closure device in these patients (Angioseal VIP, St. Jude Medical). Instructions for use with this device recommend against deployment in patients with thrombocytopenia (platelets < 100,000), raising questions whether such patients should undergo transfusion to avoid puncture site complications. We evaluated the efficacy, safety, and follow-up angiographic findings following closure in our HCC population.

Methods: We reviewed HCC patients who had undergone closure from December 2007-February 2011. Platelet transfusions were not performed. At the end of each procedure, contrast study of the access site was performed to assess appropriateness for closure: artery diameter > 4mm without atherosclerotic plaque. Access location was either common femoral (CF), superficial femoral (SF) or profunda femoral (PF) artery. Clinical success was defined as immediate hemostasis upon deployment of the closure device without supplemental compression. Comparative success at different platelet thresholds was evaluated: greater than 100,000 platelets as well as mild (<100,000), moderate (<75,000) or severe (<50,000) thrombocytopenia. Patients were evaluated for complications at follow-up in-house and in IR clinic. For patients undergoing additional treatments, follow-up angiograms were assessed to determine the maintenance of arterial patency after previous closure.

Results: 161 HCC patients underwent 333 closures. 202/333 (60.7%) were performed with some degree of thrombocytopenia. Clinical success was achieved in 323 of 333 closures (97.0%). In all device failures, hemostasis was achieved with approximately 5 minutes of manual compression. Table 1 summarizes the success rates for closure at the three different thresholds of thrombocytopenia compared to normal. Fisher's exact test showed similar outcomes between groups at all platelet counts. T-test revealed no statistically significant difference in the platelet counts of successful and failed closures (p=0.54). 2 minor (0.6%) and 1 major complications (0.3%) occurred. Minor complications included 1 hematoma and 1 episode of post-procedural bleeding without a hematoma. Both patients had mild thrombocytopenia. The 3rd patient had a platelet count of >100,000 and developed a pseudoaneurysm requiring surgical repair following exertion the day of the procedure. 86 patients underwent 157 subsequent angiographic studies after closure (median 1 additional, range 1-6) (Table 2). Median time to follow-up angiography was 38 days (range 6-633 days). Closure location was CF: 152, SF: 5 and PF: 0. Repeat angiography demonstrated no change in the access site appearance in 155/157 cases (98.7%). One of the patients with narrowing had 1 previous closure of the CF and the other had 4 previous closures of the SF.

Conclusions: Percutaneous closure is safe, effective, and repeatable even in the setting of moderate to severe thrombocytopenia.

Table 1

Platelet Count	N Closures	Success (%)	p value
>100,000	131	127 (96.9%)	
<100,000	202	196 (97.0%)	1.00
<75,000	84	81 (96.4%)	0.72
<50,000	32	31 (96.9%)	1.00

Table 2

	Number of Follow-up Closures					
	1	2	3	4	5	6
Total Procedures	80	42	22	7	5	1
Normal Appearance	80	41	22	7	4	1
Abnormal Appearance	0	1	0	0	1	0

Poster 23: Early Diffuse Recurrence of Hepatocellular Carcinoma after Percutaneous Radiofrequency Ablation: Analysis of Risk Factors

H. Rhim, M. Lee, Y. Kim, H. Lim

Objectives: The purpose of this study was to evaluate the risk factors affecting early diffuse recurrence within one year after percutaneous radiofrequency ablation (RFA) for hepatocellular carcinoma (HCC).

Methods: Out of 146 patients who received transcatheter arterial chemoembolization (TACE) for treatment of recurrent HCC within one year after RFA, we selected 23 patients with early diffuse recurrence (17 men, 6 women; mean age, 65 years). Early diffuse recurrence was defined as three or more new recurrent HCCs in the liver within one year after initial RFA. As a control group, we selected 23 patients, matched exactly for age and sex, in which there was no local tumor progression or new recurrence after initial RFA. To analyze the risk factors, we examined patient factors (pre-RFA alpha-fetoprotein, Child-Pugh classification, cause of cirrhosis) and tumor factors (size, location, margin, contact with portal vein, hepatic hilum, or hepatic capsule, presence of ablative margin on CT). Recurrent HCC was defined as an enhancing mass in arterial phase with washout in the portal or delayed phase of dynamic liver CT. We used Cox-regression tests with univariate and multivariate analyses to identify the risk factors affecting early diffuse recurrence after RFA.

Results: Recurrent tumors occurred from 30 to 365 days after RFA. The median time from initial RFA to recurrence was 203 days. Nine out of 23 patients (39.1%) had four or more recurrent HCCs. Of the patients, three (13.0%) had intra- and extra hepatic recurrence at the time recurrence was diagnosed (lung metastasis, n=2; abdominal wall metastasis, n=1). Uni-variate analysis indicated that larger tumor size and poorly defined margin of tumor were significant risk factors for early diffuse recurrence after RFA (P<0.05). Multivariate analysis indicated that poorly defined margin of tumor was a significant risk factor (P<0.05).

Conclusions: Large tumor and poorly defined margin of tumor may be risk factors for early diffuse recurrence of HCC within one year after RFA. Tumors with such risk factors should be treated with a combination of TACE to minimize the potential of therapeutic failure.

Poster 24: Laparoscopic Thermal-Ablation of HCC with Microwave: Preliminary Experience and Results

R.M. Lauro, P. Reggiani, L. Caccamo, U. Maggi, E. Melada, G. Rossi

Objectives: The Hepatocellular Carcinoma (HCC) is the most responsive tumor to thermal-ablation techniques leading to their extended use in cirrhotic patients especially when enrolled for liver transplantation, according to BCLC guidelines. A new thermal-ablation technique with promising preliminary results has recently come out.

The aim of our preliminary study is to analyze our mid-term results using the Laparoscopic Microwave (LMW) treatment in 30 cirrhotic patients suffering from HCC.
Methods: From May 2010 to December 2011, cirrhotic patients harboring at least a HCC in stage A of the BCLC classification, within the Milano Criteria and located in critical sites (abutted the diaphragm, close to the gut, beneath the Glisson's capsule), underwent LMW treatment. The diagnostic work-up was always completed according to the BCLC guidelines. The LMW treatment was always carried out using the US-guide. The MW AMICA probe HS (2,45 Mhz). Hospital service was used for the ablation treatment. A single Microwave (MW) antenna delivering a power from 45 to 60 Watts for 5-10 minutes was always used. Lesions bigger than 30 mm had 2 or 3 antenna insertions. To assess the efficacy of the MW treatment, a CT-scan was obtained after one, three, six and nine months.
Results: Thirty patients (21 male, 9 female, median age 69.2 (range: 47-84), 21 Child-Pugh A and 9 Child-Pugh B) had the laparoscopic approach with a single MW antenna. The etiology of cirrhosis was HCV in 19 patients, HBV in 7 patients, Ethanol in 3 patients and NASH in 1 patient. The medium size of the nodules was 26 mm (range 21-39 mm). Eighteen patients had 1 nodule, 8 patients had 2 nodules and 2 patients had 3 nodules. Single Laparoscopy was undertaken in all patients with multiple ablation when needed. The post-operative time was uneventful with a maximum hospital stay of 3 days (median 2.4 days). No deaths were reported. After one month, 27 (90%) patients showed the complete necrosis of the nodules which was also confirmed after three, six and nine months. Three patients out of the 27 mentioned above, showed new-onset nodules at 3 months without local recurrence (10%).Two patients showing partial response (residual disease) after 1 month (6.7%),were indicated to repeat ablation either laparoscopic or trans-arterial depending on the sites of the residual disease. One patient was lost during the follow-up (3rd month). Two patients showed a partial thrombosis of a second order portal vein branch which was cleared with heparin in a month of treatment.
Conclusions: Our preliminary experience showed that the MW treatment by laparoscopic approach is safe. Compared to the RFA (Radiofrequency Ablation), the efficacy of the treatment with MW is really promising, especially for lesions bigger than 30 mm. Furthermore, according to our experience, the MW treatment seems to offer shorter application time without affecting the performance and also appears to obtain good ablation of bigger lesions along with superior necrosis rate. It stands to reason that the LMW treatment, should be preferred for lesions close to the Glisson's capsule or just beneath it, considering the notable power of the methodology.

Poster 25: Side Effect Profile of Patients Undergoing Concurrent Sorafenib and Chemoembolization Treatments for Hepatocellular Carcinoma

A.Y. Kim, E. Depopas, M. Glading, N. Rudnick, K. Sharma

Objectives: To determine the side effect profile and safety of concurrent sorafenib and transarterial chemoembolization treatments.
Methods: A retrospective database review was performed in 189 patients who were treated with transarterial chemoembolization (TACE) within the past five years. Of these, 39 patients were treated concurrently with sorafenib and TACE. Assessments of their side effects were made before and after initiation of sorafenib. The patients were then subdivided into groups who were treated initially with sorafenib versus those treated initially with TACE. A comparison of MELD scores was made for the two subgroups, before and after their first TACE.
Results: 39 patients were treated with concurrent sorafenib and TACE. Documentation after initiation of sorafenib was available on 33 patients. All of the patients were started on a regimen of 400mg BID and all 33 had documented side effects temporally associated with initiation of sorafenib. The most common side effects were fatigue and hand and foot syndrome, seen in 13/33 and 12/33 patients, respectively. Other relative common side effects included skin rash, diarrhea, weight loss and epistaxis. 13/39 patients were started on sorafenib before initiation of TACE whereas 25/39 patients were treated with TACE before sorafenib. No documentation of the date of sorafenib initiation could be found in 1 patient. Overall, the average MELD score before and after the first TACE was 11.1 and 11.8 respectively. For the subgroup started on sorafenib before TACE the average MELD score before and after the first TACE was 11.0 and 12.4. In contrast, the average MELD score before and after the first TACE was 11.2 and 11.5, for the group treated initially with TACE. Eight patients in this subgroup then subsequently underwent a TACE procedure after initiation of sorafenib. For this subgroup, the MELD score was 10.5 and 11.3 before and after the first TACE after initiation of sorafenib.
Conclusions: Our data suggests that concurrent sorafenib and transarterial chemoembolization is safe. The side effect profile from this dual therapy is similar to those for sorafenib only treatments. The side effects associated with TACE was low, with two patients developing treatment related hepatic insufficiency. Interestingly, there was a moderate increase in post TACE MELD score in patients initially treated with sorafenib, compared to no change in patients initially treated with TACE. Further evaluations should be made to determine if concurrent sorafenib and TACE treatments lead to worsening hepatic function and if sorafenib should only be started when the patient is no longer a TACE candidate.

Poster 26: Quantitative Analysis of Higher Order Hepatic Arterial Flow Following Conventional and Drug Eluting Bead Chemoembolization

B. Hartmann, K. Royalty, S.B. White, S. Dybul, W.S. Rilling, E.H. Hohenwalter

Objectives: Conventional transarterial chemoembolization (cTACE) and drug eluting Bead (DEB) chemoembolization are frequently utilized for liver-directed therapies in the treatment of primary hepatocellular carcinoma and hepatic metastases. Decreased flow in higher order hepatic arteries occuring as a result of cTACE / DEB TACE will affect the impact of subsequent liver directed therapies. In this study, novel software was used to analyze hepatic angiograms and evaluate changes in higher order hepatic arterial flow using several temporal parameters relating to contrast bolus kinetics both before and after cTACE / DEB TACE.
Methods: IRB approval was obtained for the retrospective review of the hepatic angiograms of 20 patients who underwent cTACE or DEB TACE for HCC or metastatic disease. A prototype software program was used to analyze the angiograms to evaluate changes in hepatic arterial flow before and after therapy, by using ROIs placed within two higher order hepatic arteries proximal to the areas treated in each patient. Kinetic contrast enhancement parameter measurements included time to peak enhancement, time of ½ maximum enhancement, and time of maximal slope of enhancement.
Results: Quantitative analysis revealed an average change of pre to post treatment time to peak enhancement of +0.70 s, time to ½ maximum enhancement +0.58 s, and time of maximal slope of enhancement +0.53 s. The student t-test was used to show that the pre to post treatment changes in these mean values were statistically significant with all p-values being < .05 (.003, .001 and .019 respectively).
Conclusions: Quantitative analysis of higher order hepatic arterial flow is feasible using the prototype software in this study. This analysis may be useful in future studies designed to compared persistent changes in higher order hepatic arterial flow between different types of liver directed therapies. Further studies will evaluate sequential changes in higher order hepatic vessels with cTACE and DEB TACE.

Poster 27: Stasis with a Single Vial of Doxorubicin Drug-Eluting Beads during Chemoembolization of Hepatocellular Carcinoma: Predictive Factors and Early Clinical Outcomes

L.M. Rivers, A.J. Frangos, J.W. McCann, D.B. Brown

Objectives: Patients undergoing drug eluting bead chemoembolization (DEB) of Hepatocellular Carcinoma (HCC) receive up to 2 vials of beads. Not uncommonly, stasis occurs with 1 vial. The purpose of this study is to evaluate factors that predict stasis with 1 vial and track early outcomes.
Methods: 44 patients with HCC underwent 79 treatments. Chi-square analysis was performed to evaluate differences in vial number between patients who: had received previous intra-arterial therapy vs. were treatment naive, had segmental/subsegmental infusion vs. lobar, or received DEB sizes > 300-500 vs. 100-300 microns. Regression analysis was performed to determine the significance of baseline tumor diameter. Patients were followed using RECIST.
Results: 1 vial of DEB was used in 59 infusions (74.7%) and 2 vials in 20 infusions (25.3%). 36/40 (90%) infusions in previously treated territories used 1 vial compared to 23/39 (59%) of treatments in treatment naïve areas (p=0.01). 42/52 (81%) segmental/subsegmental infusions used 1 vial compared with 17/27 (63%) lobar infusions (p=0.08). 9/15 (60%) procedures with > 300-500 micron beads used 2 vials compared to 11/64 (17%) infusions with 100-300 vials alone (p=0.01). Mean tumor diameter was slightly greater when larger DEB were used (46 + 46 mm vs. 34 + 24 mm for 100-300 beads, p=0.16). At regression analysis, a larger tumor size did not predict a requirement of 2 vials (p=0.20). 42 patients had evaluable disease at a mean of 10 + 2.5 months (range 2.5-20 months). 6 patients (14%) developed progressive disease (PD) at a mean of 6.7 + 4.1 months. The remainder had Stable Disease (n=18, 43%) or Partial Response (n=18, 43%). The 6 patients with PD underwent 13 infusions, 11 of which involved delivery of 1 vial.
Conclusions: Patients who have undergone intra-arterial therapy had a significantly greater chance of stasis with 1 vial of DEB. Segmental/subsegmental delivery and use of larger beads did not predispose patients to stasis with 1 vial, likely due to tumor size. PD with LCB was relatively uncommon but longer-term follow-up is important to determine whether progression is more likely following the delivery of a single vial.

Poster 28: Ultrasound-guided Percutaneous Microwave Ablation of Hepatocellular Carcinoma Adjacent to the Gastrointestinal Tract Under Temperature Monitoring

X. Yu, P. Liang, J. Yu, Z. Cheng, Z. Han, F. Liu

Objectives: The liver tumor adjacent to gastrointestinal tract was thought as the contraindication of thermal ablation by some doctors for the risk of gastrointestinal tract perforation. The purpose of the study was to prospectively evaluate safety and efficacy of MWA assisted with ethanol injection for HCC abutting gastrointestinal tract.

Methods: 474 patients with 532 tumors that underwent percutaneous MWA with curative intention were included. 175 lesions of 175 patients located less than 5 mm from gastrointestinal tract were in GI group (mean tumor size 3.7±1.8 cm). 357 lesions of 299 patients located more than 5 mm from hepatic surface, gastrointestinal tract and first or second branch of hepatic vessels were in control group (mean size 2.8±1.5 cm). The temperature of marginal ablation tissue proximal to gastrointestinal tract was monitored and controlled to fluctuating between 45 °C and 59 °C for more than 10 min for GI group. Ethanol (1–21ml) was injected into marginal tissue in 145 of 175 lesions of the GI group.
Results: 165 of 175 patients (94.3%) in the GI group and 287 of 299 patients (96.0%) in the control group achieved complete ablation assessed by contrast-enhanced imaging and serum AFP level one month post-ablation (P=0.40). According to the follow-up contrast-enhanced imaging, the rate of local tumor progression was 10.9% (19/175) and 7.0% (21/299) in the GI group and control group, respectively (P=0.15). There were neither immediate nor periprocedural complications in both groups. There was no delayed complication of gastrointestinal and bile ducts injury. Major complications happened in 10 (4.2%) of the gastrointestinal group and 9 (2.5%) of the control group (P=0.27).
Conclusions: Under strict temperature monitoring, microwave ablation assisted with ethanol injection is safe and achieves a high complete ablation rate for hepatocellular carcinoma adjacent to gastrointestinal tract.

Poster 29: Iatrogenic Celiac Axis Dissections During Transarterial Treatment of Hepatic Tumors

S. Shamimi-Noori, M.C. Soulen, S. Stavropoulos, M. Itkin

Objectives: To study the incidence and outcome of iatrogenic dissection of the celiac axis and its branches during TACE for hepatic tumors.
Methods: An IRB-approved retrospective review of the IR QI database and hospital electronic medical records was performed to identify the incidence of arterial dissection during the procedure and subsequent treatment approach. 1667 trans-arterial catheter directed procedures targeting the hepatic tumors were performed during the 124-month period. The follow up imaging and procedural result were then collected.
Results: Iatrogenic dissection of the celiac axis or its branches was reported in 14/1667 (0.84%) patients (Male 8, female 6, mean age 58.9). The incidence of flow limiting dissection was 5/1667 (0.3%). In 3/14 (21%) procedures the dissection was caused by 4-5 Fr diagnostic catheters and in 11/14 (79%) by microcatheters used for coaxial selection of the arteries. In 5/14 patients, the procedure was aborted after the detection of the dissection (3/5 flow limiting). Treatment of the dissection at the time of the procedure was attempted in 4/14 cases, including nitroglycerine (1/4 patient) and heparin administration(1/4 patient) and heparin with angioplasty (2/4 patients). Of these 4 patients, 1 had completion of the TACE procedure on the day of the dissection and 2 had successful TACE procedures at a later date. 7/14 cases had follow up imaging, which revealed complete resolution of the dissections in 6/7 patients and minimal residual stenosis in 1/7 patient. Following dissection repeat TACE was attempted in 6 patients and was successful in all of them.
Conclusions: The incidence of iatrogenic dissection of the celiac axis or its branches during TACE procedures is low. These dissections often heal with or without treatment and do not limit the ability for subsequent TACE procedures.

Poster 30: Post Radioembolization Extrahepatic Biliary and Hilar Changes Identified During Transplant Surgery: The Cleveland Clinic Experience

F. Aris, S. Shrikanthan, F. Aucejo, G. El-Gazzaz, G. McLennan, A. Gill

Objectives: Hepatocellular carcinoma (HCC) is the sixth most common form of cancer and the third leading cause of death. The incidence of HCC continues to rise in the United States. The majority of these patients present with non-resectable disease. The gold standard for treatment of nonresectable HCC that meets the Milan criteria is transplantation. This is however limited by the availability of donor organs. Radioembolization to delay disease progression has emerged as a possible bridging therapy to transplantation. While intrahepatic biliary and gallbladder complications have been described with radioembolization, little is known about the effects of radioembolization on extrahepatic biliary and hilar structures and their impact on the subsequent transplantation surgery.
Methods: We retrospectively reviewed our database of patients who have received radioembolization for HCC and who subsequently underwent liver transplantation in order to examine these effects.
Results: Between January 2009 and December 2011, 60 HCC patients received Yttrium 90 radioembolotherapy at our institution. Of these patients, 5 underwent liver transplantation. At time of the surgery, scarring and/or ischemic changes were noted in the gallbladder and/or the extrahepatic biliary tree in 2 patients. Review of the pre-embolization angiograms including the C-arm cone-beam computed tomography demonstrated the presence of patent cystic arteries in both of these patients and the Y90 particles were injected proximal to the origin of the cystic artery. Hilar adhesions were noted in 3/5 patients. The surgeons reported difficulty with the dissection of the hilum due to adhesions and one patient had sclerotic common bile duct and had to undergo hepaticojejunostomy. All patients had right lobar disease and all had received radioembolization to the right lobe. Immediate (within 24 hours) post-procedure nuclear medicine imaging (SPECT and/or PET) was performed in 4/5 patients due to a change in practice confirmed extrahepatic activity in 3 of these cases.
Conclusions: Our data suggests that radioembolization may complicate subsequent liver transplantation surgery. Further research is necessary to elucidate the relationship between radioembolization and subsequent liver transplantation.

Poster 31: Safety and Efficacy of Tace for HCC in Patients with TIPS

N. Bagadiya, S.S. Shah, A.M. Fischman, E. Kim, F.S. Nowakowski, J.L. Weintraub

Objectives: To assess the efficacy and safety of Transarterial Chemo Embolization (TACE) in patients diagnosed with Hepatocellular Carcinoma (HCC) after Transjugular Intrahepatic Portosystemic Shunts (TIPS) procedure.
Methods: A retrospective review of patients with pre existing TIPS who underwent TACE for HCC was performed. The HCC was diagnosed at an average of 18.04 months after the index TIPS procedure was performed. The TIPS were performed from 2003 to 2011: total (n=9), ascites (n=7), bleeding varices (n=2). Patients were evaluated for acute technical success, pre- and post-procedure MELD, successful liver transplantation, survival time following diagnosis, and major adverse events.
Results: Acute technical success of TACE after TIPS was 100%. Mean MELD after TIPS of 15.4 increased on average 3.8 (range +0.54 to +14.02 increase) from the pre-TIPS value. Mean MELD post TACE of 14.9, increased on average 1.5 (range -3.51 to +8.14 increase) from the pre procedure value. Liver transplantation was successfully performed in 4 of 9 patients (44.4%) and 1 of 9 patient is currently awaiting transplant (11.1%). Four patients did not proceed to surgery due to progression of malignancy (n=2) or comorbid conditions unrelated to HCC (n=1) treated with RFA instead; one patient was lost to followup (n=1). One patient experienced significant postembolization syndrome of fever and abdominal pain due to hepatic ischemia (11.1%). Average follow up time ranges from 1 to 59 month; one patient (11.1%) expired 3 months after TACE with hypoxia respiratory failure and encephalopathy.
Conclusions: TACE is a safe and effective adjuvant technique to increase survival in patients with HCC after TIPS procedure. Careful patient selection may reduce complication rates. Additional prospective studies should be performed to evaluate the efficacy of TACE in patients with HCC diagnosis after a TIPS procedure.

Poster 32: Long-Term Survival of Patients with Unresectable, Huge Solitary HCC Following Minimally Invasive Treatments: a Single Center Experience

I. Dedes, E. Sinakos, A. Drevelegas, E. Akriviadis

Objectives: Hepatocellular carcinoma (HCC) represents one of the most common malignancies globally. Management of huge solitary HCC (10 cm or larger in diameter) often involves novel non-surgical treatments due to poor surgical outcomes. This cohort study provides a retrospective report of 8 patients with huge solitary HCC who were treated with minimally invasive methods in our center, during the period 2006-2011. Primary objective of this study was mean overall survival. Secondary objectives included safety and tolerance.
Methods: Eight male patients with huge, solitary unresectable HCC were included. One patient had extrahepatic metastases. All patients had a cirrhotic liver, while seven patients out of eight had chronic hepatitis B and one had alcoholic liver disease. At the time of initial diagnosis 5 patients were classified as Child-Pugh A while 3 patients as Child-Pugh B. Overall the mean radiological initial tumor size per patient on CT and DSA was 12.4 cm. All patients underwent at least one superselective transarterial chemoembolization (TACE). In three patients, the tumor downsized adequately to be treated with radiofrequency ablation (RFA). Sorafenib was also added as adjunctive antiangiogenic therapy in two patients. The initial sorafenib dose for both patients was 400 mg b.i.d.
Results: Mean overall survival was 34.5 months. Total number of TACE sessions performed was 30 and the mean TACE session per patient was 3.75. Total RFA sessions performed were 5. All procedures were generally well tolerated. Post embolic syndrome presented in all patients after TACE. After RFA in one patient a biloma developed and was successfully treated conservatively while in another patient a mild pleural effusion was formed. Sorafenib administration caused diarrhea and fatigue in both patients. No major complications occurred.
Conclusions: These data suggest that minimally invasive, non-surgical treatments such as TACE and RFA combined or not with antiangiogenic therapy might be a safe and well tolerated treatment option for unresectable, huge solitary HCC and prolong survival. Large trials are needed to assess the overall survival benefit.

Poster 33: Outcomes of Combined, Concurrent, and Sequential Interventional Therapy for Huge Hepatocellular Carcinoma

X. An, J. Wang, K. Li

Objectives: To evaluate the clinical efficacy of combined, concurrent, and sequential interventional therapy for huge hepatocellular carcinoma (greater than 10 cm in diameter)

Methods: Thirty-five patients with huge hepatocellular carcinoma (above 10 cm in diameter) were treated with comprehensive interventional therapy, including transcatheter arterial chemoembolization and followed subsequently radioactive seed iodine 125 brachytherapy or percutaneous ethanol injection. Inhibition of hepatitis B virus (HBV) expression and replication together with traditional Chinese medicine were performed during therapy. Clinical effects after multidisciplinary treatment were synthetically estimated by AFP level, HBV-DNA content, Child-Pugh grade, Karnofsky performance score, ultrasound sonography, CT and DSA imaging, etc.

Results: Two patients had serious liver function damage and recovered uneventfully after supportive treatment and good protective care. The one year, two year and three year survival rates were 77.4%, 54.8% and 29.0%, respectively. Complete response and partial response were achieved in four and seven cases, respectively. AFP level and HBV-DNA content dropped in all the cases. Multivariate analysis of these variables mentioned above identifed the HBV-DNA content and Child-Pugh grade as the independent significant prognostic factors.

Conclusions: On the basis of arterial chemoembolization, iodine 125 brachytherapy or ethanol injection deal a crushing blow to residual liver tumor cells in order to improve the prognosis, while the former is better in therapeutic effect than the latter but cost a fortune. Both antiviral treatment and traditional Chinese medicine are effective auxiliary methods of increasing the survival rate, but these charge extra and also need good compliance.

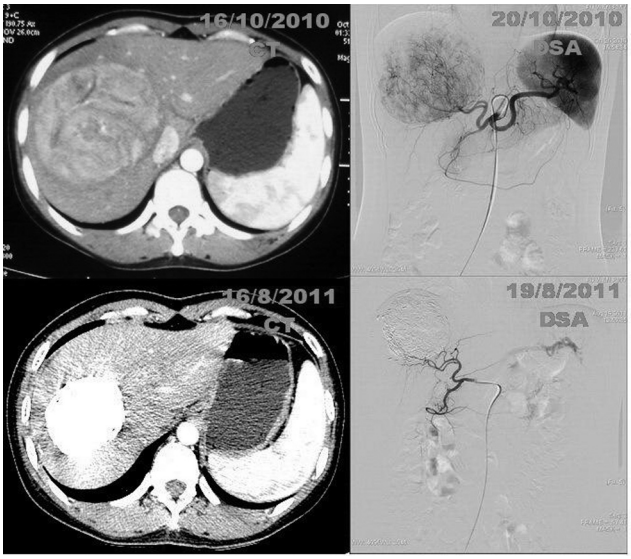

CT and DSA imagings before and after comprehensive interventional therapy for ten months

Poster 34: Transarterial Chemoembolization of Liver Tumours with Drug Eluting Beads

S.S. Kulkarni, N.S. Shetty, T.P. Dharia, A.M. Polnaya, M. Thakur, G. Sangani

Objectives: To evaluate the feasibility, efficacy and safety of transarterial chemoembolization using doxorubicin-loaded drug eluting beads in patients with hepatocelluar carcinoma and hepatic colorectal metastases.

Methods: From May 2009 to December 2011, 60 patients with histopathologically proven hepatocelluar carcinoma (HCC) or colorectal metastases were treated transarterially with doxorubicin-loaded drug eluting beads (DEBs) of particle size 100-300 microns. 42 males and18 females with median age 50 years (35 to 65) underwent 80 sessions. The complete dose of 4 mL of DEBs loaded with 50 mg doxorubicin was injected during 56 sessions and 1-3.5 mL of DEBs was injected during 24 sessions. Pre and post procedure clinical data, imaging findings and laboratory results were documented. The morphological response was evaluated using contrast enhanced CT scans at 6 weeks as per the RESCIST criteria.

Results: Post-procedure CT scan done 6 weeks after using DEBs showed a partial response in 32 of 40 patients (80%), stable disease in six (15%) and progressive disease in two (5%). The mean size of largest metastasis in each patient decreased from 42 mm ± 24 (median, 39.5 mm) to 33 mm ± 23 (median, 29 mm). After a median follow-up of 15 months (range, 6-24 months), 18 patients' disease remained controlled without tumor progression and 20 patients had progressive disease. The median time to progression was 15 months. Postembolization syndrome lasted less than 7 days after 46 sessions (67%) and more than 7 days after fourteen sessions (22%), and no symptoms were observed after eight sessions (11%). Two patient developed abscess on the second day of treatment which was aspirated immediately. There was increase in the liver enzyme levels 48-72 hours after the procedure with peak aspartate aminotransferase (AST), alanine aminotransferase (ALT) and bilirubin levels being 35 - 490 IU (mean, 125 IU ± 77; normal, <35 IU), 20 - 440 IU (mean, 149 IU ± 155; normal, <45 IU) and 8-90 mol/L (mean, 26 IU ± 25; normal, <17 IU) respectively, at 2-3 days. We did not have any procedure related hepatic failure or death in our series.

Conclusions: Our preliminary results of TACE with doxorubicin loaded DEBs suggest that it is a safe, effective and well tolerated procedure. A comparative study with a standard transarterial chemoembolization regimen is warranted to define the best protocol for transarterial treatment of hepatic metastases and HCC.

Poster 35: Treatment for Hemothorax Caused by Spontaneous Rupture of Hepatocellular Carcinoma

F. Ono, M. Hiraga, N. Omura, S. Onochi

Objectives: Hemothorax is a very unusual complication of hepatocellular carcinoma (HCC), accompanied by a high mortality because the negative pressure inside the pleural cavity makes spontaneous hemostasis difficult. The objectives of this study were to present an extremely rare case in which we experienced presenting with ruptured HCC complicated by hemothorax and to also review the pertinent literature so as to assess the efficacy of transcatheter arterial embolization (TAE) in the treatment of hemothorax secondary to HCC rupture.

Methods: The PubMed, Google Scholar and Japan Medical Abstracts Society databases were searched for articles in English and Japanese languages reporting on ruptured HCC complicated by hemothorax. The articles were then systematically reviewed.

Results: Case: The case pertains to a 56-year-old female who was transported to our hospital due to hemorrhagic shock. She was diagnosed with ruptured HCC in the caudate lobe accompanied by concomitant hemothorax and hemoperitoneum. Successful hemostasis was obtained by TAE (Figure), and surgery was conducted one month after TAE. In this case, no lesions as possible sources of bleeding were observed in the thorax and blood from the liver seemed to have traversed the intact diaphragm to enter the pleural cavity soon after the HCC rupture. This unusual phenomenon was considered to be strongly associated with the location of the tumor and the formation of a hematoma inside the omental bursa. It is said that TAE is not always effective for ruptured HCC in the caudate lobe because of the multiple tumor-feeding arteries. Successful TAE in the present case was very beneficial for performing subsequent surgery. Review: As far as our research tells us, 16 cases of ruptured HCC complicated by hemothorax have so far been reported in the literature, and the details of a total of 17 cases, including our case, were analyzed. These cases consisted of 13 males (76%) and 4 females (24%) between the ages of 31 and 79. Of them, 5 cases (29%) had ruptured primary HCC with (n=4) or without (n=1) direct invasion into the pleural cavity, while the others (n=12, 71%) had ruptured metastatic HCC in the thorax. Regarding the treatment outcomes, 16 cases were available for evaluation in this study. Of these, 9 cases (56%) underwent no special procedures to achieve hemostasis and 8 of them (8/9=81%) died within 2 weeks. In addition, 1 case (6%) was treated by emergent surgery, but nevertheless died 6 days thereafter. On the other hand, 6 cases (38%) underwent TAE as the initial treatment for hemothorax and 5 of them (5/6=83%) obtained successful hemostasis and thereafter survived for 3 months or more. The successfully embolized arteries after TAE included the hepatic artery, the phrenic artery and the superficial cervical artery, while gelatin sponges, ethanol or coils were used as embolic material.

Conclusions: A rupture of HCC is capable of causing hemothorax, which leads to very poor outcome. TAE is believed to be an extremely useful treatment for hemothorax secondary to HCC rupture.

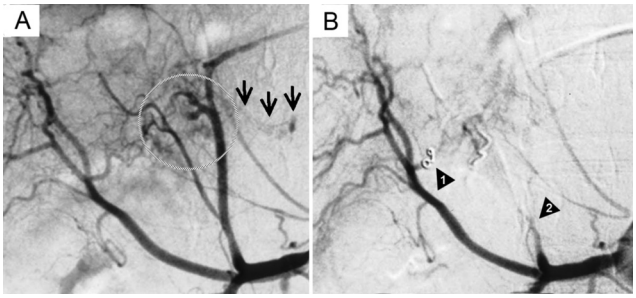

Abdominal angiography demonstrated a hypervascular tumor (A, circle) and contrast medium extravasation (A, arrows), both of which disappeared after the embolization of the caudate artery derived from the anterior branch of the right hepatic artery (B, arrowhead 1) and the proximal portion of the left hepatic artery (B, arrowhead 2).

Poster 36: Evaluation of Safety, Tolerability and Overall Survival Following Whole-Liver, Lobar or Segmental Radioembolization in Unresectable Hepatocellular Carcinoma (HCC)

G. Vallati, L. Carpanese, G. Pizzi, R. Kayal, R. Sciuto

Objectives: Evaluation of Safety, Tolerability and Overall Survival Following Whole-Liver, Lobar or Segmental Radioembolization in Unresectable Hepatocellular Carcinoma (HCC)
Methods: This was a multicenter retrospective study conducted in 325 patients with unresectable HCC who received 90Y-resin microspheres between 09/2003 and 12/2009. Typically, patients were Child-Pugh class A (82.5%), had underlying cirrhosis (78.5%) and good ECOG performance status (PS) 0–1 (87.7%); but many had multinodular disease (75.9%) invading both lobes (53.1%) and/or portal vein occlusion (23.3%).
Results: Most patients received whole-liver (150; 46.2%) or right-lobe administration (123; 37.2%) and a few left-lobe (29; 8.9%) or selective segmental treatment (24; 7.4%), as a single session (>95% of cases). Delivered median activity (1.7 vs. 1.2 GBq; p=0.0023) and target liver volume (1772 vs. 450 mL; p<0.001) was greater with whole-liver than segmental treatment. Treatment approach differed significantly according to the number of nodules, distribution (uni- vs. bi-lobar), PS and BCLC stage (p<0.001). Patients with early (stage A) vs. advanced (stage C) HCC were more likely to receive segmental treatment (45.8% vs. 33.3%) than left-lobe (32.1% vs. 42.9%), right-lobe (13.8% vs. 52.0%) or whole-liver (10.0% vs. 66.0%) treatment. Median survivals [95%CI] for patients treated with segmental, left-lobe, right-lobe and whole-liver approaches were 23.7 [9.0–not reached], 13.8 [8.7–27.4], 12.8 [10.2–16.8] and 12.4 [10.4–15.5] months (p=0.191). No treatment approach further compromised liver function (bilirubin, albumin, ALT, INR or platelets) as measured by an increase in CTCAE grade >3 from baseline to 3 months (p>0.05). Transient fatigue was common (54.5%) and more frequent with whole-liver than lobar/segmental treatment (p<0.001). The incidence of GI ulcers was 3.7% (overall) and 6.0% (with whole-liver treatment).
Conclusions: Radioembolization using 90Y-resin microspheres tended to be tailored to burden of HCC and the liver was not further compromised irrespective of the extent of hepatic volume treated. Disease stage, rather than treatment approach, was the main driver of survival.

Poster 37: Survival and Tolerability Following 90Y-RESIN Microsphere Radioembolization in Patients with Unresectable BCLC Stage C Hepatocellular Carcinoma (HCC)

G. Vallati, L. Carpanese, G. Pizzi, R. Kayal, R. Sciuto

Objectives: To better understand the safety profile and factors driving prognosis following radioembolization in patients with unresectable Barcelona Clinic Liver Cancer (BCLC) stage C HCC defined by the presence of ECOG performance status (PS) 1 or 2, portal vein occlusion (PVO) and/or extra-hepatic [N1, M1] disease (EHD).
Methods: A retrospective study was conducted of patients receiving radioembolization using 90Y-resin microspheres between 09/2003 and 12/2009. Differences in CTCAE (v3.0) grade from baseline to day 90 between cohorts were assessed by the Kruskal-Wallis test. Kaplan-Meier analysis stratified by key prognostic indicators estimated survival.
Results: Of 183 patients, 46 (25.1%) were Child-Pugh class B; 145 (79.7%) were ECOG 1 (59.3%) or 2 (20.3%); 73 (39.9%) had branch (23.5%) or main (16.4%) PVO; and 28 (15.3%) had EHD. Post-radioembolization AEs were mostly grade 1 or 2, including: fatigue (61.2%), nausea and/or vomiting (31.0%); abdominal pain (28.4%), fever (12.0%) and gastrointestinal ulcer (4.4%). Fatigue affected a higher proportion with ECOG 1/2 than ECOG 0 (p<0.001). Grade 3/4 changes in bilirubin were observed in 6.0% of patients (p=0.002) and only in those with ECOG 1/2. Other changes in LFTs were not significant. Median survival [95%CI] was 10.0 months [7.7–10.9] and similar in patients with or without PVO (10.2 [7.7–11.8] vs. 9.3 months [7.4–11.4]; p=0.826). Survival diminished with symptomatic disease (ECOG 0 vs. 1 vs. 2: 10.8 [6.5–11.9] vs. 10.0 [7.7–11.8] vs. 6.6 months [5.5–20.8]) and extra-hepatic spread (no EHD vs. EHD: 10.2 [8.2–11.7] vs. 7.4 months [4.3–13.1]), but these differences were not significant. Survival was similar by Child-Pugh class A vs. B (p=0.668); but differed by number of nodules <5 vs. ≥5 (p=0.020), pre-treatment ascites (p=0.007), INR >1.2 (p=0.037) or bilirubin >1.5 mg/dL (p=0.009). Multivariate Cox proportional hazards model found only nodules >5 (HR 1.59) and INR >1.2 (HR 1.52) were independently prognostic for survival.
Conclusions: Radioembolization was well-tolerated in patients without significant differences in survival for the defining characteristics of BCLC stage C HCC (PVO; PS; EHD).

Poster 38: Transarterial Chemoembolization of Unresectable Hepatocellular Carcinoma with Doxorubicin Eluting Beads: A Single Centre Experience

A. Veiss, J. Savlovskis, K. Kupcs, H. Kidikas, J. Vilmanis, G. Purkalne

Objectives: To present the results of our initial experience in using the drug eluting beads (DEB) loaded with doxorubicin in patients with hepatocelular carcinoma (HCC).
Methods: Our retrospective study was conducted over 10 months (March 2011–February 2012). 9 patients with liver cirrhosis and unresectable uni- or multifocal HCC underwent transarterial chemoembolisation (TACE) with doxorubicin beads (DC Bead™). The underlying cause of liver cirrhosis was hepatitis C. Patients presented with Child Pugh stage A (n = 2) and B (n = 7). The mean intrahepatic tumor size, considering the sum of diameters of all lesions treated, was 7.2 cm (rangee, 3-12 cm). Liver function and hematological parameters were documented before and after each TACE. Computer tomography imaging was performed before and 4 weeks after TACE.
Results: 9 patients received a total number of 23 TACE treatments with DC beads (mean dose 120 mg). At 9 months, a complete response was seen in 11.1%, an objective response in 77.8%, progressive disease in 11.1%. Mean tumor necrosis 74.8% (range, 30%–100%). Severe procedure-related complications were not observed. Postembolization syndrome was observed in all patients. At the time of data analysis, 5 (55.5%) out of 9 patients were alive.
Conclusions: TACE with drug eluting beads in unresectable HCC offers efficient treatment resulting in tumor response within a very short time. The technique is simple to perform and seems to be well tolerated by patients.

Poster 39: Follow-up Yttrium-90 Internal Pair Production PET/CT Imaging in Patients with Primary or Metastatic Liver Tumors as compared with Brehmsstrahlung Imaging: A Prospective Case Series

M.L. ONeill, J. Salsamendi, M. Georgiou, T. Froud, S. Bhatia, M.M. Cristescu

Objectives: To demonstrate non-target embolization much more precisely and quickly, where applicable Demonstrate improved accuracy in the depiction of the treatment distribution, as well as quantify the degree of radioactivity in any individual portion of the tumor in the form of point values.
Methods: This is a prospective non-blinded case series involving the acquisition of a pair production PET/CT as soon as possible after an already performed Y-90 Sirspheres treatment of hepatic malignancy. The feasibility of this method has been demonstrated in a few pilot studies, although no large prospective series have been performed to our knowledge. It will be performed in addition to the standard Brehmsstralung SPECT scan. The measures used will include: Degree of correlation with expected vs. achieved tumor coverage by the treatment; Degree of anatomic dose correlation between treatment distribution depicted by the two modalities; Determination of average intensity values of treated areas vs. non-treated background liver parenchyma, for later correlation with various patient outcomes; Detection of non-target embolization, where applicable, and qualitative comparison between the two modalities as to the conspicuity of the abnormality.
Results: We have thus far demonstrated high quality and accurate PET/CT studies in all subjects, which correlate well with both the known distribution of tumor burden and with the angiographic findings. For example, in one case, the PET/CT helped define that the dose distribution covered all of hepatic segment 4, rather than the planned selective treatment of segment 4b, for example. In another subject, who has multifocal disease, the PET/CT demonstrated the dose distributions more accurately than the Brehmsstrahlung imaging. In both of these examples, the added information obtained with the PET/CT was clinically useful, because it could better define the treated area and help exclude non-target embolization. Other patients studied so far had similarly successful and useful results.
Conclusions: Pair production Yttrium-90 PET/CT is a practical and highly accurate method to confirm anatomic dose distribution of Y-90 in the setting of hepatic tumors. It appears to be more accurate that Brehmsstrahlung imaging alone, and has also previously reported to more accurately depict non-target embolization. Therefore, we anticipate that it may in fact ultimately emerge as the standard of care in the post Y-90 treatment setting.

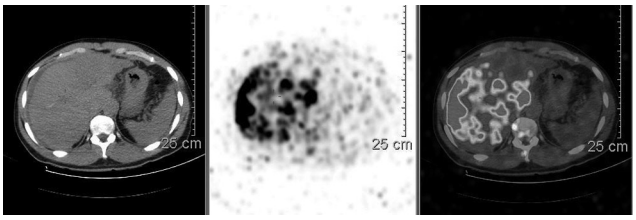

Patient with multi-focal distribution of tumor:
(Left to Right)
a.) Axial non-contrast CT
b.) Brehmsstrahlung SPECT
c.) Y-90 PET/CT

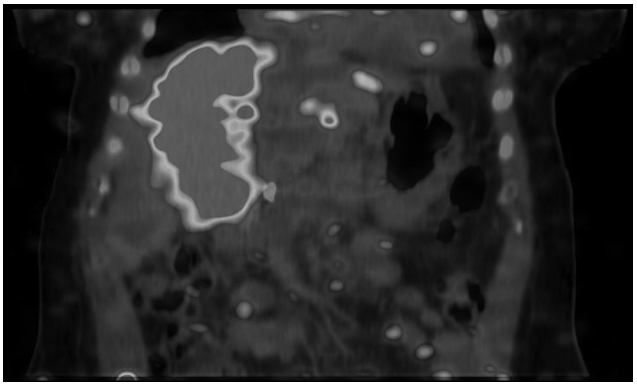

On a different subject with underlying tumor mostly limited to hepatic segment 4b. Coronal Y-90 PET/CT demonstrates homogenous signal in the region of both 4a and 4b, consistent with a slightly larger treated area than expected.

Poster 40: Safety and Feasibility of Whole-Liver Yttrium-90 (Y90) Radioembolization

R.P. Dang, A.M. Fischman, E. Kim, F.S. Nowakowski, J.L. Weintraub, R.A. Lookstein

Objectives: For primary or metastatic liver cancer with involvement of both lobes, transarterial radioembolization (TARE) with Yttrium-90 (Y90) is typically administered separately and sequentially to each lobe in order to avoid the potential toxicity and associated morbidity of whole-liver treatment. The purpose of this study is to evaluate the safety and feasibility of whole-liver TARE.

Methods: From March 2005 to November 2011, 100 whole liver TARE procedures were performed in 90 patients (58 males and 32 females) aged 28 to 81 (mean age of 61) for primary or metastatic liver cancer using SIR-Spheres. All imaging and electronic medical records were retrospectively reviewed for demographics, history, technical success, 30-day mortality rate, incidence of major and minor complications at 60 days, and metabolic laboratory data at baseline, 6 weeks, and 15 weeks. Tumor histology included 82.2% metastatic tumors (74/90) and 17.8% primary hepatocellular carcinoma (16/90). Metastatic lesions included: 54.4% neuroendocrine (49/90), 10% colorectal (9/90), 5.6% lung (5/90), 3.3.% adenoid cystic (3/90), 3.3% cholangiocarcinoma (3/90), 2.2% renal cell (2/90), 2.2% sarcoma(2/90), and 1.1% breast (1/90). 33.3% of patients had extrahepatic metastases (30/90). 65.6% of patients had prior liver treatments (59/90). 74.4% of patients had prior chemotherapy (67/90).

Results: Acute procedural technical success was 100 %. The mean administered dose of Y90 was 1.39 GBq (range 0.72 GBq-2.48 GBq). Mild hyperbilirubemia and transaminitis were observed in the follow-up period. Mean total bilirubin level was 0.7 mg/dl at baseline. Mean total bilirubin level was 1.2 mg/dl at 6 weeks and 2.2 mg/dl at 15 weeks. Mean AST and ALT levels were 58.7 and 40.6 U/L at baseline, respectively. Mean AST and ALT levels were 73.4 and 48.5 U/L at 6 weeks and 135.6 and 72 U/L at 15 weeks, respectively. 30-day mortality rate was 0%. The incidence of minor complications at 60 days was 4% (4/100), including 1 patient with jaundice (1%) and 3 patients with new onset ascites (3%). The overall incidence of major complications at 60 days was 5% (5/100). One patient developed acute cholecystitis (1%) and 4 patients developed gastroduodenal ulceration (4%). There were no cases of radiation induced liver disease.

Conclusions: This data suggests that whole-liver TARE may be a safe and feasible method for treating primary or metastatic liver cancer with involvement of both lobes.

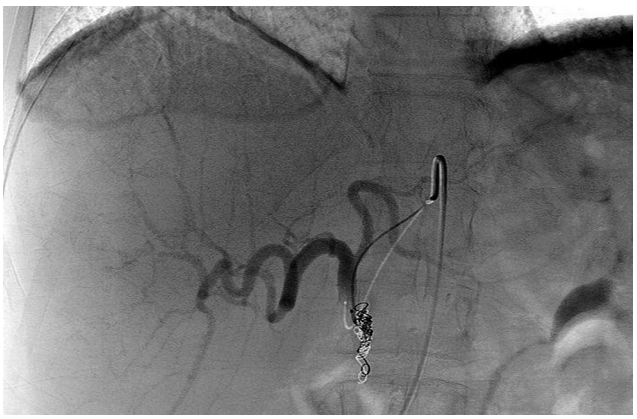

59 year old female with mestatic lung carcinoma. Proper hepatic artery injection of SIR-Spheres post coil embolization of gastroduodenal artery.

59 year old female with metastatic neuroendocrine tumor. Proper hepatic artery injection of SIR-Spheres post coil embolization of right gastric artery and gastroduodenal artery.

Poster 41: Y-90 Radioembolization as Second-line Therapy for Hepatic Metastases

A. Cholapranee, M. Dagli, J.I. Mondschein, S. Stavropoulos, M.C. Soulen

Objectives: Chemoembolization is effective first-line therapy for many hepatic metastases, providing disease control in the majority of patients. Responders with liver-dominant progression can be retreated with chemoembolization to re-establish disease control. Radioembolization offer an alternative approach to 2nd-line therapy. We compared TTP and survival among a cohort of patients treated with 2nd-line Y-90 to a concurrent cohort treated with Y-90 first line.

Methods: IRB-approved review of our Y-90 database identified 22 patients with liver metastases (13 NET, 3 colon, 2 cholangiocarcinoma, 4 other) who developed liver-dominant disease progression 29 +/- 30 months (range, 5-119 mo) following first-line chemoembolization. 40 radioembolizations with Y-90 resin microspheres were performed (1-4/pt). A concurrent cohort of 45 patients (20 colon, 13 NET, 6 cholangio, 2 RCC, 6 other) who elected Y-90 as 1st-line therapy received 67 Y-90 instillations. All patients had clinical and laboratory assessment one month after each Y-90 instillation, then every three months.

Results: Technical success was 100%. >90% of the prescribed dose was administered in 76% of procedures in the 2nd-line group vs. 76% in the first-line cohort, p=NS. Progression by RECIST occurred in 57% of the 2nd-line group at a mean of 17 months, and in 53% after 1st-line therapy at a mean of 9 months. Mean survivals from diagnosis of liver metastases, from first chemoembolization, and from first Y-90 were 69 mo, 47 mo, and 20 mo in the 2nd-line group and 45 mo, [n/a], and 13 mo in the 1st-line group.

Conclusions: Radioembolization with resin microspheres can be performed as second-line therapy following prior chemoembolization without compromise to delivery of the prescribed dose. Tumor control and survival following second-line therapy are within the range expected for Y-90 therapy; the difference between cohorts reflects the preponderance of NET patients in the 2nd-line group vs. colorectal mets in the 1st-line cohort.

Poster 42: inSIRT Trial - Single Center Phase II Study of Yttrium-90 Radioactive Resin Microspheres in the Treatment of Liver Predominant Metastatic Colorectal Adenocarcinoma After Failure of 1st-Line Combination Chemotherapy

T. Reid, K. Shimabukuro, P. Fanta, S. Dad, S. Rose, E. Roeland

Objectives: Liver metastases develop in half of colorectal cancer (CRC) cases and once metastatic, ~90% die due to their consequences. We are evaluating the aggressive management of liver metastases through the incorporation of selective internal radiation therapy (SIRT) using Yttrium-90 (Y-90) radioactive microspheres after evidence of progressive disease following 1st-line FOLFOX ± bevacizumab. Optimal timing for microsphere treatment relative to chemotherapy is not clearly established.

Methods: Subjects with predominant hepatic metastatic CRC despite 1st-line FOLFOX based therapy ± bevacizumab are eligible. Interventional radiology and nuclear medicine assess the liver lesions and the subject receives SIRT followed by 2nd-line FOLFIRI 4-6 weeks after the final SIRT.

Results: To date, 9 metastatic CRC subjects have been treated and 10 subjects enrolled (goal 30 subjects). One subject was withdrawn due to progressive lung metastases. 4 of 9 subjects (45%) achieved PFS at 6 mos and average TTP is 7 months (0.7-21.3 mos). Overall treatment has been well tolerated, except one possible study related SAE of liver failure. The OS endpoint has not been achieved.

Conclusions: Historically, 2nd-line FOLFIRI has achieved a 2.5 mos median PFS. Our preliminary results of 9 subjects with metastatic CRC show a PFS up to 21.3 months and 45% PFS at 6 mos. These encouraging results demonstrate the utility of an innovative direct approach to metastatic CRC after failure of 1st-line combination chemotherapy. Based on our promising preliminary results, our aim is to enroll 30-35 metastatic CRC patients.

Table shows the results for the PFS of patients on this study

Subject #	1st-Line	# of SIRT	2nd-Line Chemo	RECIST Best Response	TTP (mos)
1	FOLFOX	1	FOLFIRI	CR	21.3
2	FOLFOX + bev	2	FOLFIRI	PD	8.6
3	FOLFOX + bev	2	FOLFIRI	PD	6.9
4	FOLFOX + bev	2	FOLFIRI	PD	11.2
5	CAPOX + bev	1	FOLFIRI + Bev	PD	0.7
6	FOLFOX	2	FOLFIRI	PD	2.3
7	CAPOX + bev	2	FOLFIRI	PD	3.6
8	CAPOX + bev	2	FOLFIRI	SD	2.6
9	FOLFOX	1	FOLFIRI	SD	5.5
10	6	20	1	0.8	34.8
		Median	5 months	10.1	37.3

Poster 43: Risk of Liver Abscess Following Y-90 Radioembolization in Patients with Prior Biliary Intervention

A. Cholapranee, M.C. Soulen

Objectives: Patients without a competent sphincter of Oddi due to prior surgical or endoscopic therapy are at high risk for liver abscess following chemoembolization despite aggressive antimicrobial prophylaxis. We examined a cohort of such patients undergoing Y-90 resin radioembolization, and compared them to a prior cohort of chemoembolized patients.

Methods: IRB-approved review of our Y-90 database identified 8 radioembolizations performed in 4 patients, two with prior Whipple and two with biliary stents. Our standard prophylactic regimen of oral levofloxacin and metronidazole two days pre-procedure continuing for 14 days after; oral neomycin/erythromycin bowel prep the day before; and IV levofloxacin/metronidazole the day of treatment was prescribed. Patients had clinical and laboratory assessment one month after each treatment, then every three months.

Results: Diagnoses were pNET, cholangiocarcinoma, ampullary carcinoma, and gallbladder carcinoma. Mean Y-90 dose was 23.2 mCi (range, 12-33 mCi). No patient developed signs or symptoms of infection, nor were subclinical abscesses detected on follow-up imaging. In the prior cohort of patients chemoembolized with CAM/Lipiodol/PVA who received the same prophylaxis, liver abscess occurred following 2/15 (13%) of procedures in 2/6 patients.

Conclusions: This preliminary experience suggests that the risk of liver abscess among patients with prior biliary intervention may be lower following radioembolization than chemoembolization, which would expand treatment options in this high-risk population.

Poster 44: Y90 Radioembolization: Comparison of Effects on Clinical Performance Status and Liver Toxicity in Patients with HCC and Hepatic Metastases from Other Primary Tumors - A Single Institutional Experience

A. Sharma, B. Kolar, A. Katz, A. Hezel, D. Lee, D. Waldman

Objectives: To compare the effects of radioembolization on clinical performance status of patients with HCC and hepatic metastases from other primary tumors

Methods: This institutional review board approved study included 26 patients with HCC and 11 patients with metastases from other primary tumors (6 - colorectal primary, 2 - neuroendocrine, 1- melanoma, 1- insulinoma, 1- breast) who underwent treatment with Therasphere Y-90 radioembolization. Clinical performance status was estimated using the ECOG scale prior to treatment and subsequently post treatment at 3 month periods. Similarly, liver toxicity was evaluated by comparing the bilirubin values and other liver enzymes prior to and post treatment (at 1month post treatment followed by 3 month periods).

Results: Comparison of ECOG status post treatment among the 11 patients with metastases (mean follow up of 5.5 months) showed that 6 of the patients had 0 score indicating normal performance status, 2 patients had died (score of 5) and 1 patient each had a score of 1, 2 and 3. Performance status of 5 patients had remained the same from pretreatment levels, worsened in 3 patients and improved in 3 patients, indicating favorable response in 72.7 % (8/11) of patients. Assessment of bilirubin levels and trends pre- and post-treatment among the group of metastases showed that all patients had normal levels of bilirubin prior to treatment and 8 of these 11 had maintained levels of bilirubin within normal range post-treatment and three had increasing levels or worsening liver toxicity (mean follow up of 5 months). ECOG performance scores in the 26 HCC patients after treatment (mean follow up of 6 months) included 5 patients with a score of 5, 1 with a score of 4, 6 with a score of 3, 2 with a score of 2, one with a score of 1 and eleven patients with a score of 0. 3 patients with score of 5 died due to worsening of liver failure or progression of disease whereas 2 others died due to comorbidities and failure of other organ systems. In nine other patients there was mild worsening of status with a drop in score of 1 or 2, ascites was incidentally noted in all these patients. 12 patients maintained their performance status compared to pretreatment status whereas there was worsening of status in the rest (14) to different degrees, indicating favorable response in 46.15% (12/26) of patients. Assessment of liver function parameters among the group of HCC patients showed that 14 had stable bilirubin trend while 12 patients had increasing bilirubin levels (mean follow up of 6 months). Correlation of ECOG with liver function parameters showed that patients with stable performance status had stable liver enzymes including bilirubin values. Three of the patients with scores of five also had worsening liver enzymes whereas the two patients with comorbidities had stable liver enzymes.

Conclusions: 1. Y90 radioembolization had a favorable response in treatment of patients with liver metastases maintaining or improving clinical performance status in a significant number of patients. 2. A comparatively less favorable response noted in HCC group of patients may be attributed to preexisting/background liver disease which may have had an independent effect or there may have been a cumulative effect of liver disease and radioembolization on liver function and performance status. 3. Maintenance of bilirubin trends and liver function parameters in group of metastases suggests that radioembolization by itself did not have a significant effect on the liver function.

Poster 45: Treatment of Stage 4 Gynecologic Malignancies by Hepatic Radioembolization

R.C. Withrow, C. Pohl

Objectives: Endometrial and cervical carcinomas are inherently radiosensitive tumors that demonstrate improved primary outcomes with adjuvant radiation therapy. Liver dominant metastatic disease from endometrial and cervical primaries should derive a similar benefit from radiation therapy, specifically Yttrium-90 (Y90) radioembolization.

Methods: Two patients were selected by a multidisciplinary team on the basis of unresectable liver dominant metastatic disease from endometrial and cervical primaries. Both patients had right lobe dominant disease, which was increasing in volume despite systemic chemotherapy. Selective right hepatic artery Y90 radioembolization was performed using routine protocol in both patients. Response to therapy is documented by a reduction in tumor volume in both patients following Y90 administration.

Results: The patient (A) with hepatic metastasis from an endometrial primary demonstrated a reduction in hepatic tumor volume of 79 cc or 54%. The patient (B) with hepatic metastasis from a cervical primary demonstrated a reduction in tumor volume of 942 cc or 62%. Both patients tolerated the procedure well with no reported adverse events. Pre-procedural PET scan of patient A demonstrated 9 highly FDG avid right hepatic lobe masses ranging from 16.3-21.5 in maximum standard uptake value (SUV) and post-procedural PET scan performed 4 months after Y90 therapy demonstrated only one FDG avid mass with a maximum SUV of 7.7.

Conclusions: Y90 radioembolization may be particularly effective in patients with liver dominant metastatic disease from primary endometrial or cervical carcinoma.

Poster 46: MRI Characteristics of Liver Metastases Treated with Stereotactic Body Radiation Therapy (Cyberknife) Following CT Guided Fiducial Placement

D. Sarkar, D. Tsai, S. Franciosa

Objectives: A pictorial essay illustrating the MRI appearance and initial treatment related changes of liver lesions treated with Stereotactic Body Radation Therapy. (Cyberknife technology).

Methods: At our institution, a cohort of 25 patients with liver metastases was followed. Patients underwent CT guided Fiducial placement and were evaluated with contrast enhanced MRI examinations pre- and post-Stereotactic Body Radiation Therapy (SBRT). The appearance of the liver lesions was monitored with attention to lesion size, changes in signal characteristics, treatment related response and outcome. SBRT was administered in 1-5 fractions utilizing Cyberknife. On average, patients received 3-5 fractions, with prescription doses ranging from 21Gy to 36Gy.

Results: Dynamic contrast-enhanced MRI was utilized to assess treatment related changes in the tumor and adjacent liver. Hepatic masses and normal liver parenchyma surrounding the tumor demonstrated unique response to SBRT. Changes in tumor size, presence of necrosis or hemorrhage, diffusion characteristics and early and late contrast enhancement patterns were assessed. Variable patterns of contrast enhancement were observed which correlated with pre-treatment dosing curves and included not only tumor response but also effects on adjacent hepatic parenchyma, closely following with the Red Shell or susceptibility zone theory. These findings are pictorially illustrated. Our results support contrast enhanced MRI as the study of choice in assessment of treatment response.

Conclusions: Stereotactic Body Radiation Therapy is a treatment option for cancer patients with liver metastases. Interventional Radiologists play a vital role in the diagnosis, staging as well as pre-treatment planning and placement of gold-tipped fiducials. Dynamic contrast enhanced MRI allows excellent follow up of liver lesions treated

with Cyberknife technology in assessment of treatment related changes and therapy outcome. These MRI characterizations may serve as the basis for monitoring of lesions and planning of additional interventions including radiofrequency ablation and chemoembolization techniques in conjunction with stereotactic radiation therapy.

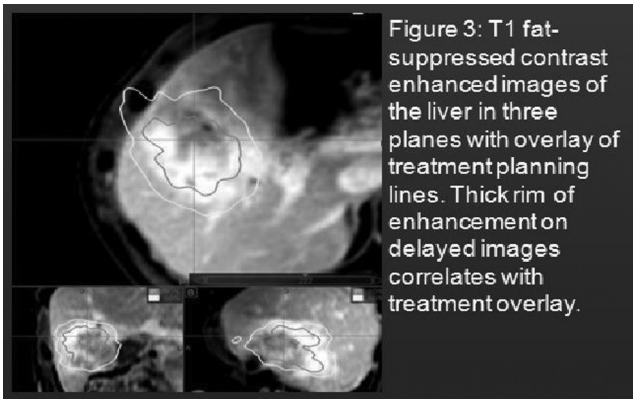

Figure 3: T1 fat-suppressed contrast enhanced images of the liver in three planes with overlay of treatment planning lines. Thick rim of enhancement on delayed images correlates with treatment overlay.

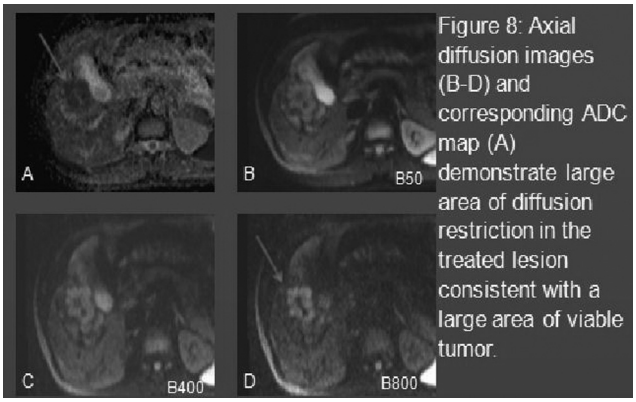

Figure 8: Axial diffusion images (B-D) and corresponding ADC map (A) demonstrate large area of diffusion restriction in the treated lesion consistent with a large area of viable tumor.

Poster 47: Diffusion Weighted Imaging For Evaluation of Liver Metastases

D. Sarkar, D. Tsai, S. Franciosa

Objectives: To pictorially demonstrate the efficacy of using Diffusion Weighted Imaging for the evaluation of treatment response in Liver Metastases.

Methods: A review of metastastic lesions followed with dynamic contrast enhanced MRI was performed. Diffusion characteristics were characterized based on tumor type and treatment response. Dynamic contrast enhanced MRI is sensitive to therapy-related changes in blood flow and vascular permeability, related to tumor angiogenesis. It serves as a noninvasive method and biomarker for characterization of tumor response to therapy. Diffusion imaging with ADC is particularly sensitive for detection of tumor.

Results: Diffusion weighted (DW) imaging is a functional MRI technique which is useful in characterization of hepatic lesions and reflects tissue cellularity and integrity of cellular membranes. Diffusion assesses movement of water molecules which is "restricted" in areas of increased cellularity, i.e. tumors. In cystic or necrotic tissues, diffusion of water protons is relatively "free" or "unrestricted." We provide various MRI images demonstrating the Diffusion-Weighted imaging appearance of liver metastases following treatments including stereotactic radioation, radiofrequency ablation, chemoembolization, and conventional 3D radiation techniques as compared to post contrast T1 weighted imaging.

Conclusions: Diffusion-weighted imaging can be used in the assessment of liver metastases. The signal intensity can provide a tissue characterization, giving information about the cellular density and particularly be useful in post-treatment imaging for monitoring of response to therapy and surveillance. Diffusion imaging is more sensitive than post contrast imaging alone. Understanding these signal differences and post-treatment changes can help in making choices regarding biopsy sites, selection of target lesions for additional treatment and margin selection.

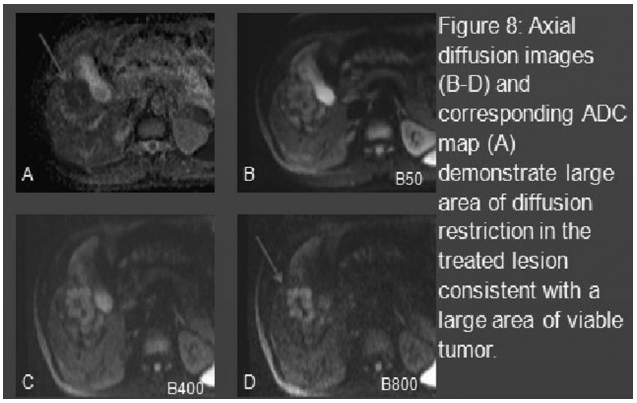

Figure 8: Axial diffusion images (B-D) and corresponding ADC map (A) demonstrate large area of diffusion restriction in the treated lesion consistent with a large area of viable tumor.

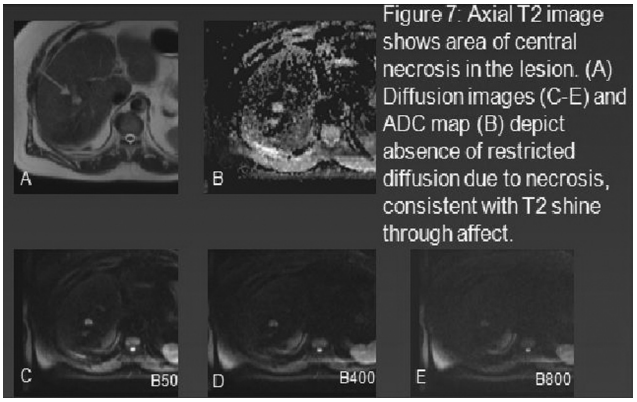

Figure 7: Axial T2 image shows area of central necrosis in the lesion. (A) Diffusion images (C-E) and ADC map (B) depict absence of restricted diffusion due to necrosis, consistent with T2 shine through affect.

Poster 48: TheraSphere Radioembolization of Metastatic Insulinoma in the Post-Transplant Liver: A Case Report and Review of the Literature

K. Kaproth-Joslin, J. McGrath, A. Sharma, J. Xue, E. Mathes, D. Waldman

Objectives: Neuroendocrine tumors (NETs) are neoplasms that arise from neuroendocrine cells of the gastrointestinal tract and pancreas. These tumors are typically highly aggressive and very vascular in nature, with a high mortality rate, and often metastasize to the liver. Orthotopic liver transplantation (OLT) is a viable treatment option for unresectable NET metastasis to the liver, with a 5-year survival rate of 60%. Unfortunately, due to the aggressive nature of these tumors, NET metastasis to the liver can occur post-transplant. In this study, we will present a case of metastatic insulinoma to the liver, status post OLT, treated via transcatheter arterial radioembolization with TheraSphere particles. This management option has provided a promising outcome in the care of unresectable NET, improving both survival outcome as well as quality of life for our patient.

Methods: We will present a case of metastatic insulinoma, status post OLT, treated with TheraSphere radioembolization. We will discuss the basic pathophysiology of NET. We will review the mechanism of TheraSphere Yttrium-90 microsphere action and discuss the steps needed to perform TheraSphere Yttrium-90 radioembolization. We will examination the special considerations for TheraSphere treatment in the post-transplant patient, as well as the risks, benefits, and expected outcomes of the procedure.

Results: Case presentation: 60 year old female, status post OLT with distal pancreatectomy for metastatic insulinoma in 2002, now with recurrent metastatic lesions to the transplanted liver. TheraSphere radioembolization was requested to treat right and left anterior metastatic lesions. Basic pathophysiology of neuroendocrine tumors. Mechanism of TheraSphere Yttrium-90 microsphere action, with discussion of the steps needed to perform TheraSphere Yttrium-90 radioembolization. Special considerations for TheraSphere treatment in the post-transplant patient, as well as the risks, benefits, and expected outcomes of the procedure.

Conclusions: TheraSphere radioembolization has been found increase life expectancy and improve the quality of life in individuals with hepatocellular carcinoma. This technique is now being applied to treat metastatic lesions of the liver as well, such as metastatic colon and stomach cancers. Use of TheraSphere radioembolization in the post-transplant patient requires unique preprocedure planning and careful consideration to prevent significant injury to the transplanted organ. In this presentation, we demonstrated safe and successful radioembolization of multiple NET metastatic lesions in the post-transplanted liver.

Poster 49: Biliary Injury Resulting from Trans-Arterial Chemoembolization Using Drug-Eluting Beads for Treatment of Metastatic Neuroendocrine Tumor in a Non-Cirrhotic Patient

J. Wagner, J.R. Leyendecker, B.E. Kouri

Objectives: This case demonstrates the potential for significant biliary injury following DEB-TACE in a non-cirrhotic patient treated for metastatic neuroendocrine tumor with the illustration of a large post-treatment biloma.
Methods: A 70 year-old male with a diagnosis of hepatic metastatic neuroendocrine tumor of appendiceal origin was referred to the Interventional Radiology service for potential TACE status-post right hemi-colectomy and left liver wedge resection. The patient's additional past medical history was significant for diabetes mellitus type II, coronary artery disease, and hyperlipidemia. Pertinent medical history included a negative history for liver cirrhosis. The patient underwent initial treatment for a single right liver lobe metastatic lesion on July 15, 2010 with traditional TACE. (Doxorubicin/ethiodol and 100-300 micron Embospheres) The patient tolerated the initial treatment well, although follow-up imaging in September 2011 discovered new lesions consistent with additional metastatic disease. The patient subsequently underwent repeat treatment on October 27, 2011. At that time, the new right liver lobe metastasis was treated with 4 cc of drug-eluting beads (100-300 um LC Beads) loaded with 100 mg of epirubicin. Again, the patient tolerated the procedure well. The MRI of the abdomen completed on December 5, 2011 demonstrated findings that were consistent with "partial response" as defined by the RECIST criteria (sum diameter of 2 target lesions reduced from pretreatment of 3.1cm to post-treatment diameter of 1.7 cm). Additionally, this MRI demonstrated impressive imaging findings consistent with focal biliary necrosis and biloma formation. Despite this large intraparenchymal biloma, the patient remained asymptomatic, and the decision was made to forego intervention unless symptoms developed. Subsequent imaging is scheduled in March of 2012.
Results: Follow-up MRI after treatment with drug-eluting beads showed partial treatment response at the site of metastatic disease, however, a non-enhancing focus of low T1/high T2 signal was also apparent in the right liver lobe, distal to the treated metastases. This focus measured approximately 6 cm in greatest axial diameter, with characteristics of biliary necrosis and biloma formation. Subsequent imaging is scheduled for March 2012.
Conclusions: Trans-arterial chemoembolization (TACE) is an accepted method of treatment for both primary and secondary tumors of the liver. Conventional TACE consists of catheter directed infusion of an emulsion of chemotherapy agents and iodised oil followed by bland particle embolization. The technique has recently been modified by the development of drug-eluting beads (DEB-TACE). These newer agents are thought to result in prolonged and more consistent local elution of chemotherapy with less systemic dose, reducing the occurrence of "post-embolization syndrome." More severe complications of both methods are also well-documented. A retrospective comparison of separate patient populations treated for primary hepatocellular carcinoma (HCC) or neuroendocrine tumor (NET) with either traditional TACE or DEB-TACE was recently published. The authors reported a significant difference in the rate of biliary injury and biloma formation in the patients treated with DEB-TACE for NET, as opposed to those treated with DEB-TACE for HCC. The authors suggest that the altered peri-biliary plexus (PBP) in those patients with HCC and underlying cirrhosis may protect the biliary system from such complications. This case is compelling in that it provides additional anecdotal support for this theory.

Poster 50: Conservative Surgery After Isolated Limb Infusion and External Irradiation in Treatment of Locally Advanced Soft Tissue Sarcoma of Lower Limbs

S. Elqammash, G. Ellabban, E. Hokkam, M. Shams, H. Hussein

Objectives: The optimal extent of treatment of advanced soft tissue sarcoma is controversial. We report our long-term results of isolated limb infusion (ILI) in cases of locally advanced soft tissue sarcoma of the lower limb
Methods: The study included two groups of patients with locally advanced soft tissue sarcoma of the lower limb. Group A included 35 patients who received treatment with Doxorubicin, followed by external beam radiation within one week. Four to eight week after, conservative surgery was performed aiming at limb preservation. Group B included 40 cases who were treated with neoadjuvant systemic chemotherapy and external irradiation followed by wide local excision of the tumour. Patients' response to treatment and the overall survival after treatment were assessed in the study.
Results: The overall response to preoperative treatment was 80% in group A and 42% in group B. Follow up duration was 5 years. Local recurrence was recorded in 36% of group A and 59% of group B. The overall survival rate was 60% in group A and 35% in group B.
Conclusions: The outcome of ILI in management of locally advanced soft tissue sarcoma of the lower limb is significantly better than neoadjuvant systemic chemotherapy in terms of tumour control and overall survival.

Poster 51: Rotational C-Arm Angiographic CT in Interventional Oncology: A Case-Based Pictorial Review from a Tertiary-Care Academic Medical Center

A. Patel, S. Virmani, A. Pillai, B. Arslan, G. Behrens

Objectives: Three-dimensional (3D) rotational DSA in combination with flat-panel detectors allows a user to create computed tomographic (CT)-like images with soft-tissue visualization from a C-arm fluoroscopy system. This technology termed "DynaCT" on Siemens C-arm angiographic units has often times served as a problem-solving tool during the procedure for many Interventional Radiologists. This case-based pictorial exhibit highlights the clinical utility of DynaCT in a variety of liver directed interventional oncology procedures.
Methods: Review of the pertinent literature regarding DynaCT. We also reviewed our institutional cases where DynaCT was utilized during oncologic interventional procedures.
Results: We provide a pictorial essay of a variety of clinical scenarios where DynaCT was used as a problem solving modality and eventually enhanced decision making during the procedure. These include a) chemoembolization of small tumors in a cirrhotic liver, b) hypovascular lesions not visualized on traditional angiogram, c) determination of aberrant vascular supply from extra hepatic arteries, d) utility as a mapping tool prior to Y90 treatment, e) differentiating a lesion from pseudo lesions or arterioportal shunts and finally f) scenarios where it improved confidence in catheter position. Each clinical scenario highlighting a clinical concern (with just the traditional images alone) will be followed by DynaCT images, demonstrating its clinical utility.
Conclusions: C-arm angiographic CT can be considered superior to traditional DSA. This educational exhibit will help in better understanding of the array of applications for this relatively new technology; especially as a problem-solving tool during various interventional oncologic procedures.

Poster 52: Radiofrequency Ablation and Vertebral Augmentation of Bone Metastasis of the Spine Early Experience of a Novel Minimal-Invasive Technology

A. Kurth, D. Proschek, R. Poser

Objectives: Spinal bone metastases are the most frequent complication of malignant non osseous tumors, and are associated with severe pain and pathologic fractures. Radiofrequency ablation (RFA) in bone tumors is a promising technique first described by Rosenthal et al. While radiation therapy is the current standard of care, localized non-ionizing procedures may address cumulative radiation dose to neural elements, local recurrence and subsequent fractures and provide complimentary therapy postponing or reducing radiation therapy. Combination of targeted tumor RFA and cement augmentation for spinal metastases using during a single minimally-invasive (MI) procedure is a fascinating option in the localized treatment of bone metastases. The unique anatomy of the spine makes MI access and controlled ablation difficult. Preclinical porcine model and first in man human feasibility data are presented to assess the safety and effectiveness of an innovative RF ablation system specifically designed for spinal metastatic lesions (STAR Ablation System), which combines a mechanically robust, articulating, bipolar RF electrode designed to permit navigation within the vertebra and enabling site specific tumor ablation. Patient outcome with regard more immediate pain relief, reduced disability and preventing compression fractures of the vertebral body are provided.
Methods: VX-2 carcinoma was implanted into distal femora of 6 New Zealand White rabbits. Tumors > 1cm in diameter received CT guided RFA using the STAR System (10 g, bipolar, articulated, extendable electrode containing multiple thermocouples and a proprietary generator with an impedance and temperature controlled algorithm. Post-procedure contrast MRI demonstrated a discrete kill zone within the hard tissue tumor, which was confirmed by histopathologic evaluation. .
Results: Two patients with solid tumor osteolytic spinal metastatic lesions (a T12 lesion from breast cancer and a T11 lesion from lung cancer) were treated. Multiple site-specific RFA was performed (STAR System) followed by targeted cement delivery (StabiliT System) to support the remaining bone through a unipedicular approach via a single working cannula. Pain and disability were shown to improve and be maintained through 3 months FU with no adverse events. Oswestry Disability Index dropped dramatically from 18 to 12 and 26 to 11.
Conclusions: These data demonstrate the STAR and StabiliT Systems are compatible and provide reliable, controllable ablation of tumor in the spine and permit safe augmentation of the remaining bone with cement. The first clinical experience suggest such technology may improve patient outcome with regard more immediate pain relief, reduced disability and preventing compression fractures of the vertebral body.

Poster 53: Microencapsulated Controlled-Release Cisplatin Formulations for Oncology Applications

P. Blaskovich, L. Pham, G. Nichols, M. Gonzalez, C. Herman, R. Ohri, X. Guan, B. Hildebrand, J. Schallom, M. Menze, J. Johnson, H. Scheibel, E. McClendon, D. Costa, H. Sard

Objectives: Localized drug delivery technologies which enable sustained-release of the anti-cancer drug, cisplatin, offer the potential for greater efficacy and reduced systemic toxicity. We report on a microencapsulation based formulation of cisplatin, which enables controllable sustained-release of the active pharmaceutical ingredient (API).
Methods: Microencapsulation of cisplatin was achieved with 75:25 poly-lactide-co-glycolide (PLGA) polymer. Microspheres were generated using a method employing a modified solid-in-oil-in-water (S/O/W) emulsion with solvent evaporation, and were collected in the 45-105 μm and 106-150 μm size ranges. The microspheres displayed uniform size and morphology, as illustrated by optical microscopy and scanning electron microscopy (SEM) (Fig 1). Additionally, consistent drug loading, in the range of 30–35% (w/w) was achieved, as measured by high performance liquid chromotography (HPLC) and inductively coupled plasma (ICP) methodologies. Further characterization with powder x-ray diffraction (p-XRD) and nuclear magnetic resonance (NMR) established that during formulation, the API retains its crystalline structure (p-XRD) as well as its cis-isoform (NMR). Gas physisorption indicates a specific surface area of 0.1 m2/g for the cisplatin microspheres. We hypothesize that surface area and porosity play a role in the mechanism of release of the API from the microspheres. The in vitro release profile, under ideal sink conditions, yielded several days of sustained API release (Fig 2). In contrast, non-encapsulated cisplatin is completely released or dissolved in less than 4 hours. This slow-releasing cisplatin microsphere formulation is currently under evaluation in cell-culture (ex-vivo) to determine efficacy (i.e. IC-50 values) along 7 different cancer cell-lines, namely A549 (lung), 5637(bladder), SKOV-3 (ovarian), HepG2 (liver), Caski (cervical), AsPC-1 (pancreatic) and Tera-1 (testicular).
Results: The results from cell-culture are pending (awaited shortly), and will be included in the poster presentation.
Conclusions: Conclusions are also pending based upon the results.

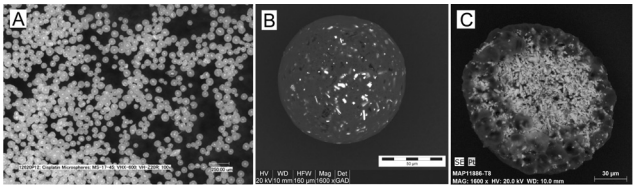

Figure 1: Images of cisplatin loaded 75:25 PLGA microspheres including (A) Optical image, (B) SEM image of one sphere, (C) SEM/EDS map of a cross-sectioned sphere.

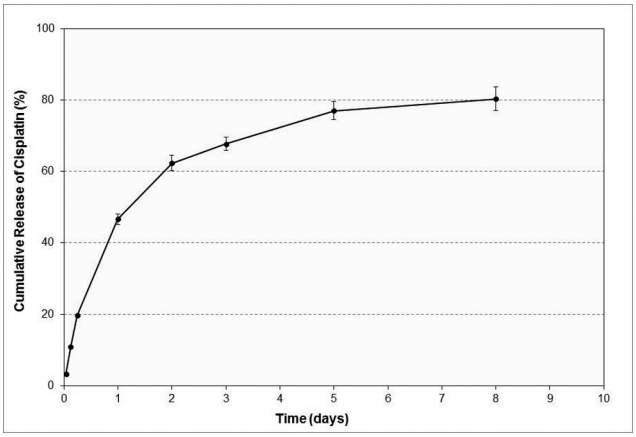

Figure 2: In-vitro kinetic drug release profile of the 35% (w/w) cisplatin loaded 75:25 PLGA microspheres measured in % cumulative release as function of time. Error bars are based on standard error mean of n=3.

Poster 54: Percutaneous Ablation and/or Osteoplasty for Palliative Treatment of Painful Tumor-Related Musculoskeletal Lesions of the Pelvis: A Single Center Experience

M. Reddick, S.B. White, W.S. Rilling, D.M. King, S.M. Tutton

Objectives: To assess pain, narcotic use, performance status and complication outcomes in a cohort of patients who underwent percutaneous treatment of painful tumor-related pelvic lesions.
Methods: A retrospective chart review was performed of 23 total procedures on 19 patients. The outcomes that were evaluated were pre and post procedure pain (VAS 1-10 scale), narcotic requirements, ECOG status and complications.
Results: Twenty-three total percutaneous procedures were performed on nineteen patients. These included 19 pelvic ablations and 23 pelvic osteoplasties. Ten patients (53%) had a combination of ablation and osteoplasty. Four patients (21%) had osteoplasty alone, and 5 patients (26%) had ablation alone. There was one de-novo screw placement and three total hardware reinforcing osteoplasties. The average pre- and post-VAS pain scale scores were 6 and 4, respectively. 19/21 (90%) of treatment sites resulted in improved pain whereas 1/21 (5%) of treatment sites had either no change in pain or worsened. 8/16 (50%) of treatments resulted in decreased narcotics, 6/16 (38%) had no change in narcotics usage while 2/16 (13%) required increased narcotics. The average pre and post ECOG performance scale scores were 1.5 and 1.1, respectively. 15/23 (65%) of treatment sites had failed prior radiation therapy. Of these, 12/15 (80%) had associated improvement in pain whereas 2/15 (13%) had no change in pain and 1/15 (7%) had increased post procedure pain. There were two complications which included an intraprocedural thermal skin injury which required elliptical excision and ultimately healed well. Another patient developed an abscess near the cryoablation site which required percutaneous drainage catheter placement which was later removed without incident.
Conclusions: This study suggests that percutaneous ablation and/or osteoplasty are a safe and effective means of treating patients with painful tumor related lesions of the pelvis. Post procedure pain decreased. Subjective quality of life was improved as a result of pain-palliation and improved mobility as reflected in a trend in improved ECOG status. Post procedure narcotic use decreased or remained unchanged in most patients, although this outcome is difficult to track due to frequent medication changes, patient compliance, and outside facility prescriptions. The lack of post-procedure fractures suggests that pelvic osteoplasty is likely an acceptable means of stabilization in appropriately selected patients. Radiation refractory patients respond well and should at least be considered for percutaneous therapy. The complications noted were relatively minor and ultimately resolved without permanent sequelae.

Poster 55: Bile Culture and Susceptibility Testing of Malignant Biliary Obstruction via PTBD

H. Yu

Objectives: A retrospective one-center study was conducted to assess the information obtainable by bile culture and susceptibility testing, especially for malignant biliary obstruction.
Methods: From July 2003 to September 2010, 694 patients with malignant biliary obstruction received Percutaneous transhepatic biliary drainage (PTBD). Bile specimens were collected during the procedure of PTBD.
Results: In the study, 694 patients were found to have malignant biliary obstruction. Of these, 485 were males and 209 were females, with an age range of 38–78 years (mean age: 62 years). There was no growth during bile culture in 57.1% patients (396/694), with 42.9% patients having a positive bile culture (298/694). Further, 57 species of microorganisms and 342 strains were identified. Gram-positive bacteria accounted for 50.9% (174/342) and Gram-negative bacteria accounted for 41.5% (142/342). No anaerobes were obtained by culture during this research. The most frequent microorganisms were Enterococcus faecalis (11.9%, 41/342), Escherichia coli (9.9%, 34/342), Klebsiella pneumoniae (8.2%, 28/342), Staphylococcus epidermidis (5.5%, 19/342), Enterococcus (5.3%, 18/342), and Enterobacter cloacae (4.7%, 16/342). The percentage of beta-lactamase–producing Gram-positive bacteria was 27.6% (48/174), and the percentage of Gram-negative bacteria was 19.7% (28/142). The percentage of enzyme-producing Escherichia coli was 61.7% (21/34).
Conclusions: Our findings suggest that the bile cultures in malignant biliary obstruction are different from those in the Tokyo Guidelines and other benign biliary obstruction researches, which indicate that the antibacterial therapy should be different. Knowledge of the antimicrobial susceptibility data could aid in the better use of antibiotics for empirical therapy of biliary infection combined with malignant biliary obstruction.

Poster 56: Single-Incision Technique for the Placement of Implantable Chest Port

J. Rosenbaum, M. Kably, J. Salsamendi, G. Narayanan

Objectives: The single incision technique for placement of tunneled central lines has been reported to have very low complication rates. This study examines the safety and efficacy of single incision technique for implantable chest port at our academic center, particularly in regard to incision site hemorrhage and infection, and patient satisfaction.
Methods: We retrospectively reviewed 42 (16 male, 26 female; mean age 56y) consecutive, single incision tunneled chest port placements from March 2011 to February 2012. A micropuncture needle bent into a C shape or in a 45 degree angle was used to access the IJV from an infraclavicular access under real-time US guidance. A

microwire and sheath were then passed into the SVC and this was followed by placement of the tunneled catheter through a vascular sheath. Outcome measures included venotomy site infection and hemorrhage. Secondary findings included procedural time, requirement for intravenous conscious sedation, fluoroscopy time, cumulative dose product, blood loss, and patient satisfaction.

Results: All placements of single or double lumen ports were successful with the majority of the ports placed via the right IJV (36/42). There were no periprocedural complications (0/42). The average total procedure time was 22.76 minutes, requiring less sedation than those for a conventional technique: a mean dose of 1.13 mg IV Midazolam and 54.89 μg IV Fentanyl. Fluoroscopy time, cumulative dose product and blood loss were all minimal with mean values of 1.94 minutes, 233.82 μGym2, and 3.18cc respectively. The lack of a second incision in the lower neck improved the cosmetic result and thus, patient satisfaction. Two patients experienced sepsis and subsequent removal of port hardware; however, both of these patients were severely immunocompromised and infection occurred at greater than 6 weeks post port placement. All other patients were free of venotomy site hemorrhage or infection

Conclusions: Single incision placement of implantable chest port is a promising technique which may further reduce periprocedural complications rates and improve cosmetic results. Overall, patients demonstrated short catheter placement times, minimal need for conscious sedation, and no related venotomy site hemorrhage or infection, while benefiting from the cosmetic result of a single incision.

Poster 57: Percutaneous Radiofrequency Ablation with Artificial Ascites for Hepatic Tumors: Usefulness of the Abdominal Band

J. Seo, Y. Lee, Y. Kim

Objectives: Percutaneous radiofrequency ablation with artificial ascites has beneficial effect to protect thermal injury of adjacent organ and to improve sonic windows of target lesions. Sometimes, large amounts of artificial ascites is needed initially and easily decreased during ablation. We report the usefulness of abdominal band in percutaneous radiofrequency ablation with artificial ascites for hepatic tumors.

Methods: The clinical and treatment-related data regarding 91 consecutive percutaneous radiofrequency ablation treatment sessions for 71 patients with hepatic tumors (HCC: 84, HGDN: 2, metastasis: 3, adenoma: 2, size: 1.0-4.6 cm, mean:2.4 cm) was reviewed. The patients were divided into two groups: group A without abdominal band (n=30) and group B with it (n=61). We compared the two groups in an assessment for amounts of artificial ascites according to target lesion location and presence of residual artificial ascites around ablated lesion at the end of radiofrequency ablation on ultrasonographic image.

Results: The mean amounts of infused artificial ascites were less in the group B with abdominal band (group A versus group B in Rt. lobe lesion: 757.5 ml versus 472.7 ml; p <0.001, in Lt. lobe lesion: 1175.0 ml versus 652.9 ml; p <0.001) (Table 1). The residual artificial ascites was observed more often in the group B compared to group A, especially in patients with Lt lobe lesion (group A versus group B in Rt. Lobe lesion: 16/20 versus 43/44; p=0.05154, in Lt. lobe lesion: 3/10 versus 15/17; p=0.007426) (Table 2).

Conclusions: The abdominal band in percutaneous radiofrequency ablation with artificial ascites for hepatic tumors is useful for decreasing the amounts of infused artificial ascites and maintaining of it. Especially, it is effective in Lt lobe lesion ablation.

Table 1, The mean amounts of artificial ascites in percutaneous radiofrequency ablation for hepatic tumors.

	group A	group B	p value *
Rt.lobe	757.5 mL	472.7 mL	<0.001
Lt.lobe	1175.0 mL	652.9 mL	<0.001

group A without abdominal band in percutaneous radiofrequency ablation with artificial ascites.

group B with abdominal band in percutaneous radiofrequency ablation with artificial ascites.

* student t test.

Table 2. The presence of residual artificial ascites around ablated lesion at the end of ablation on the ultrasonography.

	Right lobe		Left lobe	
Presence of residual artificial ascites	group A	group B	group A	group B
(-)	4	1	7	2
(+)	16 (80%)	43 (97.7%)	3 (30%)	15 (88.2%)
p-value *	0.05154		0.007426	

* chi-square test.

Poster 58: Increasing Medical Student Knowledge and Interest in Interventional Oncology: The Impact of a Dedicated Interventional Oncology Training Symposium

R. Gupta, R.K. Ryu, K. Memon, R. Salem, R.A. Omary, R.J. Lewandowski

Objectives: Interventional oncology (IO) is a highly specialized field within radiology. Recruiting motivated individuals and providing dedicated, focused training are essential to ensure continued leadership, research and innovation in this field. We aim to test the hypothesis that a dedicated IO symposium for medical students would significantly increase their knowledge and interest in IO as a career choice.

Methods: A 1-day symposium was held to introduce medical students to the field of IO. Lecturers focused on the clinical and research aspects of IO and featured a panel discussion including current trainees. A hands-on workshop allowed participants to use percutaneous ablation devices in an animal model and practice catheter-based skills with a bench top coil embolization model. Attendees were prospectively asked to complete a Likert scale-based questionnaire assessing their knowledge and interest in IO prior to and following the symposium. Statistics were calculated using the Chi-square test. The null hypothesis was rejected at $p<0.05$.

Results: 101 trainees from across the country participated in the symposium. 39 (39%) completed questionnaires were collected. Prior to the symposium, attendees reported knowledge of IO at 2.12 on a scale from 1 to 4 (1 = no knowledge, 4 = significant knowledge). Following the symposium, attendees reported knowledge of IO at 3.54, a significant increase (P value < 0.0001). Prior to the symposium, attendees reported interest in IO at 2.64 (1 =1 little or no interest, 4 = highly interested). Following the symposium, attendees reported interest in IO at 3.64, also a significant increase (P value < 0.0001).

Conclusions: This study shows that a focused symposium highlighting the clinical and research aspects of IO can have a significantly positive impact on medical student a) knowledge and b) interest in IO as a career. The long-term impact on career choice is unknown. A longer-term study to assess the longitudinal impact of the IO training symposium is underway.

Poster 59: Successful Salvage of Carcinoma Esophagus Patient with Aberrant Right Subclavian Artery Esophageal Fistula by Endovascular Angioembolization - A Case Report

A.M. Polnaya, S. Kulkarni, N.S. Shetty, T.P. Dharia, M.H. Thakur

Objectives: To describe emergent salvage treatment offered to a patient with carcinoma esophagus with aberrant right subclavian artery (ARSA) esophageal fistula by endovascular glue embolization.

Methods: Development of a fistula between an ARSA and the esophagus is a rare cause of massive hematemesis. The present report describes the first case of arterioesophageal fistula with an aberrant right subclavian artery caused by proximal esophageal growth and prolonged nasogastric intubation who was successfully salvaged from the catastrophy. 42 Y female patient presented with complaints of progressive dysphagia of 4 months duration. Preliminary work up revealed a growth in the upper third esophagus which was confirmed to be squamous cell carcinoma. CT study confirmed the presence of growth and ARSA at the level of involvement. Patient was planned for chemoradiation when she presented massive hematemesis, hypovolemic shock which was aggressively resuscitated. Endoscopy was not feasible and patient was posted for emergency angioembolization. Catheter angiography revealed a pseudoaneurysm secondary to tumour involvement in the proximal portion of ARSA with fistulous communication with the adjacent esophagus in the form of active contrast extravasation into the esophagus. Salvage was planned by 50% glue embolization of the fistulous tract for stopping the on table torrential bleeding. Post-embolization check angiogram revealed complete stoppage of active extravasation and non visulalization of the pseudoaneurysm. Patients vitals stabilized with cessation of active bleed. Post-embolization day 2 patient was taken up for stent graft placement; however, check angiogram revealed short segment complete occlusion of the involved segment of ARSA with good forward flow maintained in the subclavian artery via the collaterals. No further endovascular treatment planned in this patient. Patient has fully recovered with no residual deficit and is undergoing completion of chemoradiation.

Results: Literature review revealed that open surgical approach is often emphasised for salvaging these patients. In our case, the target problem was resolved by endovascular means. Though an emergency endovascular glue embolization of the fistulous tract and aggressive critical care management were key to successful outcome in our patient, a more definitive endovascular covered stent graft placement across the involved segment is highly recommended.

Conclusions: Transcatheter embolization and stentgraft placement is suggested as a potential alternative to surgery in the treatment of the aberrant right subclavian artery-esophageal fistula.

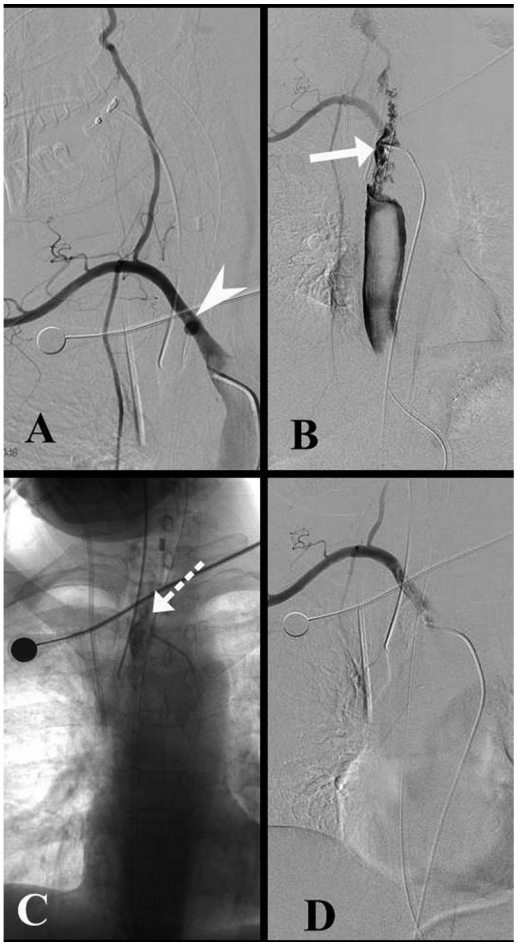

Angioembolization images :
A ARSA gram reveals pseudoaneurysm (Arrowhead).
B Fistulous communication demonstrated (Solid arrow) between ARSA and Esophagus with active extravasation.
C Glue cast in the fistulous tract (Dotted arrow).
D Post-embolization checkgram shows no more fistulous communication.

Poster 60: Cryoablation as Salvage Therapy of Locally Recurrent Squamous Cell Laryngeal Cancer

J.G. Mammarappallil, C. Sullivan, J.J. Urbanic, M. Porosnicu, J. Meyers, H. Clark

Objectives: To present the successful utilization of cryoablation as salvage therapy for locally recurrent squamous cell carcinoma of the larynx.
Methods: A 73-year-old man presented with stage 1 (T1N0M0) squamous cell carcinoma of the supraglottic larynx. He elected definitive external beam intensity modulated radiation therapy (70 Gy in 35 fractions to the primary site and 50 Gy in 25 fractions to the lower neck). Local tumor recurrence 1 year later led to laryngectomy. Two years later, recurrent disease in the left peristomal region was managed with re-irradiation and chemotherapy (60 Gy, Altima and Tarceva). Surveillance PET/CT 5 months following radiation therapy showed a 3 cm hypermetabolic mass in the same region with no additional sites of disease detected. Stomal resection with reconstruction was not offered due to limited chance for cure and likelihood of major morbidity and mortality. Additional radiation therapy was also not advised. Cryoablation was offered as salvage therapy. The Galil cryoablation system (Galil Medical, Incorportated. St. Paul, MN) was employed incorporating four Ice Rod probes. General anesthesia was utilized with intubation through the pre-existing tracheostomy for airway management throughout the procedure. CT fluoroscopy was used to position the ablation probes. The ablation was completed following the typical 10 minute freeze, 8 minute thaw, 10 minute freeze protocol. Due to the superficial location of the tumor and its erosion through adjacent skin, cryoablation was expected to be followed by a surgical tissue flap to cover the subsequent cutaneous injury.
Results: Other than mild hemorrhage into the trachea, no complications were realized during or immediately following the cryoablation. Post-procedure, the patient was hospitalized for airway management and pain control. Within several weeks of treatment, necrosis occurred in the adjacent, proximal tracheal wall and posterior stoma. On post-treatment day 38, debridement was performed. Soft tissues of the superficial left neck and tracheostoma were reconstructed with a pectoralis myocutaneous flap and a deltopectoral flap. Pathology revealed no evidence of cancer in the debrided tissue. PET/CT performed at four months showed no recurrence.
Conclusions: Treatment of laryngotracheal stomal recurrence is typically managed with extensive surgical resection that is highly morbid and without significant chance for cure. Such a procedure was not considered an option in this case. For this patient, cryoablation has established local control of recurrent parastomal laryngeal tumor with minimal associated morbidity. In general, cryoablation is proving to be a robust means of treating primary and metastatic neoplastic disease involving the lung, liver, kidney, bone, and prostate. As our experience and understanding of this technology evolves, we will continue to define its appropriate use in these organ systems as well as expand its application to other regions of the body. Though long-term results are still pending, this case demonstrates an atypical utilization of cryoablation in the successful management of locally recurrent laryngeal cancer.

Poster 61: Investigation of the Safety and Usefulness of Computed Tomography-Guided Percutaneous Needle Biopsy of Paraaortic Lymph Nodes

T. Aramaki, M. Moriguchi, E. Bekku, K. Asakura, M. Endo

Objectives: Various factors such as malignant lymphoma cause abdominal lymph node enlargement. A histological diagnosis of malignant lymphoma is important in planning therapy, and although superficial lymph node biopsies are often obtained, target lesions occasionally arise only around the abdominal aorta. These require surgical, or more recently, endoscopic biopsies. To intraoperatively determine whether target lymph nodes are correctly resected during a surgical biopsy can be difficult, and therapy could be delayed due to postoperative complications.The aim of this study is to assess the safety and effectiveness of percutaneous biopsy of paraaortic lymph nodes under computed tomography (CT) fluoroscopic guidance.
Methods: We retrospectively investigated puncture success rates based on findings of diagnostic imaging, size of target lymph nodes, rate of confirmed diagnosis, frequency of changes in therapeutic plans and incidence of complications among 36 patients after percutaneous needle biopsy using an 18G cutting needle between September 2002 and March 2009.
Results: The pre-biopsy diagnoses for the 36 subjects who underwent percutaneous needle biopsy included: malignant lymphoma (n = 26), lymph node metastasis of esophageal cancer (n = 3), lymph node metastasis of lung cancer (n = 3), lymph node metastasis of pancreatic cancer (n = 3) and unknown (n = 3). The median size of the target lymph nodes was 25 mm (range: 9–102 mm). The results of diagnostic imaging indicated that all punctures were successful. The diagnoses were confirmed in 33 of the 36 patients (91.7%). Histopathological findings confirmed malignant lymphoma (n = 21), squamous cell carcinoma (n = 2), poorly differentiated adenoma (n = 2), other malignancies (n = 5), benign lesions (n = 3) and unknown in 3. Therapeutic strategies were altered based on the results of CT-guided percutaneous needle biopsies in 12 of the 36 patients (33.3%). Three patients developed 4 adverse events comprising grade 1 radiation dermatitis (n = 1), grade 1 hematoma (n = 2) and grade 1 pneumothorax (n = 1).
Conclusions: Target paraaortic lymph nodes can be accurately punctured using CT-guided percutaneous needle biopsy, and the specimens were too small to examine the flowcytometry or chromosome analysis; however, it was enough to confirmed the diagnosis according to WHO classification of malignant lymphoma. Percutaneous biopsy of paraaortic lymph nodes under CT fluoroscopic guidance is useful for confirming diagnoses with a low risk of serious deep organ damage.

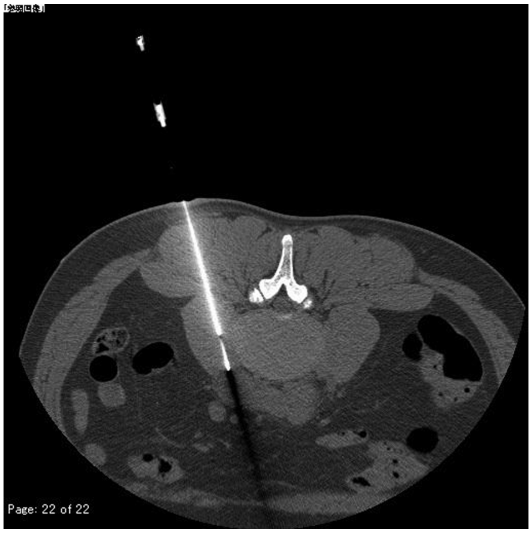

Poster 62: Cryoablation of Metastatic Lesions Residing in Intraosseous Structures: Local Control, Pain Palliation, and Survival Observations

H.J. Bang, P.J. Littrup, B.P. Currier, D.J. Goodrich, J. Kuo, H.D. Aoun

Objectives: Multi-site cryoablation (MCA) was conducted to assess complications, local tumor recurrences, pain reduction, and overall survival (OS) in the treatment of metastatic lesions residing in bone locations.
Methods: 36 CT and/or US-guided percutaneous PCA procedures were performed upon 32 tumors in 20 patients. Mean patient age was 62 years with a male:female sex distribution of 12:8, respectively. Tumor locations were grouped according to common metastatic sites. Cementoplasty was utilized in cases with compromised bone stability. Complications were assessed according to Common Toxicity Criteria for Adverse Events Version 3.0 (CTCAE). Median overall survival (OS) was determined using the Kaplan-Meier Method. Data on pain palliation was available for 7 patients.
Results: A mean of 1.8 (36/20) MCA's per patient were performed with a median clinical follow-up of 12 months. Anatomical location of treated bone lesions are as follows: 20 chest wall and/or rib, 6 pelvis/sacrum, 2 lumbar vertebrae, 2 scapulae, and 2 mandible. Primary cancer diagnosis for the 20 patients include 8 renal, 4 lung, 3 colon, 1 ovarian, 1 breast, 1 liver, 1 bone, and 1 alveolar soft part sarcoma. Major complication and local recurrence rates were 9% (3/32) and 5% (1/20), respectively. The average worst pain pre-operatively was 7 (range: 5-9) and the average pain post-operatively was 1 (range: 0-2) within one month. Median OS was 13.9 months.
Conclusions: MCA had low morbidity and local tumor recurrence rates for all anatomic sites and also proved safe and effective when paired with cementoplasty in lesions with extensive bone infiltration. Although data on pain reduction was limited, the observed results warrant future considerations for the use of MCA in the palliation of painful/symptomatic metastatic lesions.

Poster 63: The Real-time MR Guidance and Monitoring Percutaneous Cryoablation of Renal Tumors: A Preliminary Report

C. Li, L. Ming, L. Yubo, C. Qianqian

Objectives: To establish initially the technique and evaluate the safety and efficacy of cryoablation of renal tumors by using a percutaneous approach guided by an intraprocedural open—configuration magnetic resonance imaging system.
Methods: Nineteen renal tumors (diameter range, 1.0–6.7 cm; mean, 2.9 cm) in 11 patients were treated with 22 cryoablation procedures under the guidance of near real—time images of a 0.23T open—configuration MR system (Proview, Philips Medical System) mounted with optical tracking system (iPath 200, Philips Medical System) at the author's institution. There were 9 male and 2 female with an average age of 63.8 years (range, 40–82 years). Cryoablation was performed using a high—pressure argon system (Cryo—Hit system) with a double freeze/thaw cycle. A 1.47, 2 or 3 mm MR—compatible cryoprobe was advanced into the target lesion according to the size of tumors. Mean duration of procedures was 136.5 (112–165) minutes. Follow-up dynamic CT and MR imagings were adopted to evaluate the efficacy of the cryotherapy (mean 12.3 months; range 4–41 months). Medical records retrospectively reviewed for evidence of renal functional outcomes.
Results: All procedures were carried out safely and accurately without any serious complications, such as bleeding, skin cold injury, infection, implantation metastasis inside the puncture path occurred. Three patients showed a residual tumor: at 5 weeks, 6 months, and 28 months after the first cryoablation. All of them received additional cryoablation later, resulting in complete tumor necrosis. Cryoablation had no influence on renal function in our study.
Conclusions: MR-guided percutaneous cryoablation of renal tumors is safe and minimally invasive. Short-term follow-up results are encouraging, although long-term follow-up is necessary to assess true treatment efficacy.

Poster 64: The Individual Design and Clinical Application of Special Shaped Tracheobronchial Stents

J. Guang-zhi

Objectives: To investigate the individual design of special shaped tracheobronchial stents and its feasibility and clinical therapeutic effects in the treatment of tracheobronchial stricture and fistula.
Methods: 20 patients were enrolled into this study, including 13 male and 7 female, aged from 37 to 78, the average age is 65.3. Airway constrictions were diagnosed in 11 patients, 4 of which had multiple stricture; the others were airway fistula, including 8 stoma-airway fistula after esophageal carcinoma radical resection and 1 left principal bronchus stump-thoracic cavity fistula after left pulmonary resection. All the patients were implanted with the special shaped tracheobronchial stents. According to the respective pathological features and the imaging data measurements of different patients, 20 special shaped individual tracheobronchial stents (8 L- shaped and 12 Y-shaped) were designed and implanted in 20 cases of airway stricture or fistula under X-ray guidance.
Results: Slight deformation and displacement happened in 1 Y-shaped stent because of uneven exertion release; the other 19 stents were placed successfully with no severe complication happened. The symptoms of dyspnea and bucking relieved and lightened immediately after the operation.
Conclusions: Placement of the special shaped tracheobronchial stents is effective for the treatment of airway stenosis and fistula. The operating technique is safe, simple and feasible.

Poster 65: Interventional Treatment for Malignant Obstructive Jaundice

Y. Li

Objectives: To approach the clinical value of interventional treatment for 56 cases of patients with malignant obstructive jaundice.
Methods: Percutaneous transhepatic biliary drainage was performed in 56 patients with malignant obstructive jaundice, including 8 cases of biliary external drainage (PTC), 28 cases of internal and external biliary drainage (PTCD), biliary-duct stent placement was performed in 30 cases on the base of biliary drainage.
Results: Skin, icteric sclera gradually relieved after Interventional therapy in 56 cases after 3 days (30 cases completely disappeared after 2 weeks); Itch of skin began to reduce 1 day (3 to 5 days later gradually disappeared). The TSB level was reduced from 126.8~382.6 micromol/L before operation to 46.5~182 micromol/L 3 to 7 days after operation. After 8 to 14 days, the TSB level was reduced to 18.2~86.3 micromole/L. No interventional therapy-related complications were occurred. The longest survival time was 22.6 months, the shortest was 3.6 months, median survival of 10.2 months.
Conclusions: Percutaneous transhepatic biliary drainage or stenting, can effectively alleviate the biliary obstruction, gradually degrade serum bilirubin concentrations, improve clinical symptoms,signs and liver function and prolong life.

Poster 66: Clinic Efficacy of CT-guided Iodine-125 Seed Implantation Therapy in Patients with Vertebral Metastatic Tumor

Z. Wang, J. Gong, K. Chen, Y. Zheng, L. Zhang

Objectives: The purpose of this study was to examine the safety and clinical efficacy of CT-guided radioactive iodine-125 seeds implantation treatment in patients with vertebral metastatic tumor.
Methods: We retrospectively analyzed 20 patients with vertebral metastatic tumor. We used treatment planning system to reconstruct the 3D image of vertebral metastatic tumor and work out the number and the dose rate distribution of 125I seeds. The minimal peripheral doses of 125I seed implantation were 90-140Gy, with median of 120Gy. 24 Vertebral metastatic tumors were treated by CT-guided radioactive iodine-125 seeds implanted. The number of 125I seeds implanted ranged from 4 to 63, with a median of 19.
Results: Follow-up ranged from 4 to 26 months with a median of 12 months. All patients tolerated seed implantation well. The rate of pain relief was 95%. The 6 and 12 month local control rates were 80% and 30%, respectively, with a median of 9 months (4-23 months). The 6 and 12 month survival rates were 95% and 45%, respectively, with a median of 10 months. Thirteen patients developed distant metastases. Three patients showed recurrence. Four patients were still alive. No myelopathies were encountered.
Conclusions: CT-guided radioactive 125I seeds implantation treatment in patients with vertebral metastatic tumor is a safe, effective, and minimally invasive method.

Poster 67: Partial Splenic Artery Embolization with Autologous Hair or Gelatin Sponge: A Comparative Study

G. Hao, B. Xia, R. Yang

Objectives: To discuss the effects and the complications of partial splenic artery embolization with gelatin sponge or with autologous hair for hepatocellular carcinoma (HCC) complicated with liver cirrhosis, portal hypertension and hypersplenism, to provide scientific information helpful for the selection of embolization materials in clinical practice.
Methods: Partial splenic artery embolization with gelatin sponge was performed in 23 patients with hepatocellular carcinoma (HCC) complicated with liver cirrhosis, portal hypertension and hypersplenism, (gelatin sponge group) and partial splenic artery embolization with autologous hair was carried out in another 27 patients (autologous hair group). The clinical data were retrospectively analyzed. The laboratory studies, complications and recurrence were observed and compared between two groups.
Results: One week after PSE, WBC and PL T counts significantly increased ($P < 0.01$), and lasted for a long time at a relatively high level.No significant difference in the thrombocyte and leucocyte counts existed between two groups ($P > 0.05$). However, the occurrence of complications in gelatin sponge group was significantly slighter than that in autologous hair group.
Conclusions: Autologous hair PSE in combination with TACE is a safe and effective measure for patients with HCC complicated with liver cirrhosis, portal hypertension and hypersplenism. Autologous hair is ideal embolic material.

Poster 68: The Observation of Effect of 125 I Seeds Implantation Combined with External Radiation in the Treatment of Tongue Cancer

Y. Wu

Objectives: To study the technical feasibility and the short-term effect of iodine-125 interstitial implantation combined with intensity-modulated radiotherapy in treating tongue cancer by direct vision and ultrasonic guidance.
Methods: 15 patients with early tongue cancer had the treatment of iodine-125 interstitial implantation by direct vision and ultrasonic guidance. 1 case operated under the general anesthesia, 14 cases by the local anesthesia. Seed needles are arranged in parallel, spacing 1 cm, target volume imaging the implanting border put 1 cm, seed spacing 1 cm. (Matched peripheral dose) MPD around tumor is 90 ~ 145 Gy, each seed activity is 0.40 ~ 0. 50 mCi, each lesions implanted 6 ~ 25 seeds. 24 hours after implantation, take the normal and lateral radiograph of head and neck or CT verification. One week later, all patients had preventive radiotherapy on cervical lymph node, taken intensity-modulated radiotherapy model, 200 cGy/time, 5 times per week, 4-4.5 weeks to complete the treatment, total dose: 40-45 Gy.
Results: After 3 to 20 months, of 15 tongue-cancer patients, 8 cases got complete remission, 5 got partial remission, 1 case got stability and 1 case got progress. Local control rate is 86.7%, and the follow-up survey has showed the rest of the patients were alive except one who occurred in lung metastases and lived for 10 months, and none had serious radiation response.
Conclusions: The short-term effect is definite for tongue cancer patients after iodine-125 interstitial implantation with intensity-modulated radiotherapy, providing a new, feasible, safe, and minimal invasive treatment method. The long-term survival rate needs further tracking and follow-up.

Poster 69: MRI Guided Experimental Cryoablation of Rabbit's Sciatic Nerve

C. Li, Q. Zhenli, L. Ming, L. Yubo

Objectives: To observe the apprearance of MRI, pathology and ultra microstructure of the rabbit's sciatic nerve after argon-helium cryoablation, evaluate the influence of the argon-helium cryoablation to rabbit's sciatic nerve, the sciatic nerve repair and regeneration after cryoablation, provide the experimental evidence for the safety and feasibility of the procedures, which are adjacent to peripheral nerve, by argon-helium cryoabation under imaging guidance in clinic.
Methods: 20 New Zealand white rabbits were randomly divided into two groups (A group and B group). Each group has 10 rabbits. Each left leg was experimental side, right as control side. Under general anesthesia, all 20 rabbits' bilateral sciatic nerves were scanned with 3.0T MRI in order to choose the experimental sciatic nerve and definite the frozen region. Argon-helium cryoablation were performed under an open 0.23T MRI guidance with 1.47 mm diameter cryoablational probe by a twice repeated freeze-thaw cycle, which 100% flow rate of argon gas was maintained to achieve freezing for 12 minutes and correspondingly helium gas was used to thaw for 3 minutes. In A group, experimental sciatic nerve with 3 mm diameter area was in the center of the ice ball. In B group, experimental sciatic nerve with 3 mm diameter area was near the ice ball. The follow-up imaging were scanned with 3.0T MRI after cryoablation immediately, 7d, 14d, 30d and 60d to observe the rabbit's sciatic nerves and their surrounding imaging changes and adjacent areas imaging changes, measure the signal intensity of sciatic nerves and muscle, and then calculate the signal intensity ratio of nerve and muscle and then examined the nerves pathology and the ultra microstructure. 2 rabbits were sacrificed in the same time. Take left and right sciatic nerve to observe the changes of tissue by light microscope and transmission electron microscope.
Results: Intraoperative imaging appearance of MRI: The ice ball appears as a dark signal void in both FE T1WI and CBASS sequences. During the cryoablation, the size of ice ball is gradually increased. The ice ball reach biggest size for 10 min. In A group, the experimental position is in the center of the ice ball. In B group, the experimental position is near the ice ball. General observation after cryoablation: The activity of the rabbit's left leg changes after cryoablation; the ankle down, toe show loss of function. Motor function are partial recovered at 60d in the A group (both 2 rabbits) and obviously recovered in the B group than A group (both 2 rabbits). Ulcers were appeared in the rabbit's foot at 30 days after cryoablation in both two groups. In A group, the ulcers do not heal at 60 days (both 2 rabbits); in B group ulcers partly heal at 60 days (both 2 rabbits). Imaging appearance of rabbit sciatic nerve before cryoablation and in immediately, 7 days, 14 days, 30 days and 60 days after cryoablation: There were no obvious changes in T1WI sequence in experimental sides in all 20 rabbits. However, in T2WI and FS-T2WI sequence, the cryoablational segment of the sciatic nerve become thick and twist, the signal of the injured nerve become higher than normal. The sciatic nerve/muscle signal intensity ratio (SIR) of the injured sides was significantly higher than the control. The difference of SIR between two group experimental side is significant. The SIR of experimental side increase immediately after cryoablation and reach the peak at 7d, whereafter, the SIR decreased in 30d and 60d after cryoablation, but still higher than control. There is no abnormality in the control side in MRI. Pathology appearance of the rabbits' sciatic nerve tissue after Argon-helium cryoablation: In the A group, the sciatic nerve appearance severe injury immediately after argon-helium cryoablation, nerve fiber degeneration, axonal swelling and myelin sheath loose. The damage reached a peak at 14d, nerve fibers sheath performed, arranged disorder. Whereafter, the nerve began to repair. At 60d, the regeneration of axons and Schwann cells appear, but necrotic nerve fibers still can be seen. In B group, the nerve also appear injury immediately after cryoablation, but not so serious as A group. There is only a part of the nerve fiber degeneration, at 7d the damage reach a peak also. Then the nerve begin to repair and regeneration, at 60d bulk fibers have repaired.
Conclusions: The formation of ice ball and the extent of the injury region could be demonstrated accurately by intraoperative MRI. The pathology and function of sciatic nerve with 3 mm diameter could be influenced by Argon-helium cryoablation under image-guided. The peripheral nerve with 3 mm could be damaged by cryoablation when the ice ball wrapped the nerve, including appeared nerve degeneration and necrosis. The nerve damage reach the peak at 14d after freezing, and then, the nerve begin to repair. In 60d, the damage can not be repaired completely. In clinical, when treating tumors which wraps peripheral nerve, we should be careful. When treating the tumors adjacent to peripheral nerve, we should be consider that the function of the nerve would loss at a long time. MRI can make the diagnosis of the freezing injury and repair of peripheral nerve with normal sequence.

Poster 70: The Use of Imitating-Viatorr in TIPS

C. Li, R. Yang

Objectives: To assess the feasibility and effectiveness of the Imitating-Viatorr in TIPS.
Methods: 110 patients with esophageal and gastric variceal bleeding due to liver cirrhosis were referred to the treatment of TIPS, all patients underwent CT scans before TIPS, according to the CT pictures, adjusted the angles of RUPS-100, after the successful puncture from hepatic vein to portal vein, balloon dilation was given and the bare stent (8mm×60mm)was released, then, the PTFE stent (8mm×40mm) was put into the bare one, under the guidance of fluoroscopy, released the PTFE stent to covered the tunnel of liver parenchyma, write down the data of portal pressure before and after the procedure.
Results: The technical success rate was 100%; the procedure-related mortality was 0%; intra-peritoneum bleeding was confirmed in three patients within six hours after TIPS, and only conservative treatment can stop it. One year follow up, 15patients rebleb (13.5%); two years follow up, 21 patients re-bleeding(19.1%); hepatic encephalopathy developed in 23 patients (20.9%); Doppler ultrasound showed the patency rates of shunt: 97 patients (88.2%) in one year; 86 (78%) in two year. Two patients underwent liver transplantation due to liver failure.
Conclusions: Before real Viatorr can be obtained, the imitating-Viatorr (bare stent combined with PTFE stent) can also improve the patency rates of shunt, similar to Viatorr; however, it seems that the modified stent increase the rates of encephalopathy.

Author Index

M

N

O

P

Q

R

S

T

U

V

W

X

Y

Z